SEISMIC ANALYSIS OF THE EMBEDDED CONTROL TOWER AT SUCCESS DAM

by

Rafael Antonio Prieto Piedrahita

A thesis submitted in partial fulfillment of the requirements for the degree of

MASTER OF SCIENCE
in
CIVIL ENGINEERING

UNIVERSITY OF PUERTO RICO
MAYAGÜEZ CAMPUS
2006

Approved by:

Ricardo Ramos, PhD — Date
Member, Graduate Committee

Luis E. Suárez, PhD — Date
Member, Graduate Committee

Miguel A. Pando, PhD — Date
President, Graduate Committee

Genock Portela, PhD — Date
Representative of Graduate Studies

Ismael Pagán, MSCE — Date
Chairman, Department of Civil Engineering and Surveying

José Mari Mutt, PhD — Date
Director of Graduate Studies

ABSTRACT

This thesis presents the analyses carried out to compute the Dynamic Soil-Structure Interaction (DSSI) effects of the embedded control tower at Success Dam, California. The particular case of the Success Dam in Sacramento, California was chosen because the control tower at this dam is partially embedded in its upstream slope. The analyses carried out included two dimensional plane strain models based on finite element and explicit finite difference formulations. Several 2D models were analyzed including models with and without the control tower, with and without the intake pipe, with different elastic properties, and incorporating soil nonlinearity using the equivalent linear method. The 3D effects involved in the problem were also studied. This was done by using 3D models and the finite elements formulation. The results obtained herein were compared with previous studies, and conclusions were drawn and recommendations for future work were provided.

RESUMEN

Esta tesis presenta los análisis realizados para calcular los efectos de Interacción Dinámica Suelo Estructura (IDSE) de la torre de control embebida en la presa Success, California. El caso particular de la presa Success en Sacramento, California fue seleccionado porque la torre de control en esta presa está parcialmente embebida en su talud aguas arriba. Los análisis realizados incluyeron modelos bidimensionales de deformación plana usando formulaciones de elementos finitos y diferencias finitas explicitas. Varios modelos 2D fueron analizados con y sin la torre de control, con y sin la tubería de toma, con diferentes propiedades elásticas, e incorporando la no linealidad del suelo usando el método lineal equivalente. Los efectos 3D del problema fueron también estudiados. Eso fue realizado por modelos 3D usando el método de los elementos finitos. Los resultados obtenidos fueron comparados con estudios previos, y se presentan conclusiones y recomendaciones para estudios futuros.

PREFACE

This study was carried out as part of a research project awarded to Dr. Luis Suarez of the University of Puerto Rico at Mayagüez (UPRM) by the Engineer Research and Development Center (ERDC) of the U.S. Army Corps of Engineers. The study focuses on the geotechnical aspects of the dynamic soil structure interaction of embedded control towers. This project is anticipated to continue on a second phase, focusing on the structural dynamics issues of this problem

I want to thank Dr. Suarez for giving me the opportunity to share his sound knowledge, his strong support to the project, and his unbreakable commitment to his students.

For their moral and effective support, special thanks to Dr. José A. Mari Mutt, Dr. Ricardo Ramos, Professor Vilma D. López, Miss Zulma Aldahondo, and my family: Consuelo, Hector and Diego.

Finally, I would also especially like to thank my fellow grad students and friends, whose permanent support is greatly appreciated. Thank you Arleen, Diana, Joanna, Lorena, Alexander, Ali, Eimar, Juan Carlos, Guillermo and Paul.

"Sólo se tiran piedras al árbol que está cargado de frutos"

Saadi De Shiraz

TABLE OF CONTENTS

Page

LIST OF TABLES

LIST OF FIGURES

1 INTRODUCTION

This thesis presents the results of a series of dynamic soil structure interaction (DSSI) analyses for the partially embedded control tower at Success Dam, California. DSSI analyses have been widely used to study seismic behavior of embedded structures built on horizontal ground. DSSI studies on sloping ground conditions have been studied to a lesser extent and further research is needed in this area. The research presented herein will specifically focus on the DSSI of a control tower structure which is partially embedded and has sloping ground conditions since it is located in the upstream slope of the Success Dam in Sacramento, California.

This chapter presents a general introduction and the motivation and objectives of this study. The organization of this report is also described in this chapter.

1.1 General Introduction and Background

The particular case of the Success Dam (California) was selected for this research project because this project has a control tower which is partially embedded in the upstream shell of the earth dam. This provided an interesting case study for DSSI of structures built in sloping ground conditions. Furthermore, this dam and its tower have been subject of several previous studies that have yielded conflicting results and recommendations. The existing studies have involved different DSSI methodologies. One of the important aspects where conflicting results seem to have been reported is in the predicted values for the base shear force of the control tower when excited under the design earthquake. The values reported for the base shear force show differences of the order of one order of magnitude despite being analyzed for the same or very similar earthquake ground motions. One of the main motivations for this research project is this issue and hence one of its objectives is to shed light on why the large differences among the reported values from previous studies.

A series of DSSI analyses were carried out using the finite element and the finite explicit differences methods. The comparison of the results from the different analyses was made in terms of the ground motions obtained in selected points within the dam and the tower, as well as in terms of the base shear force and moment in the control tower. The models were prepared using all the information available for the dam, including geophysical data recently obtained for the Success Dam.

1.2 Motivation

Many earth dams are built with intake towers which are auxiliary structures that help drain the water from the reservoir. In some instances dams have control towers which have a similar function than intake towers, but typically do not have direct contact with the water intake opening. Control towers are typically located over a drainage conduit that runs across the bottom of the dam cross section. Control towers contain the mechanical and electrical equipment to operate gates that control the flow of water across this drainage conduit. These towers are usually built within the dam and hence are partially embedded. It is crucial that these structures remain standing and operational after a strong earthquake.

Seismic analysis of embedded control towers must account for several effects such as the effect of the surrounding soil in the embedded portion of the structure, the possible soil nonlinearity (particularly when subjected to strong ground shaking), and the sloping ground condition of the free surface of the dam from where the tower stems.

A survey conducted by Dove (1996) revealed that most intake and control towers in the United States are lightly reinforced and thus are likely to sustain inelastic deformations in the event of a strong earthquake. This author therefore recommends performing a nonlinear analysis of the structure to obtain realistic results, especially if a decision regarding the retrofitting of the towers is to be made.

This research project will entail analyses of the Dynamic Soil Structure Interaction (DSSI) of an embedded control tower. These analyses will study the interaction of the structure (control tower) and the soil (earth dam) during strong seismic events. This is a highly complex interaction phenomenon which modifies the soil and the seismic response of the structure (displacement, acceleration, rocking, etc.) during the earthquake.

The motivation for the research aims to develop further knowledge of the particular influence of embedment, and soil interaction on the seismic response of embedded control towers. As mentioned before, the proposed research will focus specifically on the control tower at the Success dam in California.

1.3 Objectives and Scope

The overall objective of this research project is to compute the DSSI effects of the embedded control tower at Success dam for the MCE.

More specific objectives include:

- Quantify the differences on the maximum base reactions (shear force and bending moment) acting on the control tower using 2D models using the finite element and the finite difference formulation.
- Compute the maximum shear force at the base of the control tower using 2D and 3D models with and without the presence of the horizontal drainage conduit.
- Compute the maximum base reactions (shear force and bending moment) acting on the control tower when the nonlinearity of the soil is included in the different models.
- Compute the variation of ground motion along the embedded length of the control tower using different DSSI formulations.

- Quantify the differences in DSSI response due to 3D effects.

1.4 Outline of this Thesis

This document is organized as follows:

Chapter 1 presents the motivation of this study, the objectives of this research project, and describes the general organization of this document.

Chapter 2 presents a summary of previous DSSI studies of Success Dam and its control tower. The summary includes a description of the methodology and models used in previous works.

Chapter 3 presents information related to Success Dam and its auxiliary structures (i.e. the control tower and the drainage conduit). This chapter also presents a summary of the available geotechnical and geophysical information used to prepare the analytical models.

Chapter 4 presents information regarding the modeling of the Success Dam, and the analytical results obtained using 2D models. Detailed information regarding the structural components in the dam including the tower and the intake conduit are also presented. This chapter also presents information regarding the seismic input used for the DSSI analyses. Several methodologies were used to evaluate the seismic response of the Success Dam. The numerical methods used were the finite element method (FEM) and the explicit finite difference method (EFDM). 2D models were prepared without structures, including the control tower, and including both the control tower and the intake pipe. Effects due to the soil nonlinearity were also investigated using the linear equivalent method (Schnabel et al. 1972).

Chapter 5 presents a summary of the results obtained using 3D FEM models. The purpose of these analyses was to study the 3D effects associated with the problem.

Two 3D models were analyzed: dam with control tower, and dam with control tower and intake pipe. The results obtained are compared with results from 2D models.

Chapter 6 presents an analysis of the results of all DSSI analyses carried out in this project, and a comparison of the results with previous studies. This chapter presents results in terms of basal reaction of the control tower (i.e. shear force, and bending moment). The results of sensitivity analyses is also presented, and used for the comparison of results.

Chapter 7 presents conclusions and recommendations obtained by this research project. This chapter also includes recommendations for future work on this subject.

2 LITERATURE REVIEW

This chapter is divided in two: a literature review on DSSI of embedded structures with an emphasis on the numerical formulation; and a summary of the previous DSSI studies available for the study project of the embedded control tower at Success Dam.

2.1 DSSI Methodologies for Embedded Structures

Table 2-1 presents a list of the most important publications on this subject relevant to this research project. This list focuses on the numerical approach and not on particular case histories.

Table 2-1 Summary of DSSI

Authors	Ground Surface	Numerical Method	Damping Type	1D, 2D, or 3D.	Observations
Goyal and Chopra (1989a)	Horizontal	FEM	Modal	1D	Capacity spectrum method
Goyal and Chopra (1989b)	Horizontal	FEM	Modal	1D	Capacity spectrum method
Goyal and Chopra (1989c)	Horizontal	FEM	Modal	1D	Capacity spectrum method
USACE (2003)	Horizontal	FEM	Modal	1D	Capacity spectrum method
Gupta and Kunnath (2000)	Horizontal	FEM	Modal	1D	Modified capacity spectrum method, adaptive pushover method
Goel and Chopra (2004)	Horizontal	FEM	Modal	1D	Modified capacity spectrum method, multi-modal pushover
Schnabel et al. (1972)	Horizontal	FEM	Strain dependant	1D	Program SHAKE. Linear equivalent method.
Lysmer et al.	Slope and	FEM	Strain	1D or	Program FLUSH. Linear

Table 2-1 Summary of DSSI

Authors	Ground Surface	Numerical Method	Damping Type	1D, 2D, or 3D.	Observations
(1975)	horizontal		dependant	2D	equivalent method includes beam elements for DSSI analyses.
HCItasca Consulting Group (2002)	Slope and horizontal	EFDM	Rayleigh formulation	1D or 2D	Program FLAC-2D. Elastic material with Mohr-Coulomb failure criterion. Includes beam elements for DSSI analyses
PEERC (2006)	Slope and horizontal	FEM	Modal or new formulation can be used	1D or 2D	Program OpenSees. Several models and failure criteria are available. Includes beam elements for DSSI analyses
HCItasca Consulting Group (2002)	Slope and horizontal	EFDM	Rayleigh formulation	1D, 2D, or 3D	Program FLAC-3D. Elastic material with Mohr-Coulomb failure criterion. Includes beam elements for DSSI analyses

2.2 Previous DSSI Studies of the Control Tower at the Success Dam

This section presents a summary of available DSSI studies of the control tower at Success Dam. For each previous study the following information is presented: Type of analysis, geometry of the model, material properties, type of damping, seismic excitation used, etc.

2.2.1 Study by Cocco (2004)

Cocco (2004) in his MS thesis entitled “Evaluation of the Nonlinear Seismic Response of Intake and Control Towers with the Capacity Spectrum Method” presented detailed analyses for the control tower at Success Dam. The author found important differences between the base shear force values at the control tower obtained using his methodology and the results obtained by previous studies presented later in this chapter. The differences found were in the order of one order of magnitude. As mentioned before, this was one of the main motivations of this study.

Cocco (2004) used the Capacity Spectrum method to calculate the nonlinear seismic response of the control tower. In this study, the tower was modeled using beam elements and the seismic excitation was applied, either in the form of a response spectrum or an acceleration time history. The possible nonlinear behavior at the critical section (usually near the bottom of the tower) was accounted for by means of a nonlinear rotational spring. The moment-rotation relationship to define this spring was based on data obtained from a series of tests done by Dove (1998, 2000), and a formula proposed by Dove and Matheu (2003).

Cocco (2004) analyzed several towers obtaining reasonable results that compared well with more rigorous analytical models. For the particular case of the Success Dam, the Capacity Spectrum-beam model with nonlinear rotational spring procedure was used to analyze the embedded control tower. Cocco (2004) incorporated the soil effects for the embedded tower by means of discrete springs using the p-y curve formulation typically used for piles. The model used by Cocco (2004) is shown in Figure 2-1. The tower properties used are summarized in Table 2-2. The parameters used for the definition of the lateral springs with the p-y curves formulation proposed by Reese et al. (1974) are presented in Table 2-3.

The pseudo acceleration response spectra of the ground motions used are presented in Figure 2-2. The selection of the ground motions was similar to previous studies of the Success Dam. The ground motions were obtained using a modified record of the 1979 Imperial Valley Earthquake registered at El Centro, a record referenced as Joshua 1992, and a third record referenced as Landers 1992. This was consistent with previous seismic studies of this dam, and the modified records corresponded to the Maximum Credible Earthquake (MCE) with a Peak Ground Acceleration (PGA) of 0.28 g and duration of about 39 s.

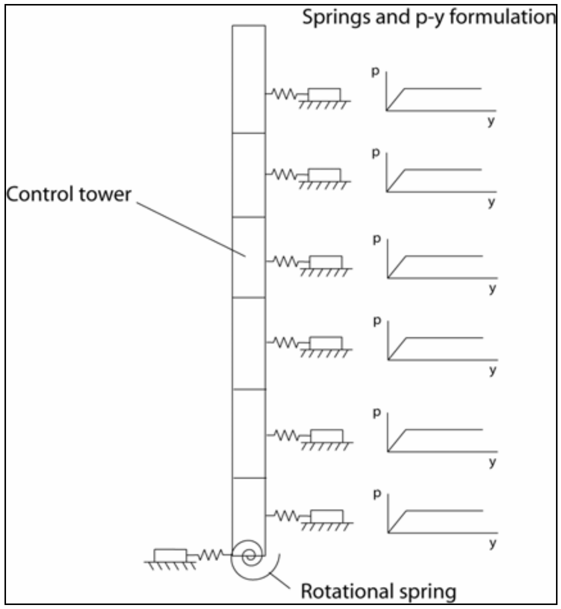

Figure 2-1 Model Used by Cocco (2004). Adapted from Cocco (2004)

Table 2-2 Cross Sectional Properties for Control Tower Used by Cocco (2004)

Section	Element Nº	Ix [ft^4]	A [ft^2]	L [ft]	Shear Factor
Base Section	20	594378.05	2989.39	8.00	1.20
1º Section	19	524490.55	2080.64	10.00	1.20
2º Section	18	564889.30	2800.64	9.00	1.20
3º Section	17	394705.35	1316.76	10.50	1.55
4º Section	16	332228.53	1039.50	9.25	1.70
	15	332228.53	1039.50	9.25	1.70
5º Section	14	223935.45	941.62	7.25	1.84
	13	223935.45	941.62	7.25	1.84
6º Section	12	55851.33	423.75	9.10	2.04
7º Section	11	40950.00	330.00	10.00	2.04
	10	40950.00	330.00	10.00	2.04
	9	40950.00	330.00	10.00	2.04
	8	40950.00	330.00	10.00	2.04

Table 2-2 Cross Sectional Properties for Control Tower Used by Cocco (2004)

Section	Element Nº	Ix [ft^4]	A [ft^2]	L [ft]	Shear Factor
	7	40950.00	330.00	10.00	2.04
	6	40950.00	330.00	10.00	2.04
	5	40950.00	330.00	9.90	2.04
8º Section	4	14876.06	98.84	10.00	1.97
	3	14876.06	98.84	10.00	1.97
	2	14876.06	98.84	12.00	1.97
Floor Slab	1	74477.50	930.00	0.83	1.20

Table 2-3 Parameters Used to Define the P-Y Curves by Cocco (2004)

Elev. [ft]	Depth z [ft]	Pult. [kips]	z/b	Coeff. As	Coeff. Bs	$E_{py\text{-}max}$ [kips]
620	10	94	0.33	2.559	2.000	2122.55
610	20	227	0.67	2.360	1.780	4245.10
600	30	398	1.00	2.075	1.542	6367.65
590	40	606	1.33	1.847	1.390	8490.20
580	50	853	1.67	1.637	1.237	10612.75
570	60	1139	2.00	1.458	1.068	12735.30
560	70	1462	2.33	1.322	0.931	14857.85
550	80	1823	2.67	1.163	0.810	16980.41

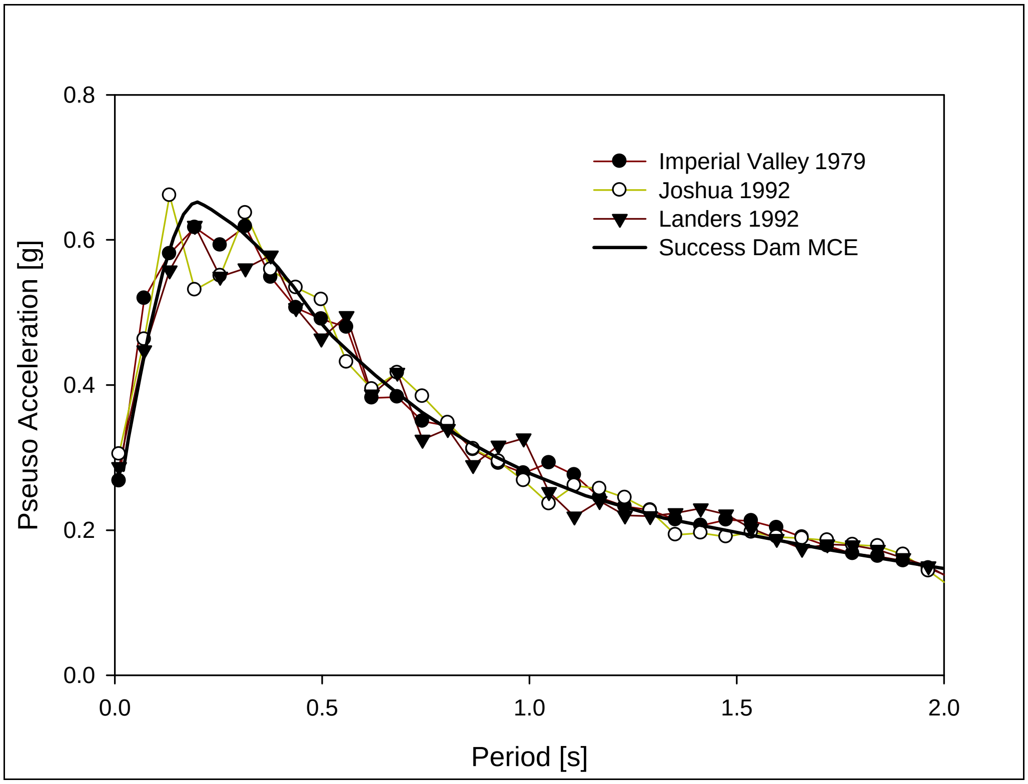

Figure 2-2 Pseudo Acceleration Response Spectra of the Input Ground Motion Used by Cocco (2004)

A careful revision of the procedure and the results obtained with the capacity spectrum method did not reveal any apparent problem. To further investigate this discrepancy in results, Cocco (2004) performed a linear elastic finite element analysis using the program SAP2000. (Computers & Structures 2002). The dam was modeled with plane strain elements and the embedded tower with frame elements. Due to the limitations of the program for this type of model, a linear analysis was performed. However, the author performed a sensitivity analysis of the most important elastic properties. The results obtained with this approach were of a similar order of magnitude to those from the capacity spectrum method under equivalent conditions. In other words, both sets of analyses by Cocco (2004) yielded basal shear forces and bending moments for the control tower that were similar in magnitude. A summary of the maximum basal reactions obtained in this study are presented in Table 2-4.

Table 2-4 Summary of Results Obtained by Cocco (2004)

Analysis Case	Soil Behavior	Maximum Base Force [kN]
CSM [1] Tower: Linear Behavior	P-Y formulation	16663
CSM Tower: Linear Behavior	None	17993
Multimodal CSM Tower: Non-Linear Behavior	P-Y formulation	14466
Multimodal CSM Tower: Non-Linear Behavior	None	12557
Multimodal CSM Tower: Non-Linear Behavior. Second critical section	P-Y formulation	14176
Multimodal CSM Tower: Non-Linear. Behavior. Second critical section	None	11263
FEM[2] - SAP2000 – Imperial valley 1979 earthquake v = 0.45	Linear	14039
FEM - SAP2000 – Joshua 1992 earthquake Poisson's ratio *v* = 0.45	Linear	12117
FEM - SAP2000 – Landers 1992 earthquake Poisson's ratio *v* = 0.45	Linear	13296
FEM - SAP2000 – Imperial valley 1979 earthquake Poisson's ratio v = 0.30	Linear	11813

Notes: (1) CSM: Capacity Spectrum Method
(2) FEM: Finite Element Method

Additional details about this study can be found in Cocco (2004), Suarez et al. (2004), and Cocco et al. (2005).

2.2.2 Study by CSI (1981)

In 1981, the company Civil Systems Inc. (CSI) presented the report Dynamic Analysis of Structures at Success Dam (CSI 1981). This study involved using a 2D plane strain model of the dam. CSI analyzed the cross section of the dam across the control tower and used the computer code SuperFLUSH which is reported as being a modified version of the code FLUSH (Lysmer et al. 1975). It is important to note that CSI (1981) modeled the tower using solid plane strain elements instead of structural elements or a single beam element. Hence, the properties of the tower elements were calibrated to account for this simplification. This study used modified mass and shear modulus values to account for the effective area of each plane strain element. Figure 2-3 presents the finite element model used by CSI (1981).

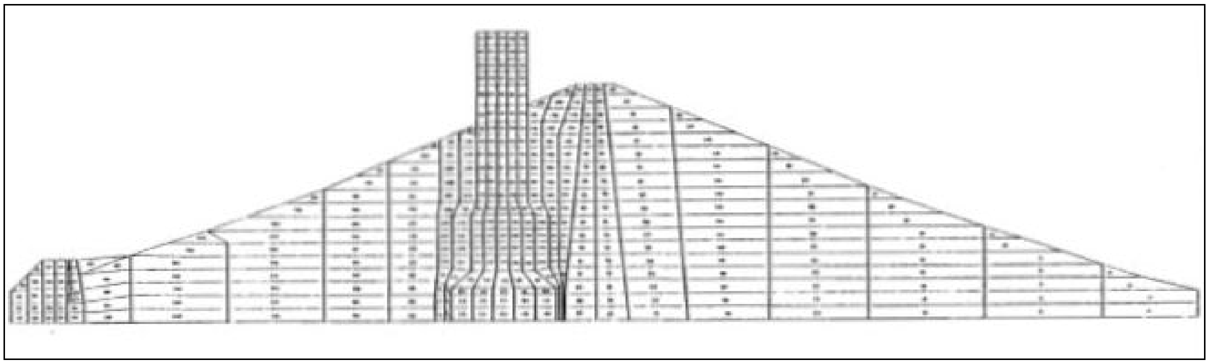

Figure 2-3 Finite Element Model Used by CSI (1981). Adapted from CSI (1981)

The seismic excitation used in this study was a modified outcropping Taft Record which was reported as being provided to CSI by USACOE. The report indicates that this record was deconvoluted to convert it to an equivalent incropping ground motion. Figure 2-4 shows the pseudo acceleration response spectra used for the analyses. For comparison purposes, Figure 2-4 also shows the spectra corresponding to the MCE at the site, which was used by Cocco (2004).

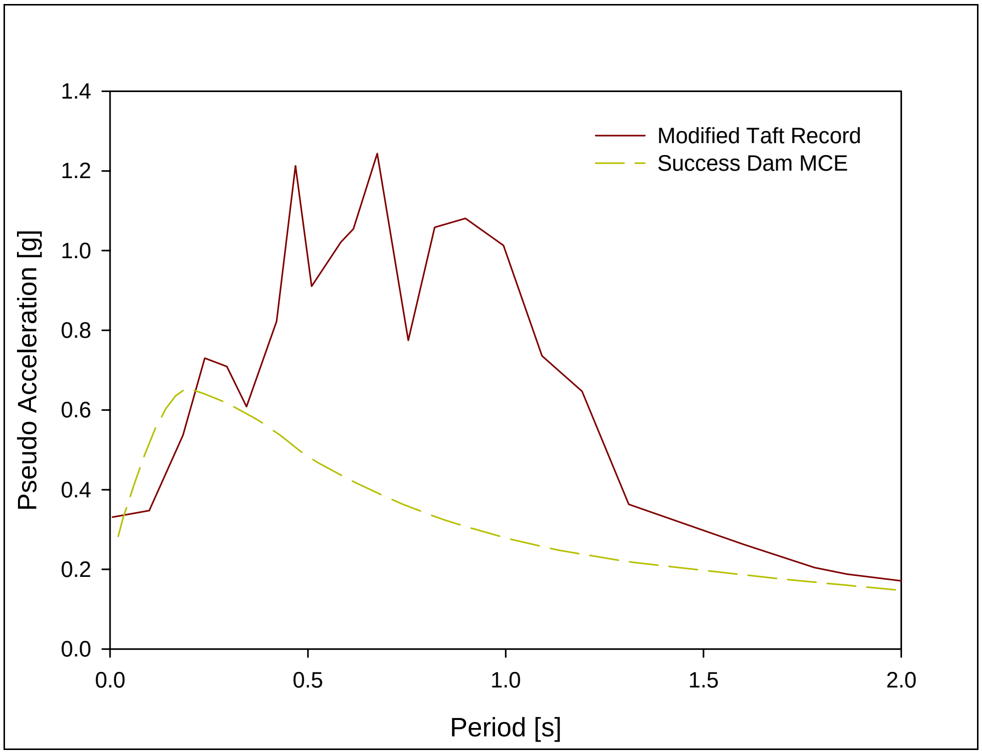

Figure 2-4 Input Motion Used by CSI (1981)

The material properties used to model the dam were reported as being based on geophysical tests gathered by CSI. The CSI report indicates the following correlation for the maximum shear modulus was found to agree well with the geophysical test results:

$$G\max[ksf] = 80\sqrt{\sigma'[psf]}$$

CSI (1981) estimated a maximum shear force and bending moment at the base of the control tower of about 244.6 MN (55000 kips), and 2.71 GN-m (24000000 kip-in), respectively.

2.3 USACOE (2004) Workshop

A screening workshop was held in Sacramento, CA by the USACOE in 2004. This workshop provided the participants with an information packet which included useful information as: detailed cross sections of the dam, detailed location of geologic units for comparison with geophysical reports, and detailed structural drawings of the control structures of the dam. Figure 2-5 presents an image of the type of information available in this unpublished information packet.

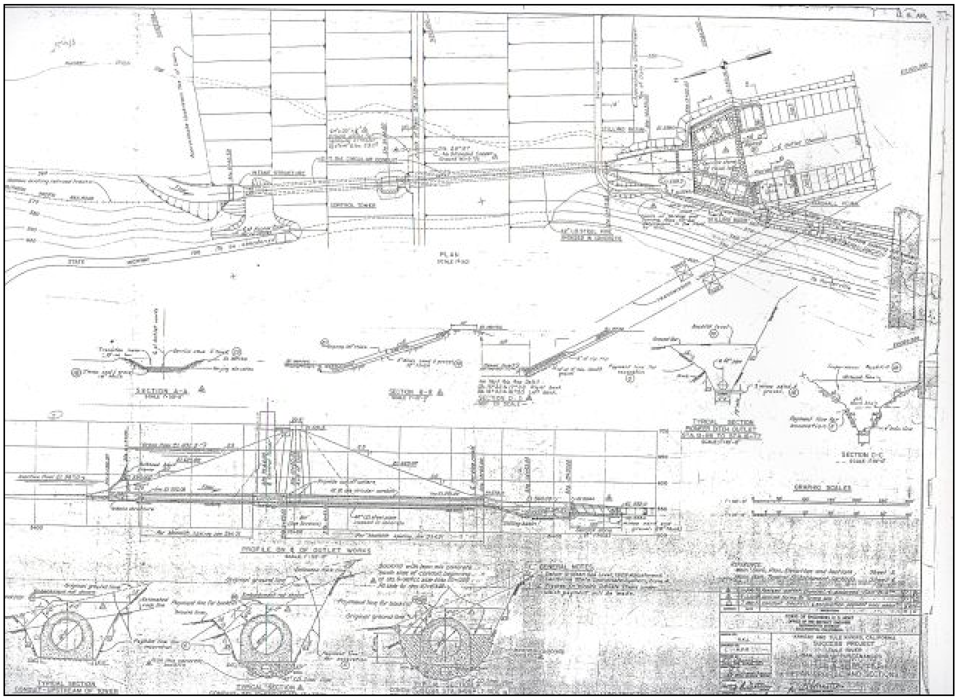

Figure 2-5 Example of the As-Built Drawings for the Success Dam, USACOE (2004)

This unpublished document was instrumental for the preparation of the numerical models of this thesis.

2.4 Geophysical Study Llopis et al. (1997)

Llopis et al. (1997) present characterization studies for the Success Dam. Shear wave velocity profiles were obtained for the Success Dam using geophysical tests. The location of the boreholes used for the tests are shown in Figure 2-6. These boring sets were used for crosshole S-wave testing, surface compression-wave (P-wave) testing, S-wave refraction testing, and/or borehole geophysical logging.

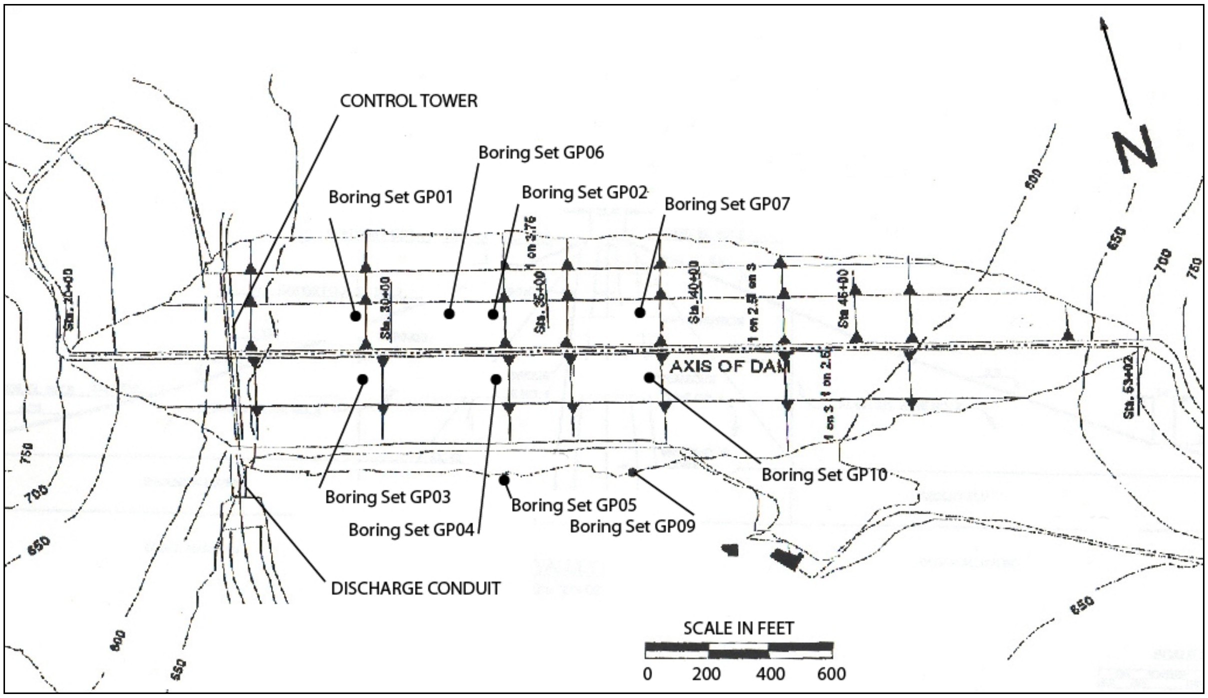

Figure 2-6 Location of Boring Sets. Adapted from Llopis et al. (1997)

Figure 2-7 presents the shear wave velocity profiles obtained by Llopis et al. (1997). The boring sets named GP01 and GP03 are the closest sets to the control tower dam section, and therefore are used to estimate the dynamic soil properties for dam model. It is important to mention that the deeper segment of the GP01 boring set reached the Saprolite geological unit. However, based on the available geotechnical data and as-built drawings, at the location of the control tower and discharge conduit this Saprolite unit is believed to be absent. Therefore, the data gathered from this boring set represents only the upstream shell of the dam body, meanwhile the data from boring GP03 is believed to better represent the downstream shell and up to some extent the foundation of the dam. This means that the rock in which the discharge conduit and tower are founded has higher shear wave velocity values than the highest reported value for the GP03 boring set.

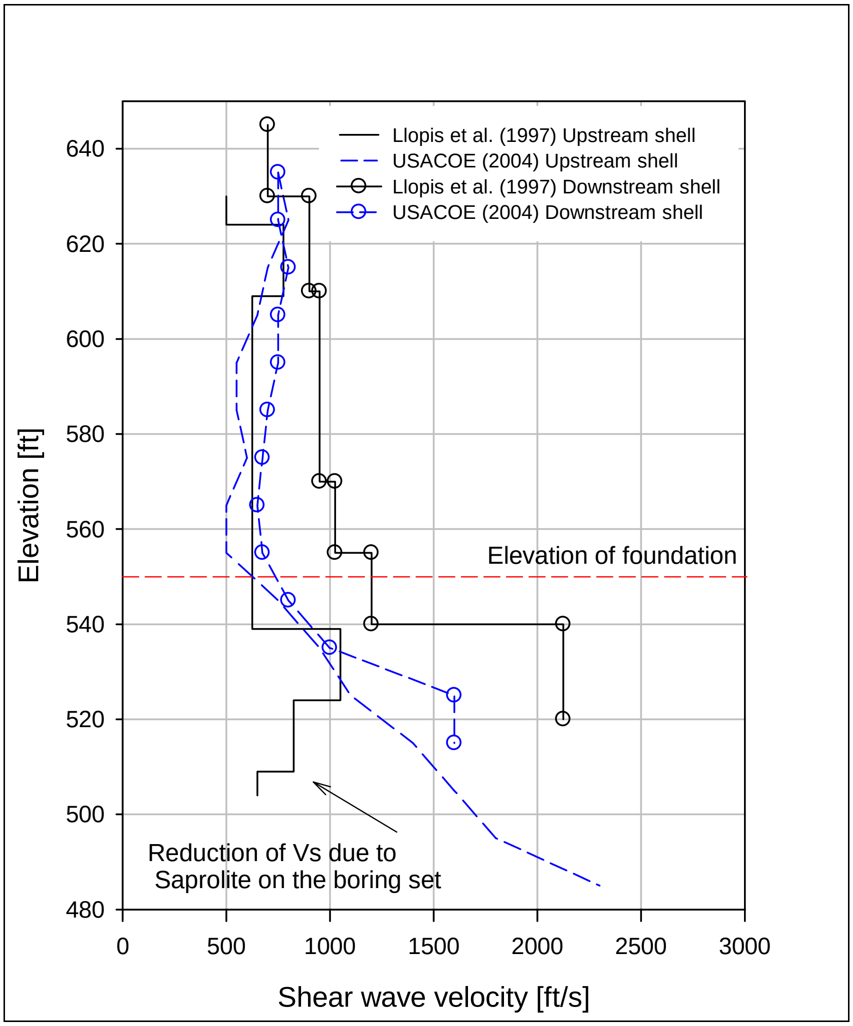

Figure 2-7 Shear Wave Velocity Profiles

3 DESCRIPTION OF THE SUCCESS DAM PROJECT

The Success Dam is a zoned earthfill dam with an approximate length of 3400 ft and a maximum height of 145 ft. The dam has a central impervious core and outer shells made with sand and rock mixtures. The upstream shell has a 3H:1V average slope, while the downstream shell slopes at 2.75H:1V. The dam was built in 1961 and is located near Sacramento, CA. This dam has been subject of several studies and is currently being considered for a mayor seismic retrofit due to stability concerns.

This chapter presents a summary of the most relevant information regarding the Success Dam. However, this is presented with particular emphasis to the area near the control tower which is the central theme of this thesis.

3.1 General Location of Success Dam

The Success Dam is located about 5 miles east of the town of Porterville in Tulare County near Sacramento, California. The dam reservoir is named Lake Success, and it is located on the Tule River. The Lake Success is a reservoir serving as recreation, irrigation, and flood control for the adjacent areas. The Success Dam is operated by the Sacramento District of the U.S. Army Corps of Engineers. The dam has geographical coordinates 36.0 º latitude and 118.9 º longitude.

The general location map for the Success Dam is shown in Figure 3-1. A plan view of the Success Dam showing the location of the control tower and the discharge conduit is shown in Figure 3-2.

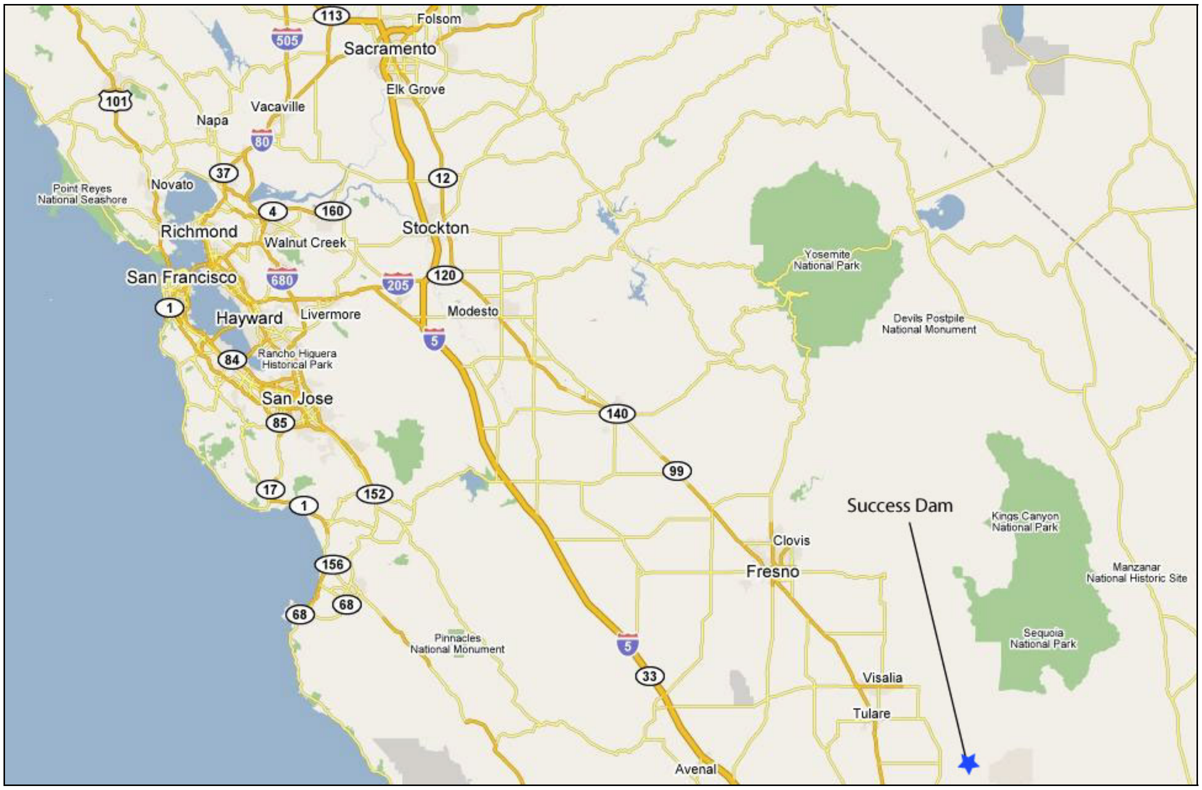

Figure 3-1 Location of Success Dam. Modified after Google – Map Data (2006), NAVTEQ (2006)

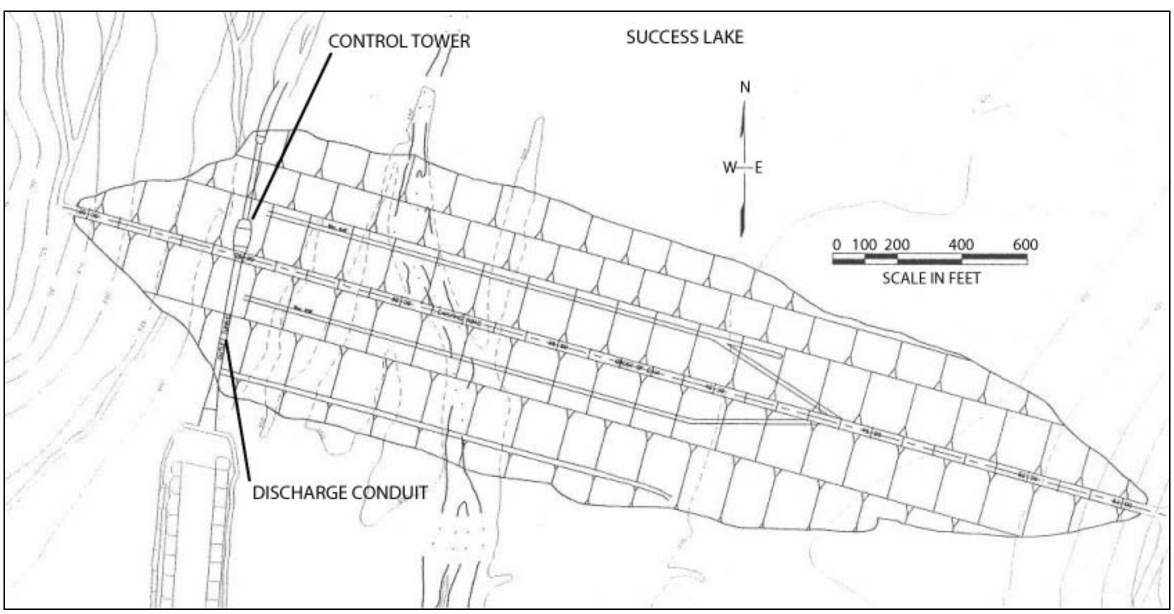

Figure 3-2 Location of the Control Tower, and the Discharge Conduit. Adapted from Llopis et al. (1997)

This dam is 3404 ft long and at its highest point has a height of 145 ft. The dam is an earthfill embankment with a central impervious core and outer pervious shells. The average upstream slope is 3H:1V and the average downstream slope is 2.75H:1V. The dam was built between 1958 and 1961.

3.2 Site Seismicity

According to USACOE (2006), the primary active faults within a 100 miles radius from the dam site are:

- Premier Fault: Closest distance to Success dam site is 13 miles, and it is believed to produce a Maximum Credible Earthquake (MCE) with a magnitude of 6.75 and Peak Ground Acceleration (PGA) of 0.28 g.

- San Andreas Fault: Closest distance to Success dam site is 72 miles, and it is believed to produce an Operating Basis Earthquake (OBE) with a magnitude of 8.0 and PGA of 0.1 g.

- Owens Valley Fault: Closest distance to Success dam site is 52 miles, and it is believed to produce an earthquake of magnitude 7.6.

- White Wolf Fault: Closest distance to Success dam site is 57 miles, and it is believed to produce an earthquake of magnitude 7.5.

3.3 Site Geology

The information related to the geology of the dam site was obtained from USACOE (2004). According to this reference, there are six geologic units present in the Success Dam footprint. These units are shown in Figure 3-3.

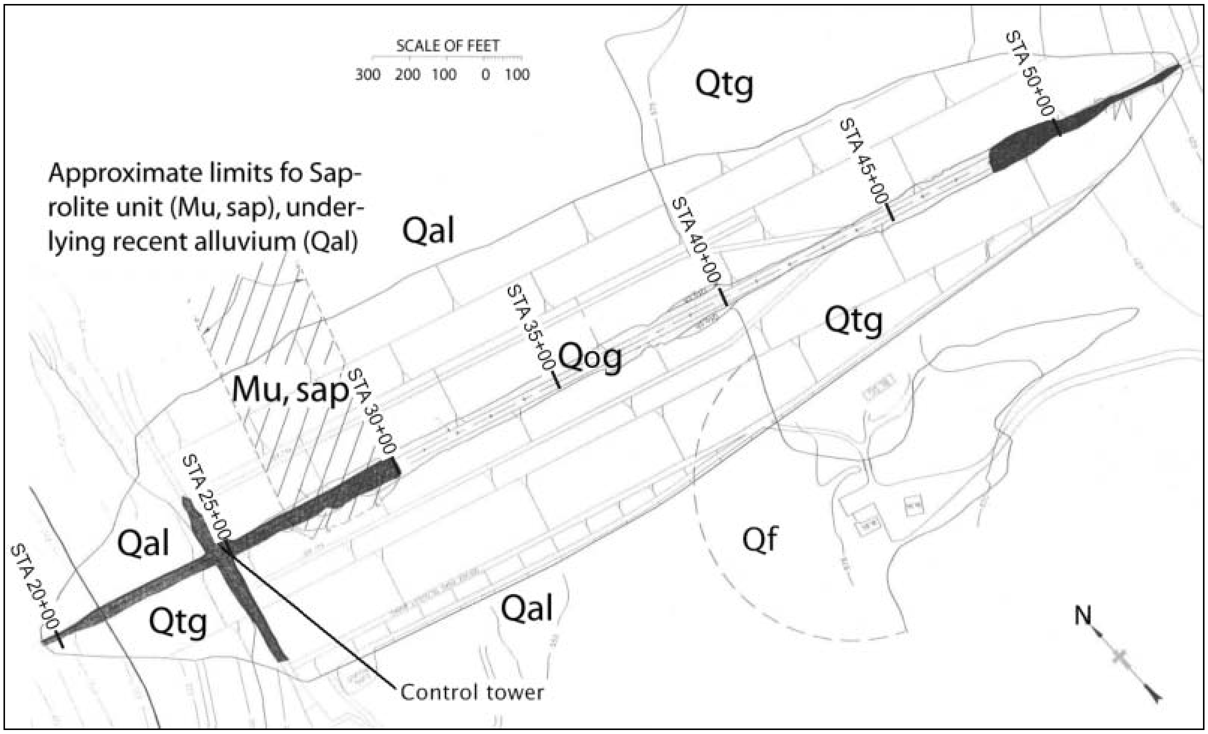

Figure 3-3 Geologic Units at Success Dam. Adapted from USACOE (2004)

USACOE (2004) describes the six geological units present at the Success Dam site as follows:

- Recent Alluvium (Qal): This unit consists of a Quaternary Alluvium. The dam is overlying this Quaternary Alluvium in almost 50% of the dam footprint. It is localized between the dam axis stations 26+00 and 40+00, with a thickness between 17 and 24 ft. The soil materials of this unit are mostly unconsolidated, loose, totally uncemented, and unweathered. The stratum is composed by interbedded sands, silts, and sandy gravels with presence of cobbles and boulders. Silt sizes are rare, except in the upper sandy portion of the deposit. The sand is medium to fine grained, and the rock sizes vary from 2 inches to 3 feet.

- Alluvial Fan (Qf): This geologic unit is only present in a small portion of the dam footprint located on the east side of the dam (opposite side of the control tower). It is composed by sediments from a stream on the east abutment which impinges on the valley. The sediments in this unit were formed by weathering of the bedrock and erosion of a terrace deposit located over the east abutment. This stratum is composed primarily by moderately consolidated clayey sands, overlying clayey gravels.

- Older Alluvium (Qog): This unit underlies the Qal deposits in most of its extent, and underlies the terrace deposits on the left abutment. It is described as a heterogeneous blend of river deposit silts, clays, sands, gravels, cobbles, and boulders. It was reported as being found below the ground water table before the construction of the dam, and is described as being composed by generally well consolidated, unoxidized, moderately to very intensely weathered, locally cemented by calcium and/or gypsum.

- Terrace Deposits (Qtg): The origin, age, and mode of deposition is the same of the Qog, and differ in the exposition to weathering conditions, since the Terrace deposits did not lie below the water table, and therefore, the terrace deposits are usually pervious and reddish brown to yellow brown. The soils are poorly cemented to uncemented. Within the terrace deposits it was possible to establish that the clay fraction was removed by percolated water and water fluctuations, leaving gravel and cobble sizes ranging from 0.5 to 5 inches in diameter.

- Saprolite Soil (Mu, sap): This soil is derived from the complete weathering of the bedrock Mu (Ultramafic plutonic rocks - Mesozoic). This unit underlies the upstream section of the dam between the dam axis stations 27+00 to 30+00. This unit is located approximately 220 ft east from the tower and water conduit. The stratum is cohesive, and is described as being high to medium plastic.

- Bedrock (Mu): This unit consists of an ultramafic plutonic rock from the Mesozoic period. This rock yielded to the Saprolite unit (Mu, sap) after complete weathering.

Using these geological units, the USACOE (2004) report presents geologic cross sections of the dam foundation. The locations of the two cross sections are shown in Figure 3-4.

The upstream geologic cross section (Section A-A) is shown in Figure 3-5. The figure shows the dam rests on young alluvium (Qal composed of interbedded sands and silts, and sandy gravels) underlain by a thin layer of older alluvium (Qog composed of heterogeneous river deposits of silts, clays, sands, and gravels), underlain by bedrock (Mu). Between stations 27+20 and 29+60 the dam foundation has a Saprolite unit (MU, sap) which is composed of weathered Mu bedrock. The control tower is outside the range of this figure since it is located at station 24+80.

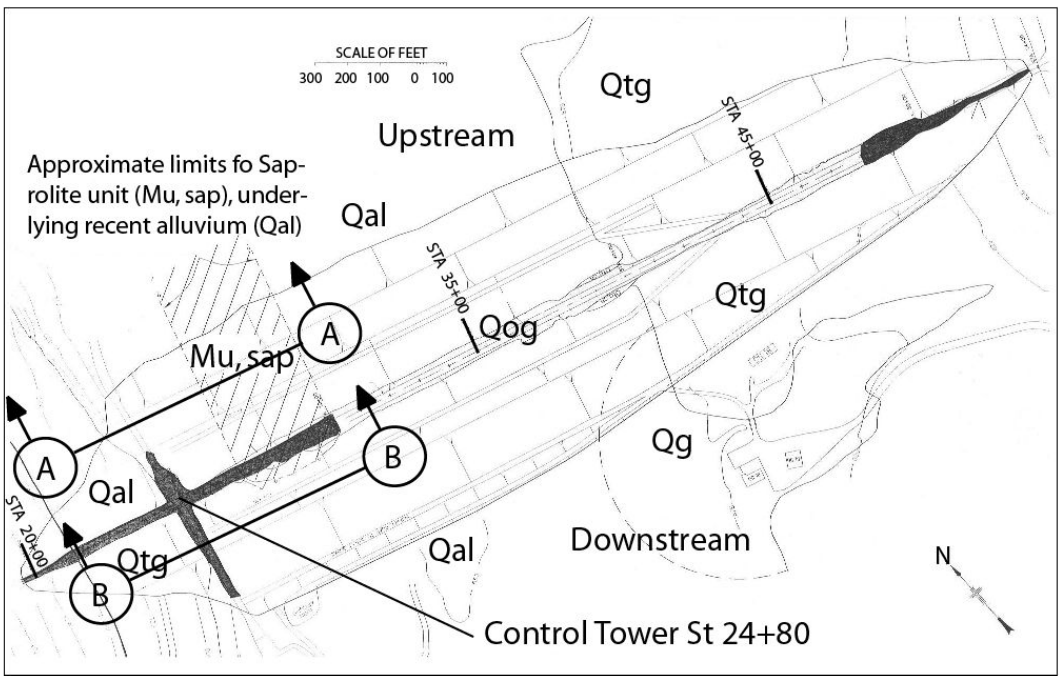

Figure 3-4 Location of Geologic Sections. Adapted from USACOE (2004)

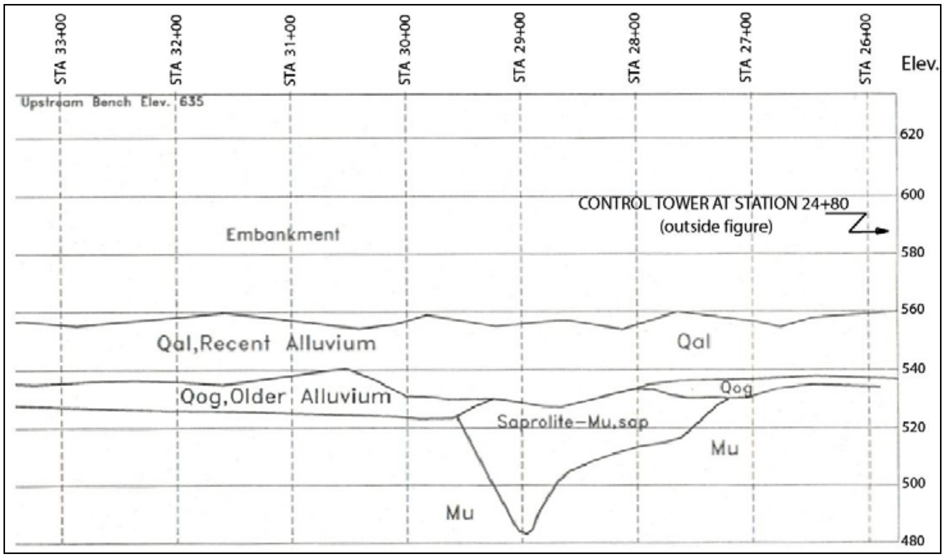

Figure 3-5 Upstream Geologic Section (A) Including Direction of the Outlet Works Location. Adapted from USACOE (2004)

The downstream geologic cross section (Section B-B) is shown in Figure 3-6. This cross section extends from about station 24+00 to 33+00, therefore includes the location of the control tower (Station 24+80). The geology of the foundation of this portion of the dam is similar to the one shown in Figure 3-5. However, this figure does not have the Saprolite unit.

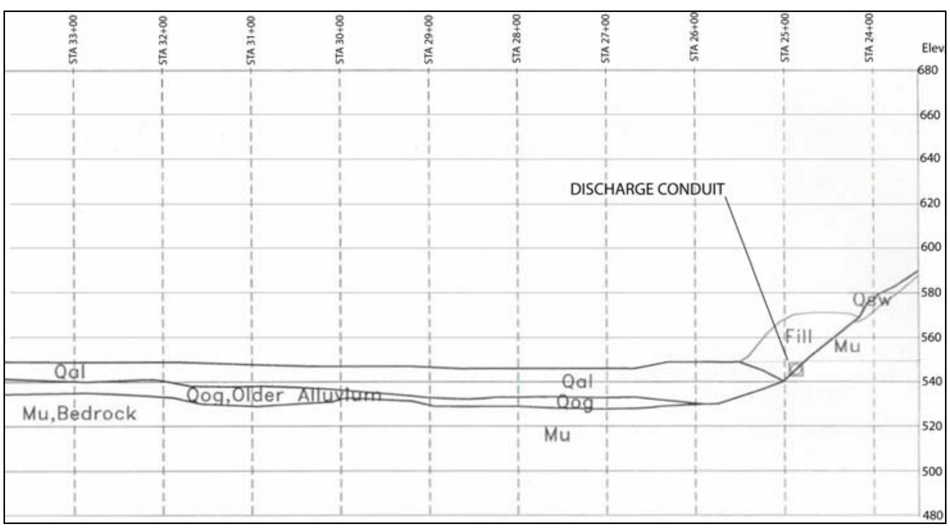

Figure 3-6 Downstream Geologic Section (B) Including Discharge Conduit Location. Adapted from USACOE (2004)

The criteria used to select the dynamic soil properties of the dam and the foundation units are presented in the following section.

3.4 Success Dam Cross Section

3.4.1 General Description

The Success Dam consists of a rolled earthfill dam composed of a central impervious core and outer pervious shells. A simplified cross section of the dam in the location of the control tower is shown in Figure 3-7.

At this location the dam is 144 feet high, the crest is 25 feet wide, and the side slopes have average inclinations of 3H:1V and 2.75H:1V on the upstream and downstream sides, respectively. The Figure 3-7 also shows the presence of transition zones. These zones are 12 feet thick and act as filters to protect the dam from piping and internal erosion. The foundation elevation at the control tower location is El. 548 feet and as described in the previous section is composed of recent and old alluvium (Qal, Qog) over plutonic bedrock (Mu).

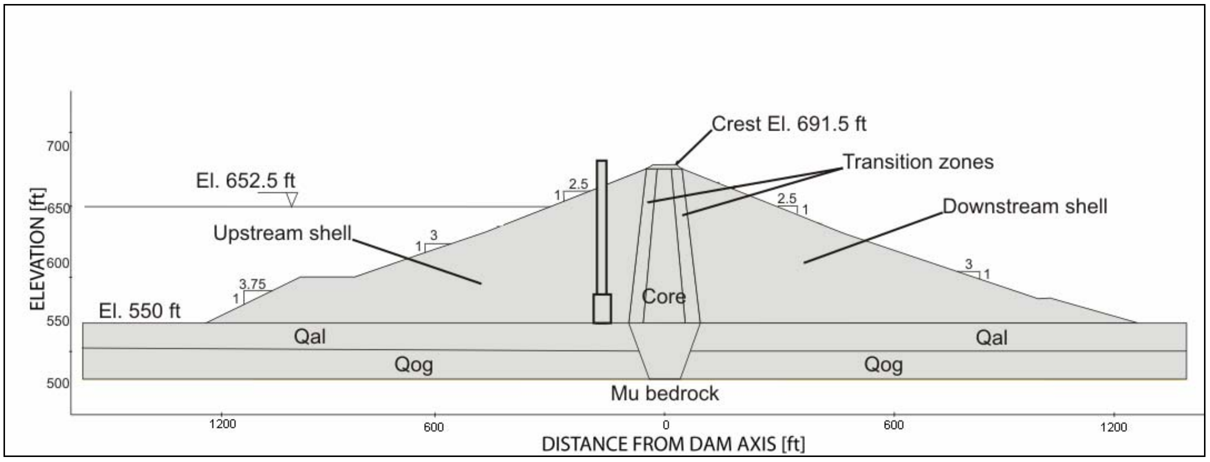

Figure 3-7 Zones in the Success Dam Cross Section

USACOE (2004) presents information about the design and construction materials used on the Success dam, and it is synthesized as follows.

The Success Dam has upstream and downstream shells, which are conformed of rock sizes ranging from 2 to 3 ft. These shells were built in layers and the main purpose is to provide upstream and downstream protection and stability. The inner section of the shells are mainly sand and rock sizes smaller than 12 inches in diameter, obtained from recent alluvium deposits less than half mile distance from the dam. The inner section of the shells was composed of gravelly sand or sandy gravel with sizes less than 12 in diameter size, and no more than 12% fine materials. The shells protecting the core of the dam were designed initially composed by 2 zones; nevertheless the USACOE (2004) indicates that no differences between the zones were found on post-construction field exploration.

The dam core was built with material consisting mainly of sandy clays and clayey sands obtained from an upstream source located about 1.5 miles from the dam. The core was constructed in 12 in lifts (loose state thickness), compacted using 4 passes of a 50 ton pneumatic-tired roller. 65% of the core material was placed at ± 5% of the optimum moisture content, 35% at 5-10% below the optimum moisture content, and 1% 5-7% above the optimum moisture content. A core trench was excavated to either weathered rock or older alluvium. A grout curtain was constructed to a depth of 75 ft between the stations 19+70 to 29+97, and 47+97 to 53+65. Then, the foundation was thoroughly cleaned by hand and high velocity air and water jets. Seventeen relief wells were installed along the downstream toe to provide relief of seepage pressure, and were replaced in 1999-2000 with a new system of 24 wells, an underground toe trench, and a surface collector trench.

There are transition zones between the core and the external shells. These materials consist of gravelly sands smaller than 6 in obtained from downstream deposits.

3.4.2 Geophysical and Geotechnical Information of Success Dam Cross Section

Geophysical tests were available from a location about 200 ft east from the control tower. The geophysical information gathered for this study is summarized in Figure 3-8. The main sources of information were the study by Llopis et al. (1997) and data presented in USACOE (2004). The data shown from Llopis et al (1997) is the closest to the control tower. This figure also shows the shear wave velocity profile chosen for the analyses carried out in this research project. It can be seen that the upstream shell was assigned shear wave velocity values ranging from 500 ft/s (152 m/s) to 750 ft/s (229 m/s). The downstream shell has shear wave velocity values ranging from 198 ft/s (198 m/s) to 1100 ft/s (335 m/s). Below Elevation 550 ft i.e. within the foundation soils, measured shear wave velocity values were as low as ~800 ft/s (corresponding to the Saprolite unit and as high as 1600 ft/s (corresponding to the old alluvium. As discussed before, the area near the control tower is reported as being free of the Saprolite unit; therefore a shear wave velocity value of 2160 ft/s (658 m/s) was assigned to the foundation soils for the numerical analysis of this thesis.

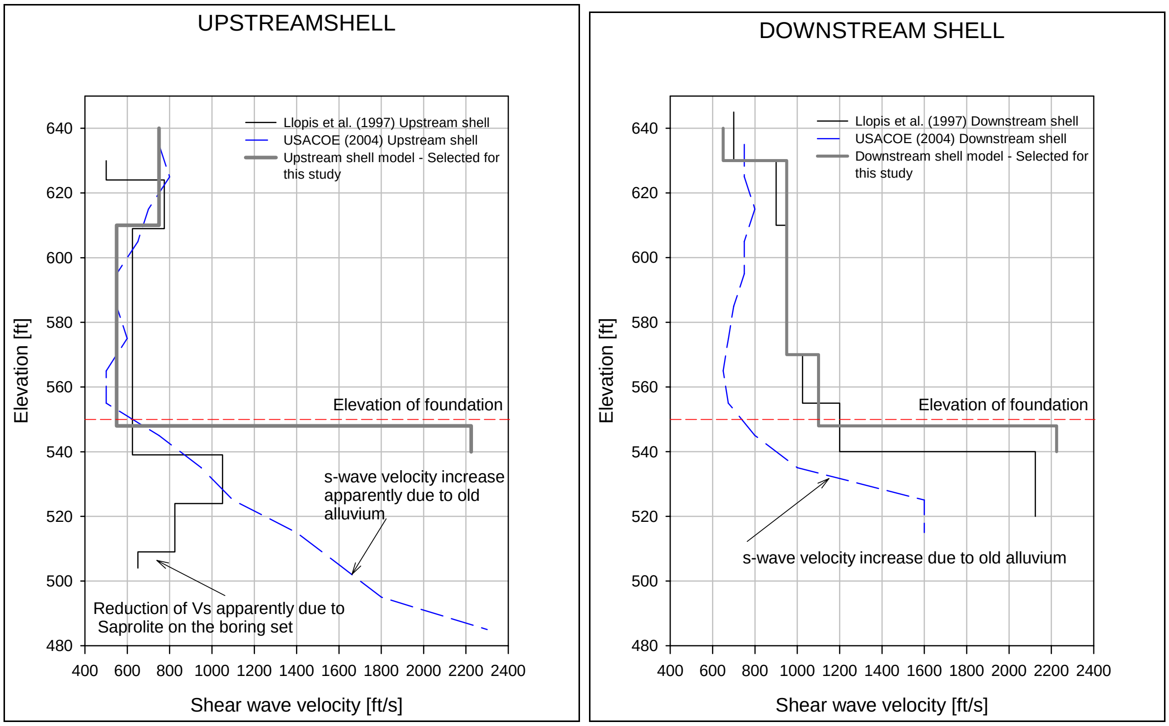

Figure 3-8 Shear Wave Profiles Close to the Control Tower Section

Some geophysical tests elevations below the discharge conduit, and based on the data gathered from these boreholes it was considered reasonable to establish that only the old alluvium on the foundation of the dam was tested, and that the underlying rock (Mu) must be stiffer than the alluvium.

As expected, differences on the dynamic soil properties were found to exist depending on the depth of the layer, as it was presented by Llopis et al. (1997). Important differences on the shear wave velocity profiles were found between the upstream and downstream shell, as can be observed on Figure 3-8.

4 TWO DIMENSIONAL DSSI ANALYSES

This chapter presents the dam modeling information including the definition of the soil and the structural properties used to generate the models, the seismic input used, and the points where the results are analyzed and compared.

4.1 Introduction

Three sets of two-dimensional models were developed to compare the results using two different methods, that is, the Finite Element Method (FEM) and the Explicit Finite Difference Method (EFDM). The first set of 2D models does not include any of the structures (control tower and discharge pipe). The second set of 2D models includes the control tower. The results of the analyses permit a direct comparison of the two methodologies, the FEM and EFDM.

The third set of models developed using the FEM includes the control tower and the intake pipe. By examining the dynamic properties and the seismic response, one can assess the importance of the intake conduit on the response of the dam and the control tower. The main characteristics of the two models are presented next.

4.2 Dam Modeling Information

The geotechnical and structural characteristics for the components of the dam cross section are presented in the following section.

4.2.1 Success Dam Materials and Foundation

The dynamic soil properties of a cross section of the Success Dam at the control tower location are defined based on the geophysical information presented in Section 3.4.2, and in available technical publications.

For easy interpretation of the dam parameters, Figure 4-1 presents the most relevant dynamic soil properties for the Success dam model.

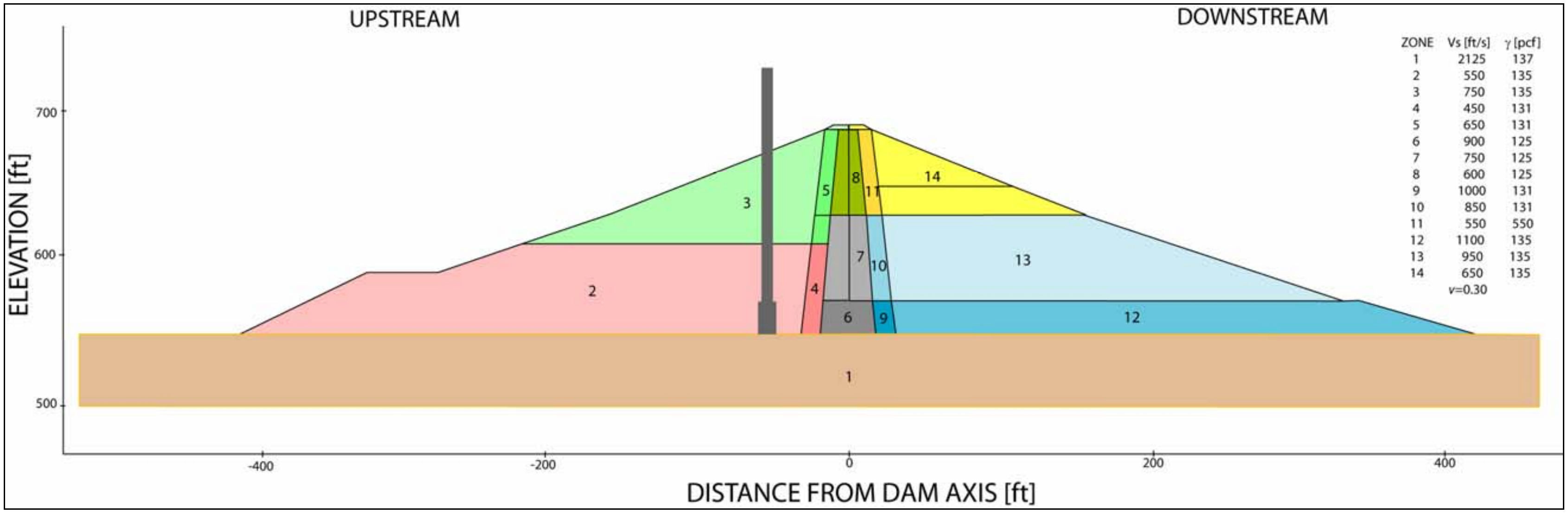

Figure 4-1 Typical 2D Model Showing the Dynamic Soil Properties at Low Shear Strain

The selected soil properties for the upstream and downstream shells required for all dynamic analyses are presented in Table 4-1 and Table 4-2, respectively.

Table 4-1 Dynamic Soil Properties of the Upstream Shell

Elevations	Parameter	Value	Units	Comments
691.5 to 610 ft	Vs	750	ft/s	After Llopis et al. (1997)
	Unit weight	135	lb/ft^3	Best estimate
	Poisson ratio	0.3	-	Estimated typical value
610 to 548 ft	Vs	550	ft/s	After Llopis et al. (1997)
	Unit weight	135	lb/ft^3	Best estimate
	Poisson ratio	0.3	-	Best estimate

Table 4-2 Dynamic Soil Properties of the Downstream Shell

Elevations	Parameter	Value	Units	Comments
691.5 to 630 ft	Vs	650	ft/s	After Llopis et al. (1997)
	Unit weight	135	lb/ft^3	Best estimate
	Poisson ratio	0.3	-	Best estimate
630 to 570 ft	Vs	950	ft/s	After Llopis et al. (1997)
	Unit weight	135	lb/ft^3	Best estimate
	Poisson ratio	0.3	-	Best estimate
570 to 548 ft	Vs	1100	ft/s	After Llopis et al. (1997)
	Unit weight	135	lb/ft^3	Best estimate
	Poisson ratio	0.3	-	Best estimate

The shear wave velocity for the foundation unit was established based on the highest shear wave velocity (about 2125 ft/s) measured by Llopis et al (1997). It is reasonable to expect that the actual shear wave velocity on the rock underlying the discharge conduit may be higher than this estimated value; nevertheless, the use of a reduced value is considered conservative. The complete set of dynamic properties used to model the foundation unit in the vicinity of the control tower section of the dam is presented in Table 4-3.

Table 4-3 Dynamic Rock Properties of the Foundation

Elevations	Parameter	Value	Units	Comments
691.5 to 610 ft	Vs	2160	ft/s	After Llopis et al. (1997)
	Unit weight	137	lb/ft^3	Best estimate
	Poisson ratio	0.3	-	Best estimate

The core of the dam is also protected by additional pervious zones, located immediately upstream and downstream of the core. Its purpose is to protect the clayey sandy material of the core from the clogging particles coming from the upstream shell and to prevent the washing out of the core materials into the downstream shell. No information the dynamic properties of these protective layers which act as filters was available. Nevertheless, based on the sources of materials mentioned in USACOE (2004), it is likely that they were built using similar, if not the same, sources of material. The dynamic properties for the transition zones were inferred from the closest geophysical boring sets presented by Llopis et al. (1997). The dynamic soil properties of the upstream and downstream transition zones are presented in Table 4-4 and

Table 4-5.

Table 4-4 Dynamic Soil Properties of the Upstream Protection Filter

Elevations	Parameter	Value	Units	Comments
691.5 to 610 ft	Vs	650	ft/s	After Llopis et al. (1997)
	Unit weight	131	lb/ft^3	Best estimate
	Poisson ratio	0.3	-	Best estimate
610 to 548 ft	Vs	450	ft/s	After Llopis et al. (1997)
	Unit weight	131	lbf/ft^3	Best estimate
	Poisson ratio	0.3	-	Best estimate

Table 4-5 Dynamic Soil Properties of the Downstream Protection Filter

Elevations	Parameter	Value	Units	Comments
691.5 to 630 ft	Vs	550	ft/s	Estimation based on Llopis et al. (1997)
	Unit weight	131	lb/ft^3	Best estimate
	Poisson ratio	0.3	-	Best estimate
630 to 570 ft	Vs	850	ft/s	Estimation based on Llopis et al. (1997)
	Unit weight	131	lb/ft^3	Best estimate
	Poisson ratio	0.3	-	Best estimate
570 to 548 ft	Vs	1000	ft/s	Estimation based on Llopis et al. (1997)
	Unit weight	131	lb/ft^3	Best estimate
	Poisson ratio	0.3	-	Best estimate

The core of the dam is reported as consisting of compacted sandy clays and clayey sands. Its dynamic soil properties were estimated based on the information available on the closest geophysical boring sets from Llopis et al. (1997). The estimated dynamic soil properties of the core are presented in Table 4-6.

Table 4-6 Dynamic Soil Properties of the Core

Elevations	Parameter	Value	Units	Comments
691.5 to 630 ft	Vs	600	ft/s	Estimation based on Llopis et al. (1997)
	Unit weight	125	lb/ft^3	Best estimate
	Poisson ratio	0.3	-	Best estimate
630 to 570 ft	Vs	750	ft/s	Estimation based on Llopis et al. (1997)
	Unit weight	125	lb/ft^3	Best estimate
	Poisson ratio	0.3	-	Best estimate
570 to 548 ft	Vs	900	ft/s	Estimation based on Llopis et al. (1997)
	Unit weight	125	lb/ft^3	Best estimate
	Poisson ratio	0.3	-	Best estimate

This section presented a summary of the dynamic properties selected or the analyses carried out in this project. The values were selected using the available information and best engineering judgment. However, a sensitivity analysis was also carried out to study the impact of varying the values of the dynamic properties of the different units of the dam.

4.2.2 Control Tower

The control tower of the Success dam consists of a reinforced concrete hollow structure with a height of 172.5 ft. Its top is at elevation 723.5 ft above the datum of the project, and it is located on the upstream face of the dam, at a distance of 56 ft from the dam axis (Figure 4-1). The tower holds the necessary mechanisms and equipment to control the flow of water through the discharge conduit.

The tower has a rectangular section with a suspended floor at elevation 691.5 ft. The sizes of the steel reinforcement bars range from 5/8 to 3/4 inches in diameter, typically spaced 12 in along each way, placed horizontally and vertically in each wall face. All reinforcement bars were specified with minimum yield strength of 40 ksi. The concrete has a specified 28 day compressive strength of 3000 psi.

The control tower structural properties used in the models of this research project were obtained from Cocco (2004). A summary of the structural and geometric properties of the control tower is presented in Table 4-7

Table 4-7 Structural and Geometric Parameters for the Control Tower

Section	Ix [ft^4]	A [ft^2]	Elevation [ft]
Floor Slab	74477.50	930.00	724.3
Section 8	14876.06	98.84	723.5
Section 7	40950.00	330.00	691.5
Section 6	55851.33	423.75	621.6
Section 5	223935.45	941.62	612.5

Table 4-7 Structural and Geometric Parameters for the Control Tower

Section	Ix [ft^4]	A [ft^2]	Elevation [ft]
Section 4	332228.53	1039.50	586.0
Section 3	394705.35	1316.76	579.5
Section 2	564889.30	2800.64	569.0
Section 1	524490.55	2080.64	560.0
Base Section	594378.05	2989.39	550.0

4.2.3 Intake-Discharge Conduit

A reinforced concrete conduit runs beneath the base the control tower and across the full width of the dam. This conduit allows the discharge of the reservoir. The nearly 600 ft conduit consists of a series of reinforced concrete segments with an internal diameter of 12 ft. The average wall thickness of the conduit is 3 ft. The conduit was built directly on the bottom of a trench excavated in competent bedrock. The upper half of the trench was filled with embankment materials.

The structural and geometric properties of the discharge conduit are presented in Table 4-8.

Table 4-8 Structural and Geometric Parameters of the Discharge Conduit

Parameter	Value	Units	Comment
Internal diameter	12	ft	From USACOE (2004)
Wall thickness	3	ft	From USACOE (2004)
Modulus of elasticity	3600	kip/in^2	Typical value for concrete
Poisson’s Ratio	0.2	-	Typical value for concrete
Unit weight	150	lb/ft^3	Typical value for concrete

4.2.4 Seismic Input

The seismic input selected for the DSSI analyses of this project is a modified record of the 1979 Imperial Valley earthquake, registered at El Centro, 230 degree component, measured at time increments of 0.02 s, and scaled to 0.28 g. This record corresponds to the Maximum Credible Earthquake (MCE) for the Success dam (84^{th} percentile). As discussed is Section 3.2, the MCE source is presumed to be related to the Premier Fault, with an estimated Mw of 6.75 and a PGA of 0.28 g at a distance of 13 km.

The selection of this acceleration time history is consistent with the previous seismic study carried out by CSI (1981). It was also used as one of the seed records to target the uniform hazard spectrum (PGA = 0.28 g) for the Success dam in the study performed by Cocco (2004) with a duration of 39.12 s. It is also understood that this accelerogram was used in a preliminary study conducted by a private consultant in California using the computer program FLAC2D (unpublished report).

A baseline correction was applied to the seismic record in this study to achieve a zero final displacement at the end of the seismic input. The time histories of displacement before and after the baseline correction are presented in Figure 4-2. The corrected acceleration time history is presented in Figure 4-3, and the pseudo acceleration response spectra before and after the baseline correction are presented in Figure 4-4. The two response spectra are also compared in the same figure with the uniform hazard spectrum for the Success Dam site.

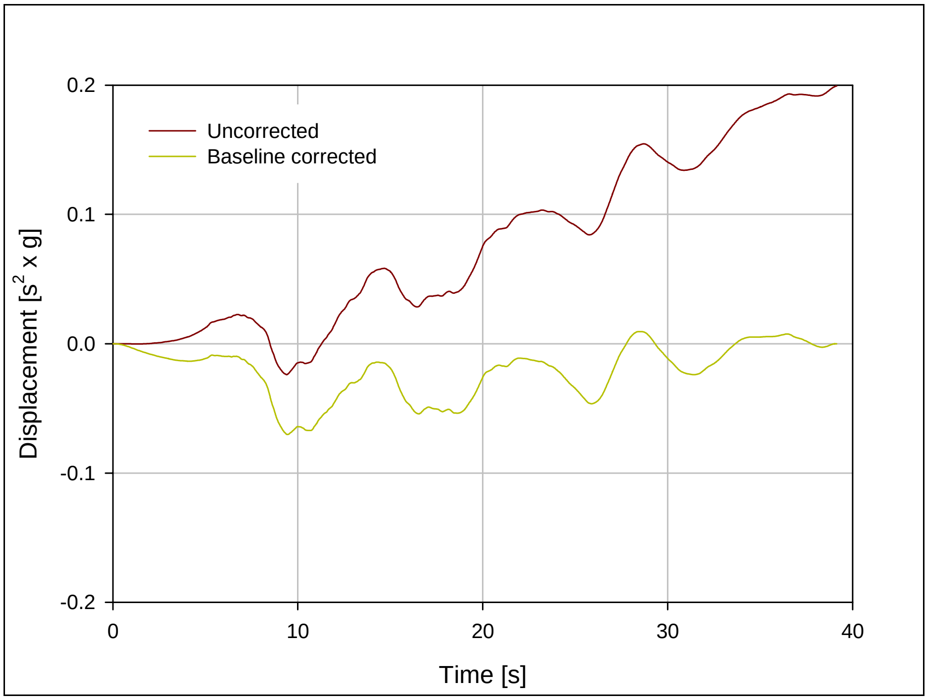

Figure 4-2 Time history of displacements of the Seismic Input before and after baseline correction

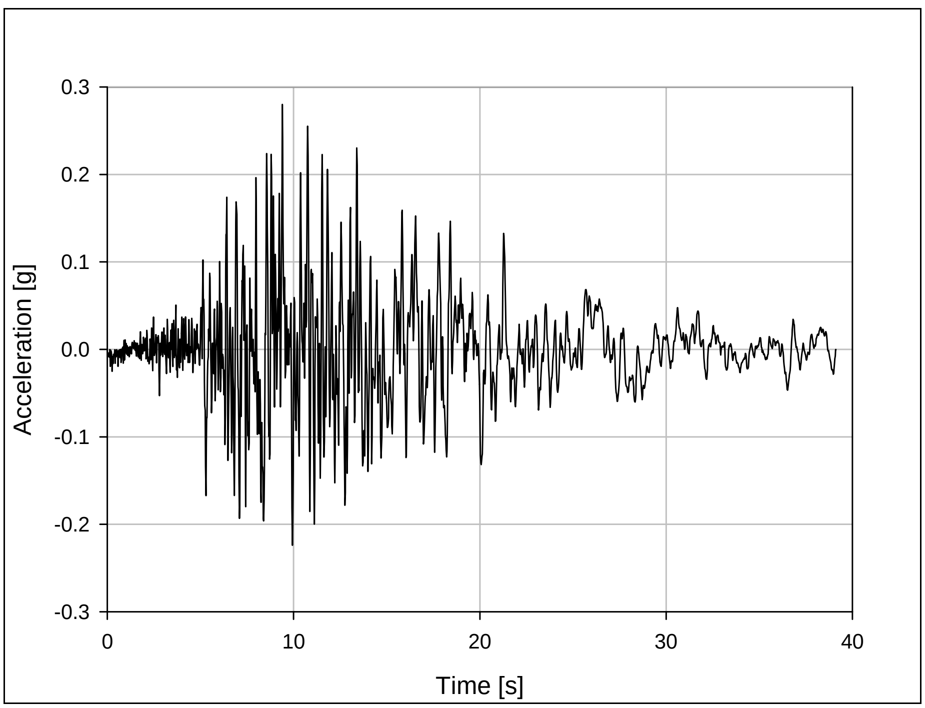

Figure 4-3 Modified 1979 Imperial Valley Earthquake Record Used as Seismic Input

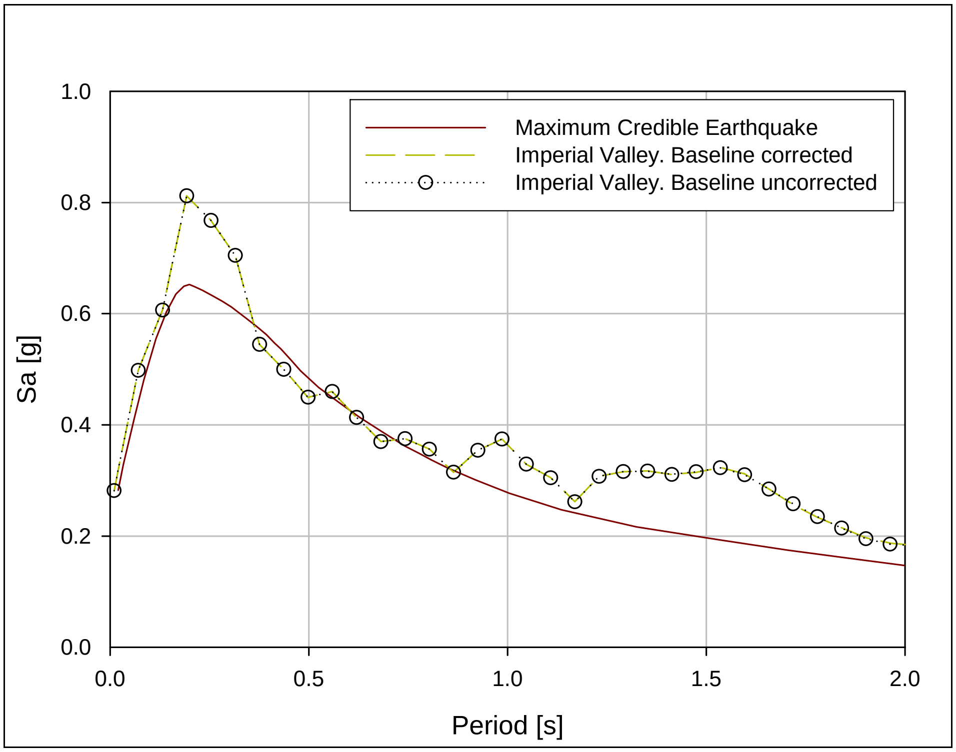

Figure 4-4 Response Spectra of the MCE and Imperial Valley Record

It can be seen from Figure 4-4 that the baseline correction practically does not modify the response spectra, and hence the use of the baseline corrected accelerogram is consistent with the spectra used in previous studies.

4.2.5 Points of Analysis

Seven points are used to report and compare the results obtained with the different models. The points were selected to facilitate the comparison with the results from previous studies, their future use in structural analyses of the control tower, and for its significance for the seismic analysis of the dam. Figure 4-5 presents the location of the points used in the analysis along with its identification.

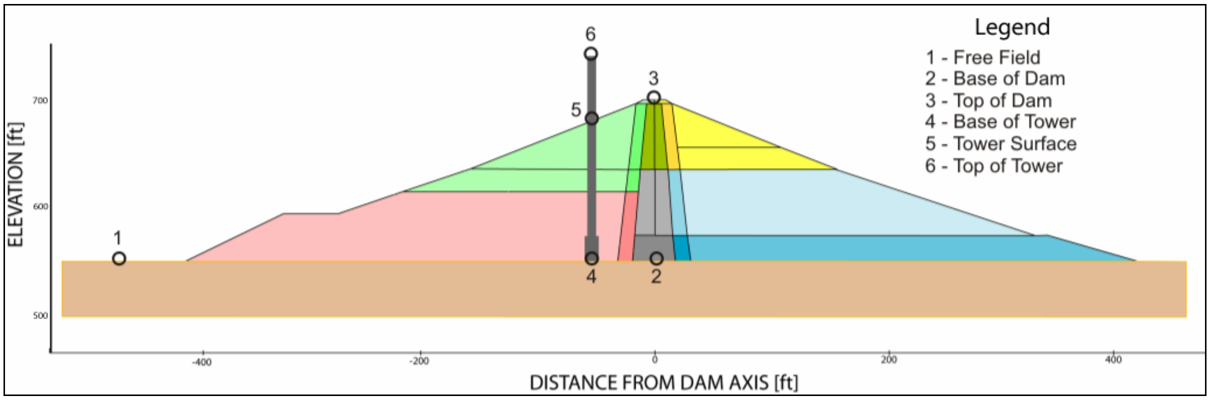

Figure 4-5 Control Points for Comparison of Results

4.3 General Description of the FEM Methodology – SAP2000

The numerical background of the finite element method is a well known subject in engineering, and thus details about the technical background will not be presented herein. Nevertheless, the criteria followed in the definition of the model are presented next.

The geotechnical material zones in the cross section of the dam are defined in the typical cross section described in Chapter 3. By doing so, all the models developed in this study will be consistent among them. Consistency with previous studies was also attempted when preparing the models. The depth of the foundation in the model was chosen based on the available geophysical information. The extension of the model in the horizontal directions was selected trying to minimize end effected but constrained by limitations of the computation time required by the EFDM solutions. For consistency of results, the FEM models were developed using the same horizontal extension. The geotechnical properties of the materials were presented in the previous chapter. Figure 4-6 shows the FEM model and the geotechnical zones used for the analyses.

The boundary conditions used are:

- 2 degrees of freedom at the base of the model are fixed. The seismic input was applied along the nodes of the base as an acceleration time history in the horizontal direction.

- The motion of the side nodes was only restrained in the vertical direction.

- All nodes had the displacements restrained in the out-of-plane direction.

- The rotations around the horizontal and vertical axes were restrained at all nodes.

- The FEM models in SAP2000 used a Rayleigh damping formulation to account for the material damping defined as a 5% of critical damping ratio.

The models were analyzed in two stages. The first stage consisted of a static analysis in which only the gravitational forces were applied. Once this first stage was completed, the displacements and strains were reinitialized to zero, while the stresses were kept and not modified. This first stage allowed the computation of the initial stress state in the model.

In the second stage, after the static solution was saved and the initial stress state computed, the seismic input was applied at the base of the model.

The FEM model had the following characteristics:

- 610 shell elements

- 674 nodes

- 11 types of geotechnical materials

- Time step 0.02 s

- Damping formulation: Rayleigh method. Critical damping ratio = 5% at the response in the first natural period.

- Integration method: Newmark with gamma = 0.5 and beta = 0.25, also called the trapezoidal rule. This method averages the acceleration in the time step.

A modal analysis was performed only to evaluate the fundamental periods corresponding to the first five vibration modes.

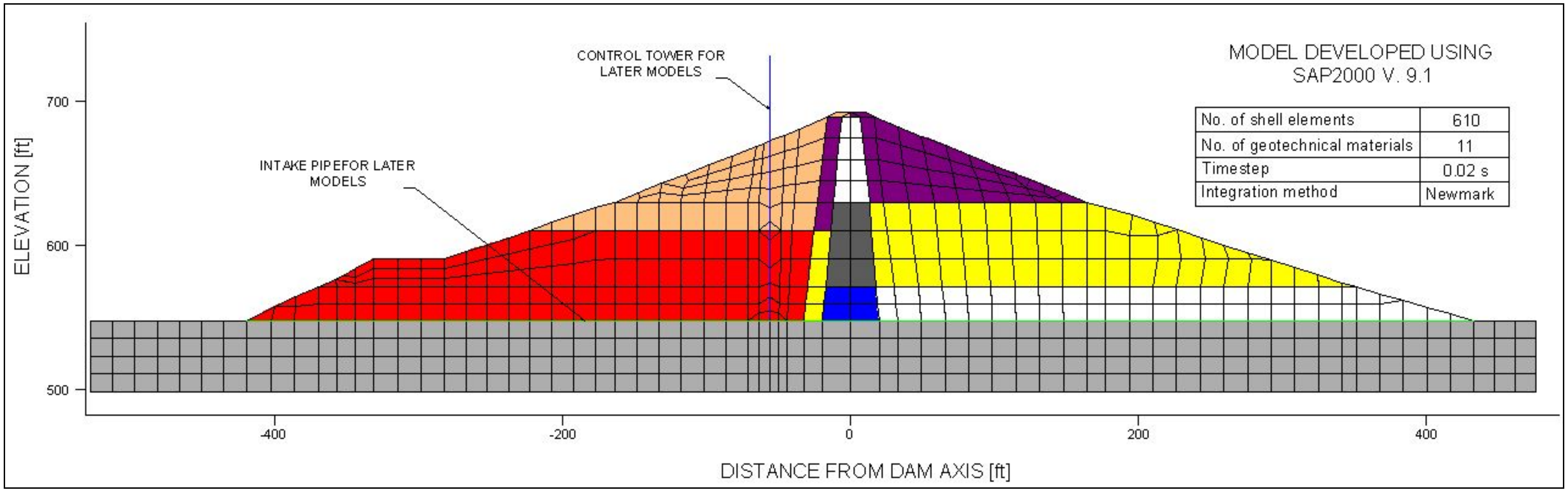

Figure 4-6 Typical Mesh Used for DSSI Analyses Using the Finite Element Method

Note: The seismic input was applied at the nodes along the base of the model

4.4 General Description of the EFDM Methodology – FLAC2D

The background behind the explicit finite difference method (EDFM) is a well known subject in engineering, and therefore it is not presented herein. Details about the numerical background behind the program FLAC2D can be found in Itasca (2000). This section provides details regarding the criteria used to define the model.

The zones with different geotechnical materials defined in the dam cross section are the same as those used in the FEM models. This allows for a direct comparison of the results obtained with the FEM and the EFDM. The depth of the foundation of the model was chosen based on the available geophysical information. The same horizontal extension used in EFDM was used for FEM models. For a model of the dam without the tower and the conduit structures was about 24 hours in a personal computer running an Intel Pentium 4 processor at 2.2GHz, with 2 GB of RAM memory. Including the concrete structures can rise the computation time to 72 hours. The geotechnical properties of the materials were presented chapter 3. Figure 4-7 shows the geometry of the EFDM model and the geotechnical zones used for the analyses. The soils were assumed to not develop important stiffness losses due to dynamic pore pressure generation, and liquefaction analysis was not considered.

The discretization process for this model was developed using the grid generation algorithm included in the computer program FLAC. The size of the side of the squared shaped zones was 1 m. Figure 4-7 presents a mesh of a EFDM model used. The mesh size shown in this figure is larger than the actual size used which was twice as fine.

The boundary conditions used were the same as for the FEM models, which were:

- 2 degrees of freedom were fixed at the base of the model. The seismic input is applied along the nodes of the base as an acceleration time history.
- The side nodes were restrained in the vertical direction.

- All nodes were restrained in the out-of-plane direction.
- The rotations around the horizontal and vertical axes were restrained in all nodes.

For consistency between the FEM and EFDM models, the FLAC-2D models used the same damping model, i.e. a Rayleigh formulation to account for the material damping defined as a 5% damping at the first natural period of the model.

The EFDM models were also analyzed in two stages. Similarly to FEM models, the first stage corresponds to a static solution in which only the gravitational forces are applied. At the end of the first stage, the displacements and strains were initialized to zero, and the stresses were stored for analyses of the second stage. After the initial stress state was computed, the seismic input was applied at the base of the model (second stage).

The EFDM models had the following characteristics:

- 21114 finite difference zones
- Dynamic time step increments of 0.00002 s
- 11 types of geotechnical materials
- Damping formulation: Rayleigh method corresponding to a critical damping ratio of 5% at the response in the first natural period.
- Integration method: Newmark with gamma = 0.5 and beta = 0.25, also called the trapezoidal rule. This method averages the acceleration in the time step.

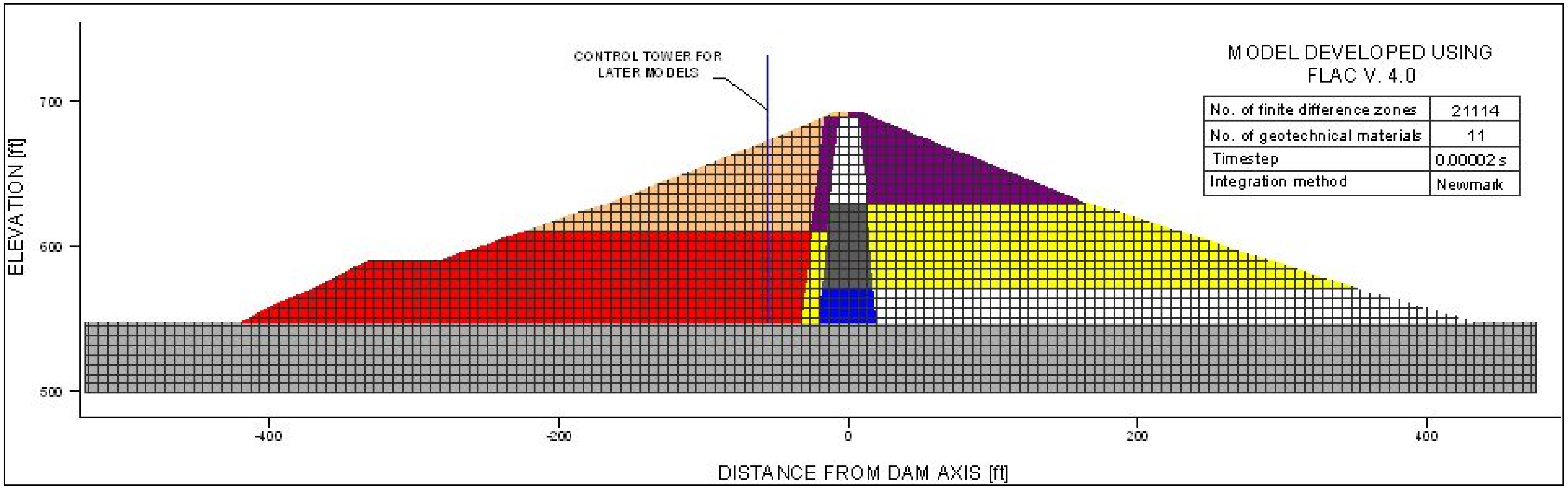

Figure 4-7 Mesh for DSSI Analyses Using the Explicit Finite Difference Method

Note: The seismic input was applied at the bottom side of zones along the base of the model. The actual mesh is twice denser than shown here.

4.5 General Description of the Linear Equivalent Methodology used

The numerical background of the linear equivalent method (LEM) is not presented herein, but details can be found in Schnabel et al. (1972). To assess the influence of soil non-linearity a combination of linear equivalent analyses and linear analyses was carried out as an approximation of the true non-linear behavior of the soil. In order to carry out this assessment additional information for the soils used in the modes is required. The LEM methodology requires definition of the approximate stiffness reduction (G/G_{max}) and increase of the critical damping ratio (β) with the shear strain amplitude (γ). The following subsection describes the procedure and criteria followed to estimate the additional information required to apply LEM.

4.5.1 G/Gmax and β Curves for the Success Dam Soils

The G/G_{max} and β versus γ curves are a way of representing the true nonlinear behavior of the soil under dynamic loading. These curves are a practical way to represent the dynamic nonlinear soil behavior without the use of complex constitutive relations of soils, and are part of the LEM methodology which is commonly used in practice to evaluate the nonlinear dynamic response of soils.

Vucetic and Dobry (1991) developed a set of curves based on laboratory test data gathered from 16 publications. The database of these 16 publications encompassed normally and overconsolidated clays, as well as sands. Vucetic and Dobry (1991) found that the plasticity index (PI) of a soil sample affects the location of these curves, i.e. rapid or slow stiffness degradation with shear strain depending on PI. Similar conclusions were drawn for the effect of IP on the critical damping ratio. At higher PI values of the soil the cyclic stress-strain the soil response tends to be more linear. Dobry and Vucetic (1991) presented G/G_{max} and β versus γ curves for PI values ranging from 0 to 200%. Figure 4-8 presents G/G_{max} and β versus γ according to Vucetic and Dobry (1991).

Seed and Idriss (1970) presented similar curves developed for sands, which usually have very lo values of PI ≈ 0. Figure 4-8 presents G/G_{max} and β versus γ according to Seed and Idriss (1970).

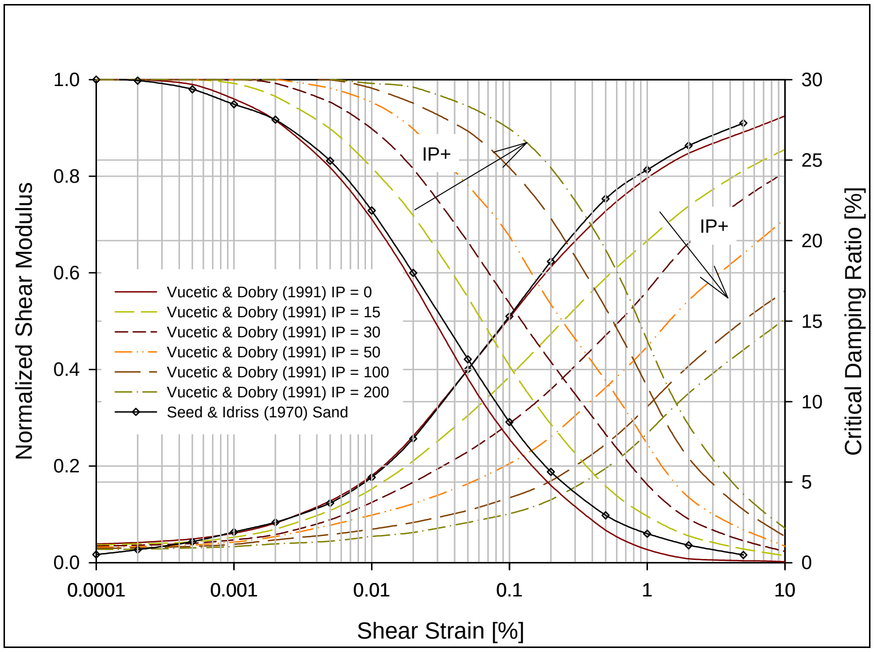

Figure 4-8 G/G_{max} and β versus γ curves according to Vucetic and Dobry (1991) and Seed and Idriss (1970)

The criteria and selection of the most appropriate curves to represent the nonlinear behavior of the soils present in the dam is described next.

External shells: Described as gravelly sand or sandy gravel with sizes less than 12 inches in diameter size, and no more than 12% fine materials. It was assumed that the G/G_{max} and β versus γ curves for sands recommended by Seed and Idriss (1970) were suitable to represent the nonlinearity of the shell materials.

Core: Described as sandy clays and clayey sands. It was assumed that the G/G_{max} and β versus γ curves corresponding to plasticity index of 30, as recommended by Vucetic and Dobry (1991) were suitable to represent the core materials.

The curves selected to model the nonlinearity of these two Success Dam material zones are presented in Figure 4-9.

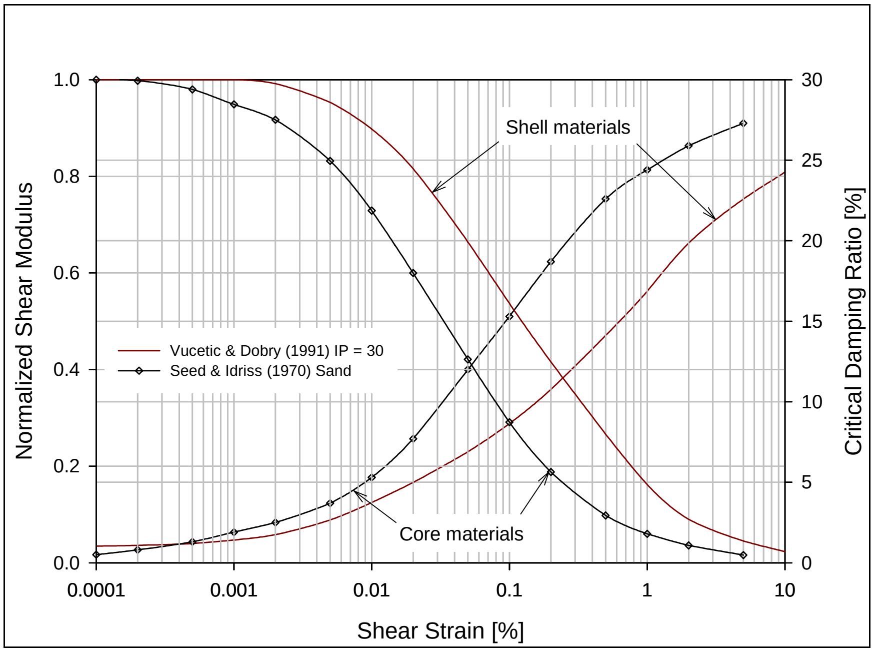

Figure 4-9 G/G_{max} and β Versus γ Curves Used in the Models

4.5.2 Outline of the Methodology Used to Incorporate the Nonlinearity

The levels of stiffness reduction and damping increase were estimated using the QUAKE/W software (GeoSlope International Ltd, 2004). This program uses a 2D plane strain finite element formulation that allows the incorporation of the G/G_{max}, and β versus γ curves described in the previous section.

The QUAKE/W software was used to develop finite element models similar to the ones used for the SAP2000 models (which only model linear elastic soils). The models did not incorporate the tower or intake pipe. The approach selected was to use the QUAKE/W model of the dam (without structures) and evaluate the levels of stiffness degradation when subjected to the same earthquake record. The finite element mesh defined for the 2D QUAKE/W model and the control points for results are presented in Figure 4-10.

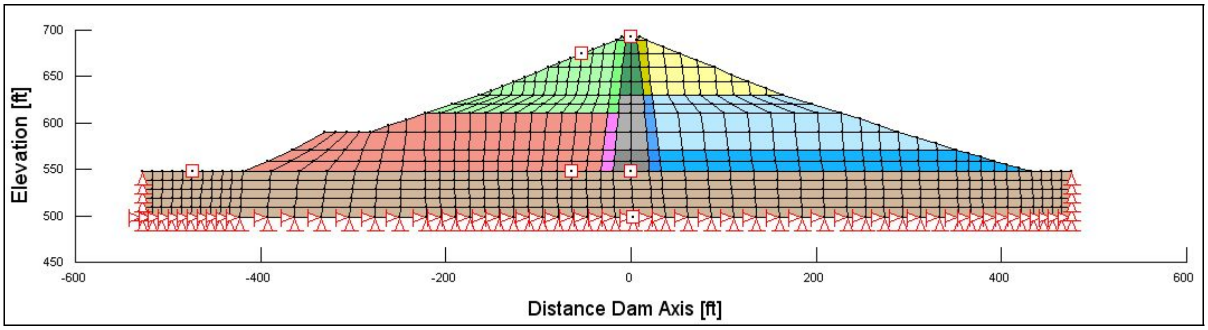

Figure 4-10 Example of Mesh Used for DSSI Analyses Using the Linear Equivalent Method

The computed final shear strain amplitudes were used to estimate zones of similar shear modulus reduction using the G/G_{max} versus γ curves of the material. This information was used to prepared linear elastic models using SAP2000. The new SAP2000 models were prepared using the identified zones with similar stiffness reduction using QUAKE/W. In essence, the approach taken was to use QUAKE/W to evaluate the shear stiffness degradation and damping increases using the capabilities of this software. With the output from QUAKE/W the SAP2000 models, that included structures, were modified according to the new material zones identified based on the QUAKE/W results. The result of the material zonations with reduced stiffness is presented in Section 4.7. A complete set of results is also presented in this section.

4.6 Results of the 2D DSSI Linear Analyses

This section presents the results obtained from the seismic analyses performed with the two 2D models, i.e. FEM and EFDM. The response is described in terms of displacements and accelerations time histories, pseudo acceleration response spectra, and base shear force time histories.

4.6.1 DSSI Analyses for 2D Models of the Dam without Structures

These models were developed to understand the seismic behavior of the dam without the structures. By comparison with posterior models one can assess the influence of the dam on the seismic response of the control tower. The displacements and accelerations time histories and the pseudo acceleration response spectra at the points of analysis are presented next. Figure 4-11 shows a cross section of the dam and the control tower with the six points selected to present the numerical results. For this section, which includes models without structures, Control Point 6 does not exist and Control Points 4 and 5 represent points at the future location of the base of the tower and the surface of the tower, respectively.

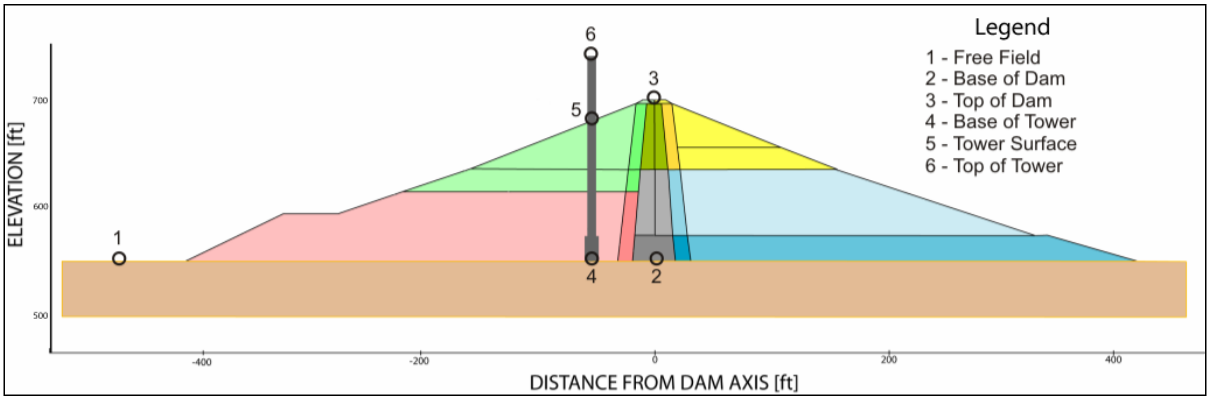

Figure 4-11 Points of the Model for Comparison of Results

4.6.1.1 Comparison of Displacement Histories

Figure 4-12 presents the relative displacement time histories in the horizontal direction at the selected points of analysis using the FEM and EFDM in each case. It can be seen from these figures that at points higher above the dam elevation, small high frequency oscillations start to occur, due to the contribution of higher modes.

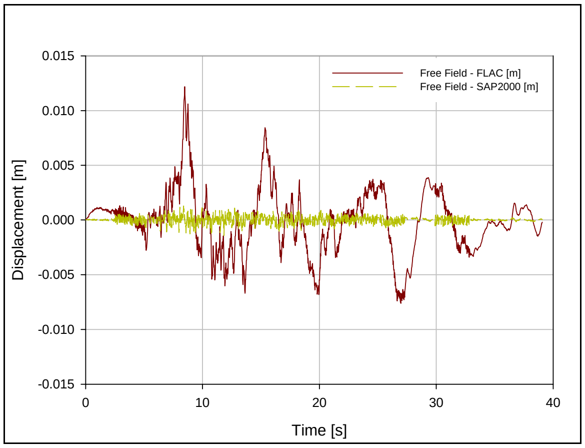

a) Control point 1. At free field

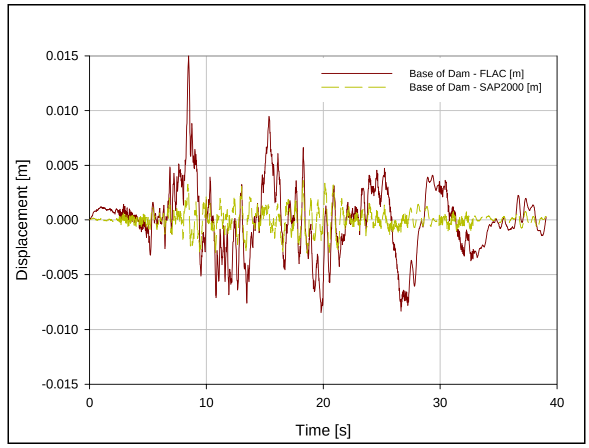

b) Control point 2. At base of dam

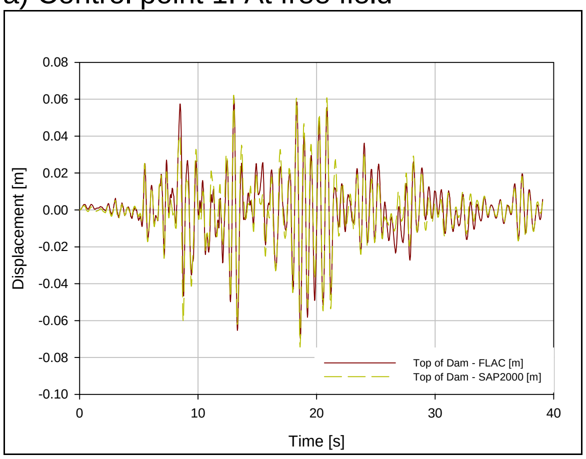

c) Control point 3. At top of dam

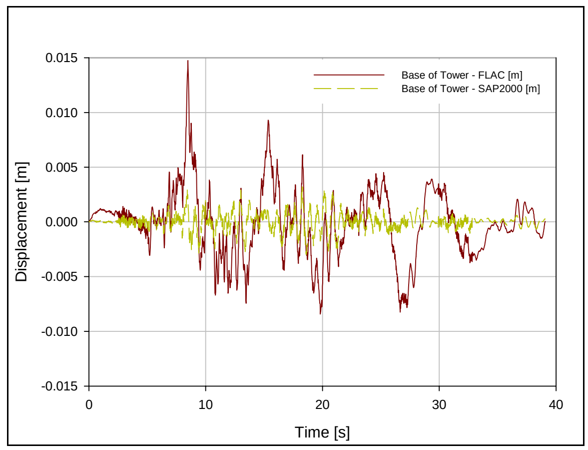

d) Control point 4. At base of tower

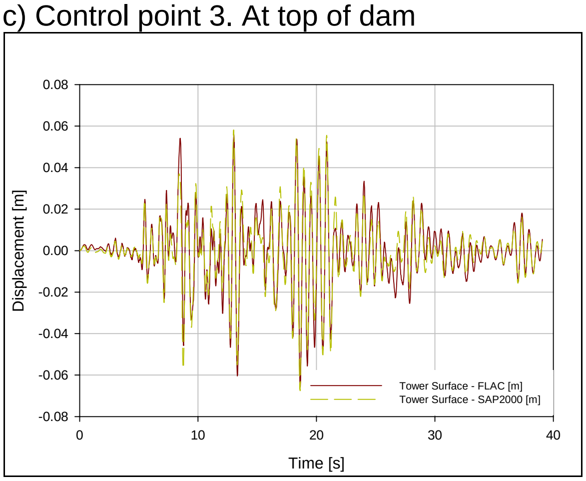

e) Control point 5. At tower surface

Figure 4-12 Displacement Time Histories at Control Points of the 2D Models without Structures

This figure shows very good agreement between the FEM (SAP2000) and the EFDM (FLAC) results for the top of the dam (Control Point 3) and the tower surface (Control Point 5). The maximum displacement at the top of the dam computed with both methodologies was 0.075 m. However, the results obtained for the free field (Control Point 1), base of dam (Control Point 2) and base of tower (Control Point 4) do not show a good agreement between the FLAC and SAP2000 results. This may be due to differences in the numerical methods (geometrical update of the model in FLAC), and the differences between the finite difference mesh (1 m squared) and the finite element mesh (3 m squared).

4.6.1.2 Comparison of Acceleration Time Histories

Figure 4-13 presents the acceleration time histories at the five points of analysis using the FEM and EFDM in each case. The accelerations shown are total (or absolute), i.e. they constitute the sum of the base and relative accelerations. The accelerations traces were trimmed at 25 s to increase the resolution to better appreciate the differences between the two methods. It can be seen in these figures that higher acceleration amplitudes are obtained as the elevation of the response point increases, which is consistent with the results obtained in terms of relative displacements presented in the previous subsection.

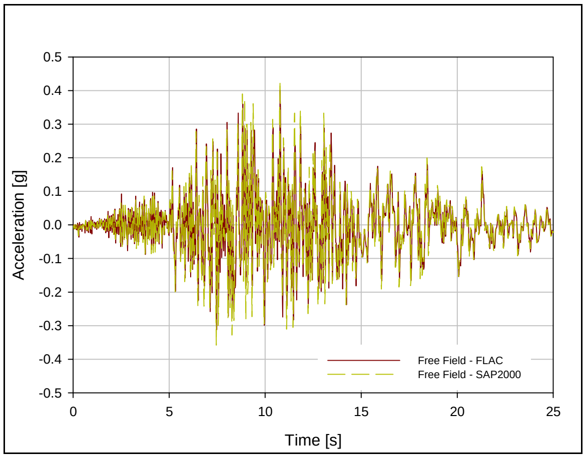

a) Control point 1. At free field

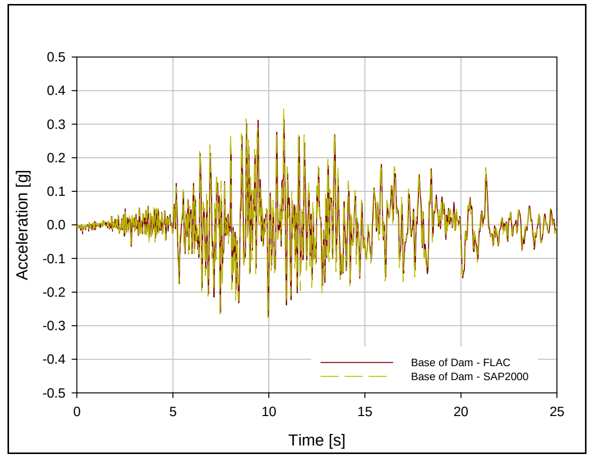

b) Control point 2. At base of dam

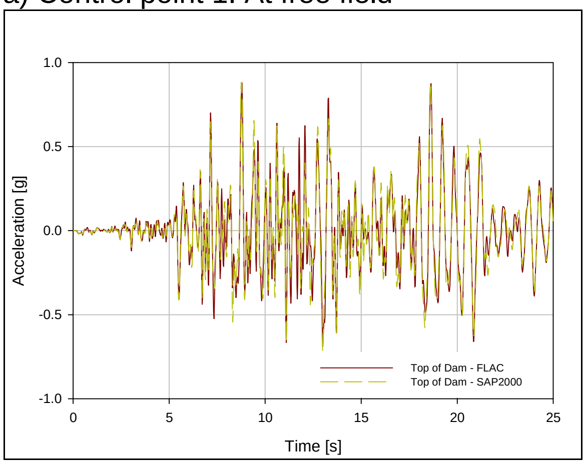

c) Control point 3. At top of dam

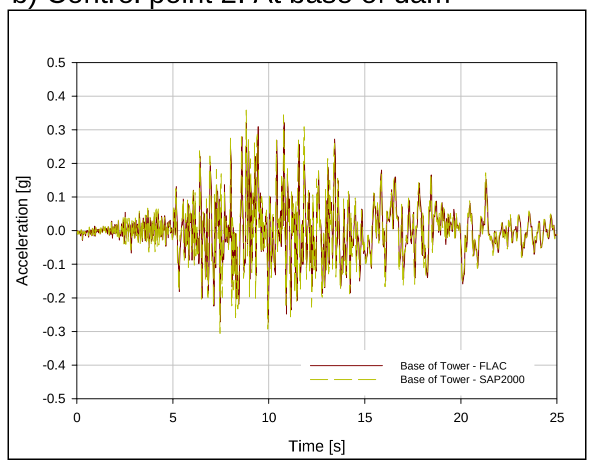

d) Control point 4. At base of tower

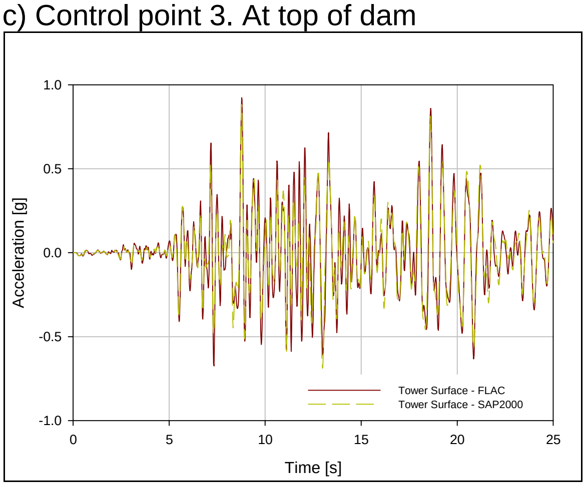

e) Control point 5. At tower surface

Figure 4-13 Acceleration Time Histories at Control Points of the 2D Models without Structures

Figure 4-13 shows very good agreement between the FEM and the EFDM results in all five control points. However, this type of plots does not provide much information due to the rapid variation with time of the data presented. Therefore, the next subsection it will present results in terms of the pseudo acceleration response spectra for an oscillator with 5% damping ratio. These curves permit a more complete description and a more detailed comparison of the results.

4.6.1.3 Comparison of Pseudo Acceleration Response Spectra

Pseudo acceleration response spectra were computed using the acceleration time histories presented before. They were computed using a 5% structural damping. Figure 4-14 presents the response spectrum curves at the five control points of analysis and for the two numerical methodologies (FEM and EFDM).

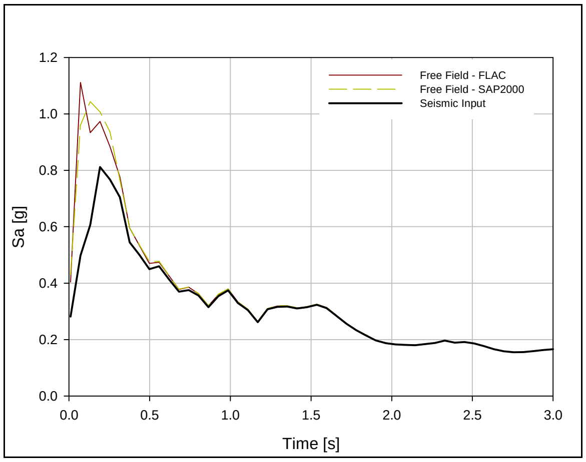

a) Control point 1. At free field

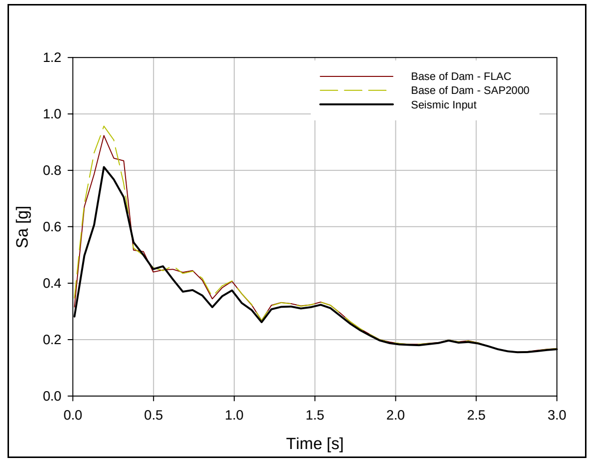

b) Control point 2. At base of dam

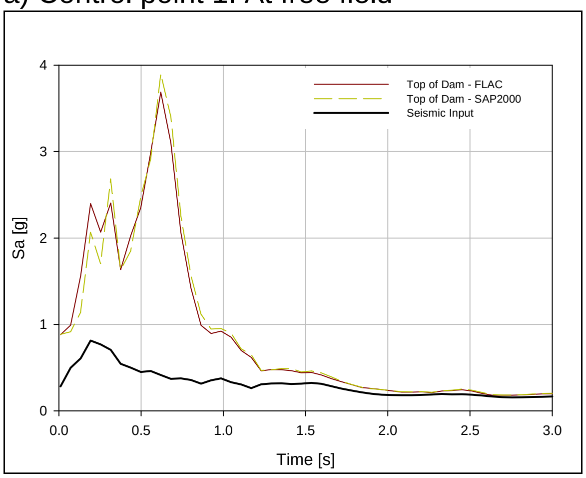

c) Control point 3. Top of dam

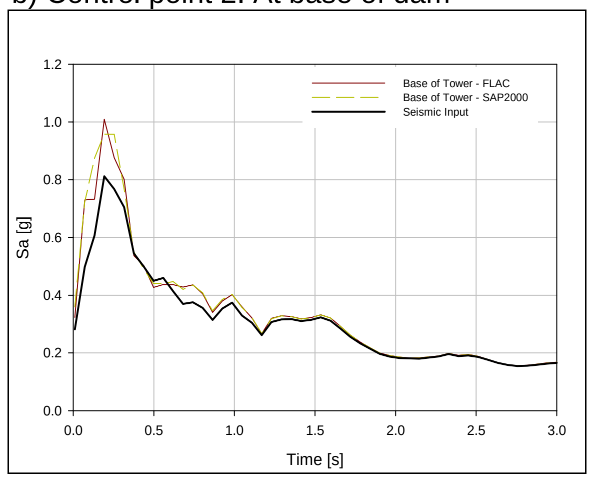

d) Control point 4. Base of tower

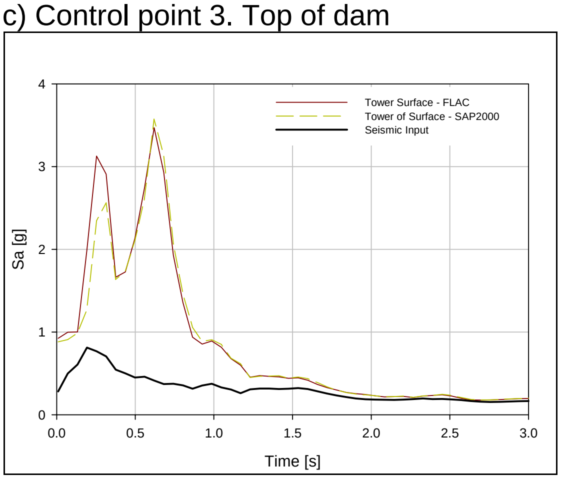

e) Control point 5. Tower surface

Figure 4-14 Pseudo Acceleration Response Spectra at Control Points of the 2D Models without Structures

For comparison purposes, the plots in Figure 4-14 show the spectrum of the input motion which corresponds to the MCE (84% percentile). The PGA for the MCE is 0.28 g and its spectrum has high acceleration ordinates of up to 0.8 g at a period of 0.2 s.

Overall the plots in Figure 4-14 showed reasonably good agreement between the response spectra obtained from the two numerical methods. Figure 4-14 (a), (b), and (d) correspond to control points at free field, base of dam, and base of tower. These points are not influenced by the natural periods of the dam, hence, as expected the predominant peaks of the computed spectra correspond closely to the peak of the input motion spectra (i.e. at a period around 0.2 s). Figure 4-14 (c) and (e) correspond to points at the surface of the dam, hence show peaks in their spectra that are influenced by the natural periods of the dam.

Knowledge of the lower natural periods of the dam can be useful when analyzing the results of the response spectra; the five shortest periods of the dam without structures as computed using FEM are presented in Table 4-9.

Table 4-9 Natural Periods of the Dam From 2D SAP2000 FEM Model without Structures

Mode Number	Period [s]	Modal Participating Mass Ratio
1	0.640	0.3325
2	0.461	0.0254
3	0.399	0.0003
4	0.373	0.00006
5	0.325	0.0008

From Figure 4-14 (c) it can be seen that three peaks of the response spectra at the top of the dam (control point 3) correspond to the first three fundamental periods of the system indicated in Table 4-9. Similarly, the two peaks of the response spectra of the control point 5 (tower surface), shown in Figure 4-14 (e), correspond to the first two fundamental periods of the dam. The amplification factors for the three peaks of the response spectra of dam crest (control point 3) were 2.6, 5, and, 8.7 for the periods of 0.2, 0.4, and 0.6 s, respectively. The amplification factors for the two peaks of the response spectra of control point 5 were 3.9 and 9.1, for periods the 0.3, and 0.6 s, respectively. For the remaining control points an amplification factor of about 1.25 is observed at the period of maximum pseudo acceleration. These relatively low amplification factors for control points 1, 2, and 4 are consistent with the high shear wave velocity estimated for the foundation soils.

In general, there was a good agreement between the results obtained using the two different methodologies. However, minor differences were observed in the response spectra obtained from the two methodologies and they may be related to the following factors:

- Time step of the calculations: The FLAC time step was $2x10^{-5}$ s, and the SAP time step was $2x10^{-2}$ s.

- Mesh differences of the two models: The shape and size of the FLAC zones and SAP finite elements were different.

- Discretization methods: The two models were evaluated using FEM and EFDM.

Based on the results of the dam section without the control tower indicates that the two methodologies (FEM and EFDM) are reasonably equivalent under the present conditions of analysis (both used linear elastic models for the soils).

4.6.1.4 Vibration Modes Shapes Using SAP2000

The dynamic response in SAP2000 (FEM) included calculations of the modes shapes of vibration including the modal participating ratios and participant factors. Visual inspection of the mode shapes can help determine whether a model with a certain natural period will contribute significantly to the seismic response.

The first five vibration mode shapes of the 2D model without structures are presented in Figure 4-15 to Figure 4-19.

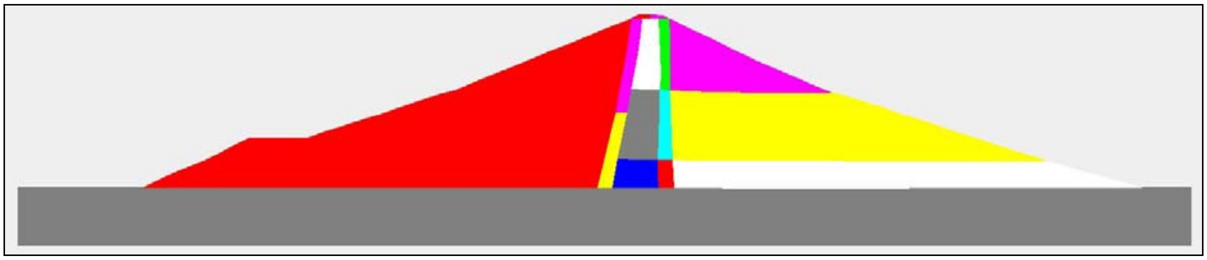

Figure 4-15 First Vibration Mode Shape of the 2D Model without Structures

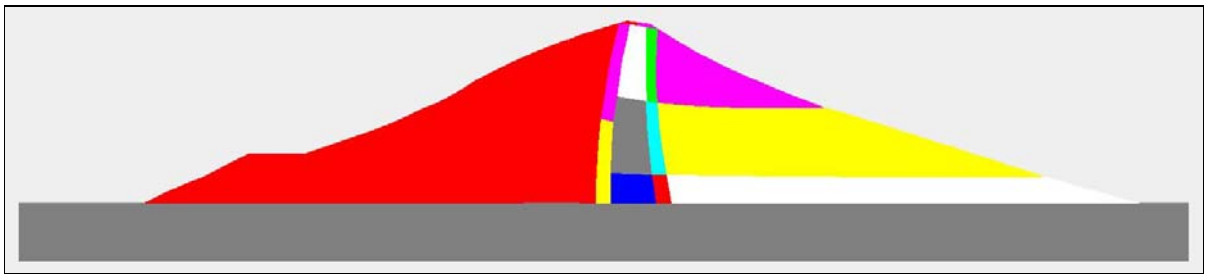

Figure 4-16 Second Vibration Mode Shape of the 2D Model without Structures

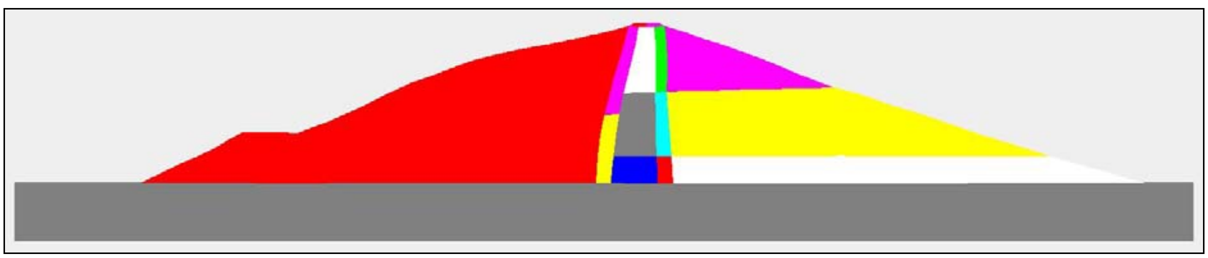

Figure 4-17 Third Vibration Mode Shape of the 2D Model without Structures

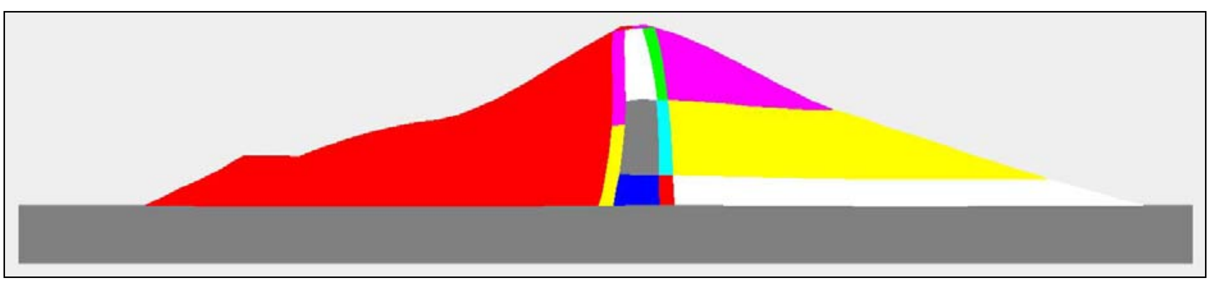

Figure 4-18 Fourth Vibration Mode Shape of the 2D Model without Structures

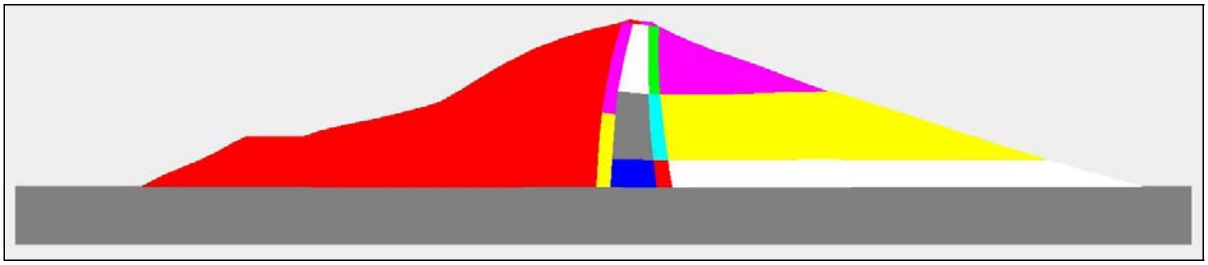

Figure 4-19 Fifth Vibration Mode Shape of the 2D Model without Structures

The following section presents DSSI results for the Success dam including the control tower. The analyses presented next continue to be linear elastic but will include computations of the base shear and the bending moments acting on the control tower.

4.6.2 DSSI Analyses for 2D Models of the Dam Including the Control Tower

These models were developed to estimate the base shear and other response quantities of the control tower. In addition, these models can be useful to evaluate the effect of the control tower embedded in the dam on the overall seismic response of the dam. Similarly as before, two 2-dimensional models were developed using the numerical techniques described earlier, i.e. the FEM and EFDM. This section presents a summary of the results obtained, and also presents a comparison with previously published studies. The response quantities selected for comparison are the relative displacements, the absolute accelerations time histories, and the pseudo acceleration response spectra at six selected control points located within the dam and control tower.

4.6.2.1 Comparison of Displacement Time Histories

Figure 4-20 presents the relative displacement time histories at the six points of analysis using the FEM and EFDM methodologies implemented in SAP2000 and FLAC2D.

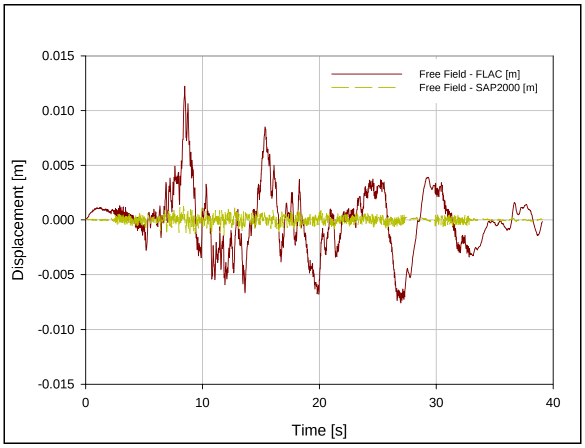

a) Control point 1. At free field

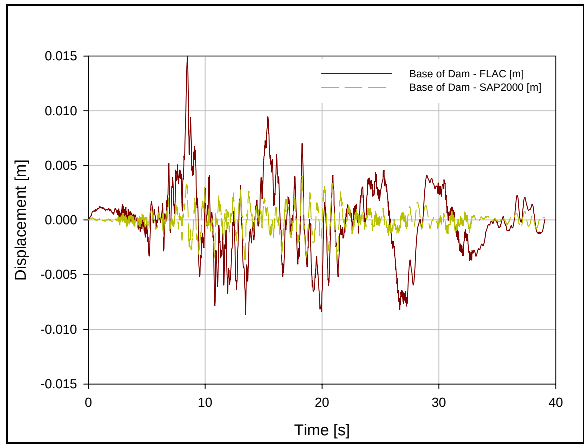

b) Control point 2. At base of dam

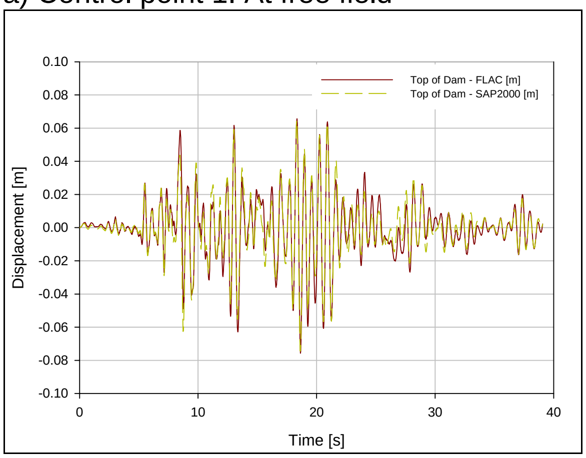

c) Control point 3. At top of dam

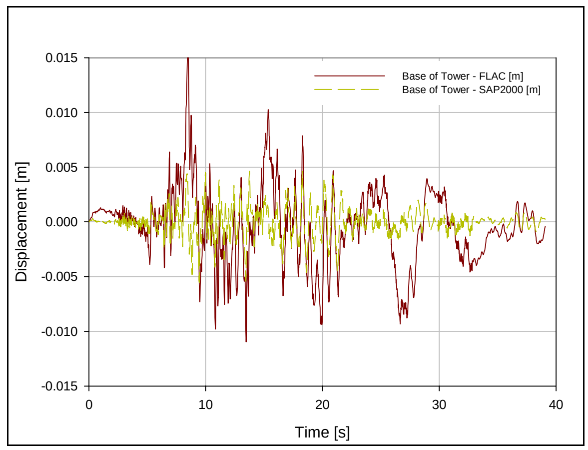

d) Control point 4. At base of tower

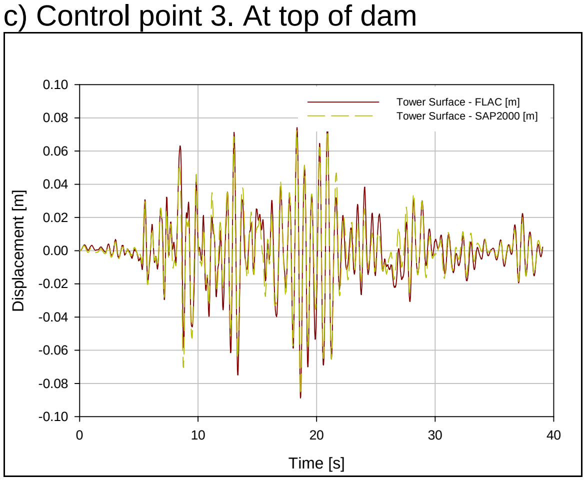

e) Control point 5. At tower surface

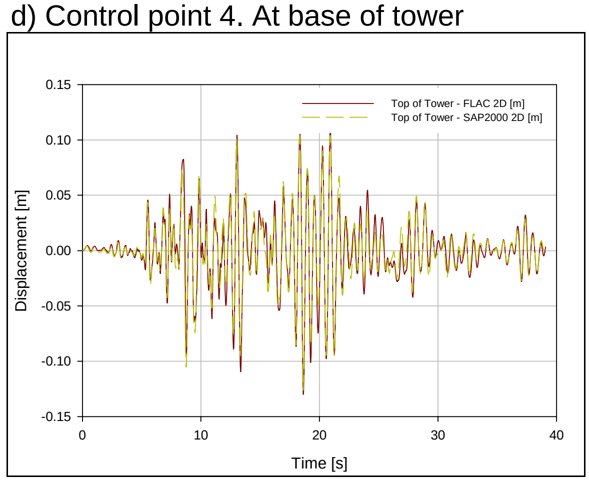

f) Control point 6. At top of tower

Figure 4-20 Displacement Time Histories at Control Points for 2D Models Including the Control Tower

The plots from Figure 4-20 showed reasonably good agreement between the FEM and EFDM results particularly for control points at higher elevations. Agreement was not as good for points near the base of the model. The maximum displacement at the top of the dam obtained from both models was 0.09 m. This constitutes a slight increase in the maximum displacement at the top of the dam when the control tower is included in the model (from 0.075 to 0.09 m). This increase may be related to the additional inertial forces acting on the heavy control tower structure. However, on the other hand, the presence of the tower also stiffens the dam, which will tend to reduce the displacements. These two opposite factors may contribute to the observed small changes in the system response (lateral displacements at the top). It is important to bear in mind that the magnitude of this lateral displacement cannot be taken as a realistic estimate if a strong earthquake hits the dam, since the results are based on models with soils modeled using linear stress-strain relationships.

The computed maximum displacement at the top of the tower and the tower surface was 0.124 m and 0.102 m, respectively, at the same instant of time. The maximum drift of the segment of the tower standing outside of the dam can be computed as:

$$Drift = \frac{0.124 - 0.102}{18m} \times 100\% = 0.12\%$$

This maximum drift of the tower occurred at 18.62 s of the inputs seismic ground motion.

4.6.2.2 Comparison of Acceleration Time Histories

Figure 4-21 presents the acceleration time histories at the six control points using the FEM and EFDM when the tower is included in the models. In general, this figure shows good agreement between the FEM and the EFDM results. As mentioned before, this type of plots does not provide much information due to the difficulty of reading the many peaks and trough characteristics of an accelerogram. Therefore, the next subsection presents results in terms of response spectra for 5% structural damping, which allow a more accurate comparison of results.

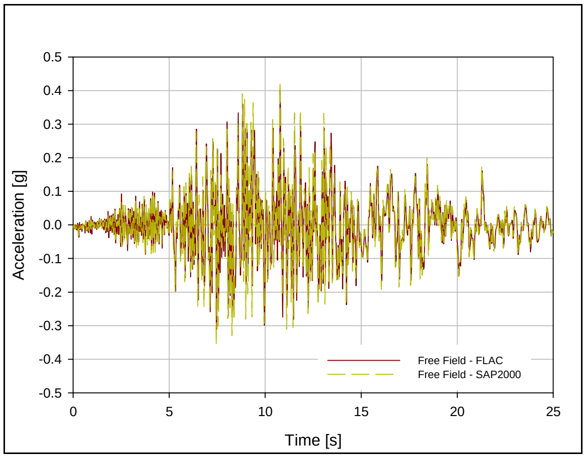

a) Control point 1. At free field

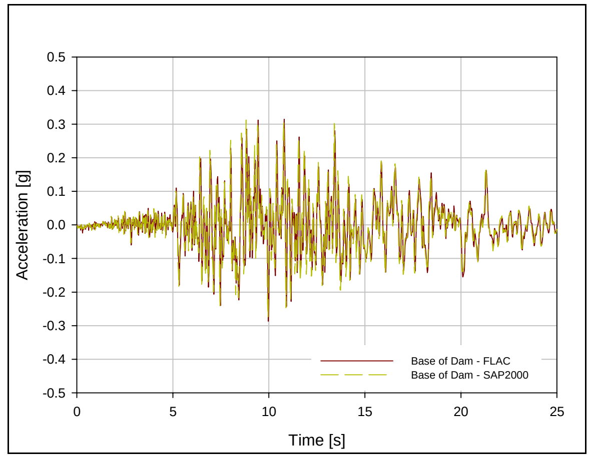

b) Control point 2. At base of dam

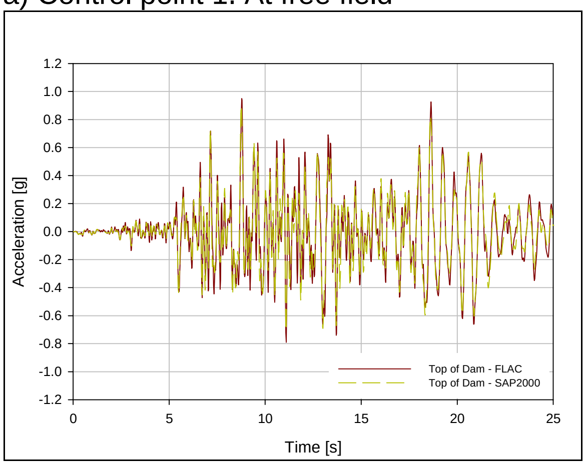

c) Control point 3. At top of dam

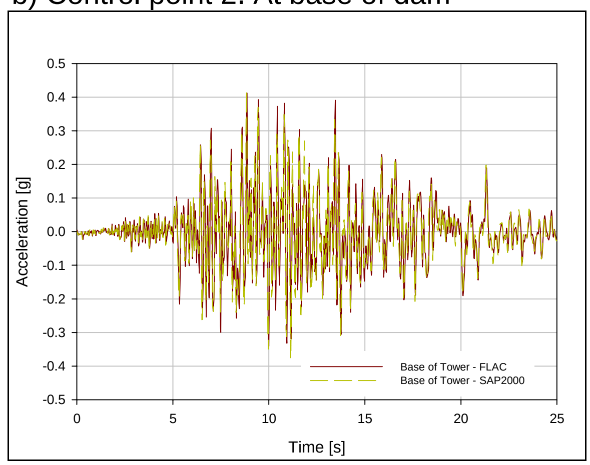

d) Control point 4. At base of tower

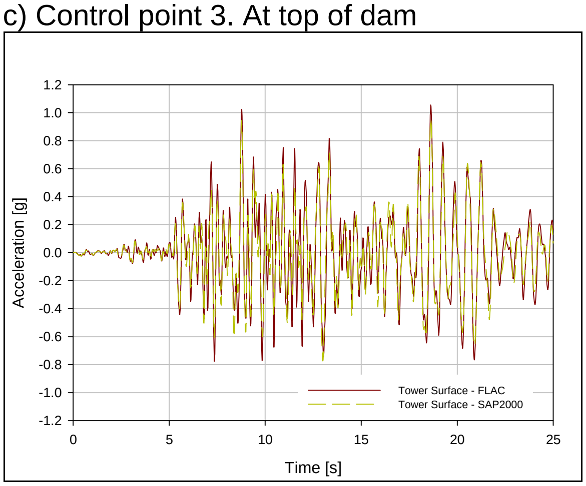

e) Control point 5. At tower surface

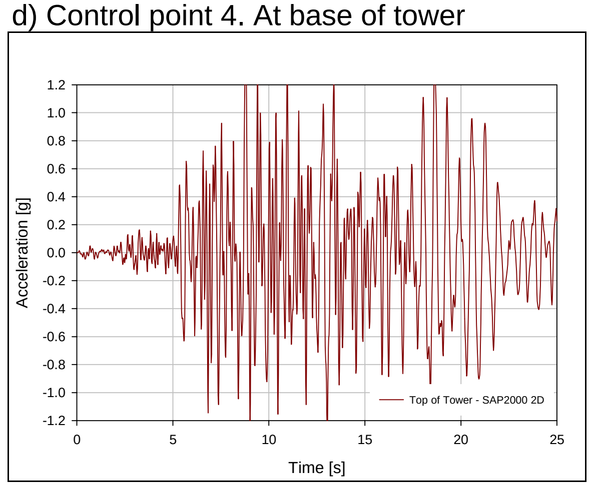

f) Control point 6. At top of tower

Figure 4-21 Acceleration Time Histories at Control Points for the 2D Models Including the Control Tower

4.6.2.3 Comparison of Pseudo Acceleration Response Spectra

Figure 4-22 presents the response spectra at the six control points of analysis. These plots were obtained by using the acceleration time histories calculated with the FEM and EFDM.

Overall the plots shown in Figure 4-22 indicate reasonably good agreement between the FEM and EFDM methodologies. The plots corresponding to the control point near the base of the models (i.e. Control Points 1, 2 and 4) showed one predominant peak at a period very close to the natural period of the input ground motion applied at the base of the models (i.e. close to 0.2 s). Figure 4-22 (c), (e), and (f) correspond to Control Points 3, 5 and 6, respectively. These points are affected by the presence of the dam and/or tower hence show more than one peak in their response spectra. To better understand these results the natural period of the dam and tower system are presented next.

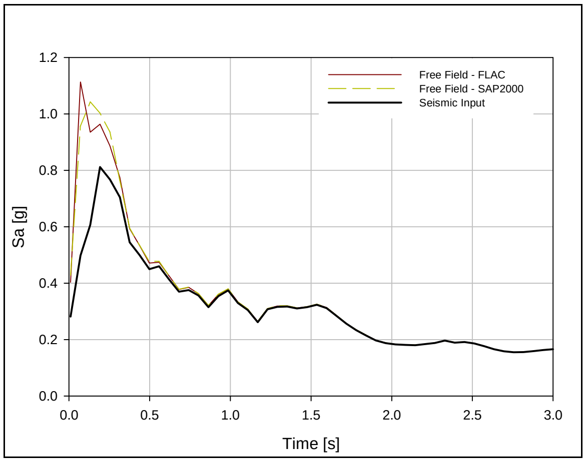

a) Control point 1. At free field

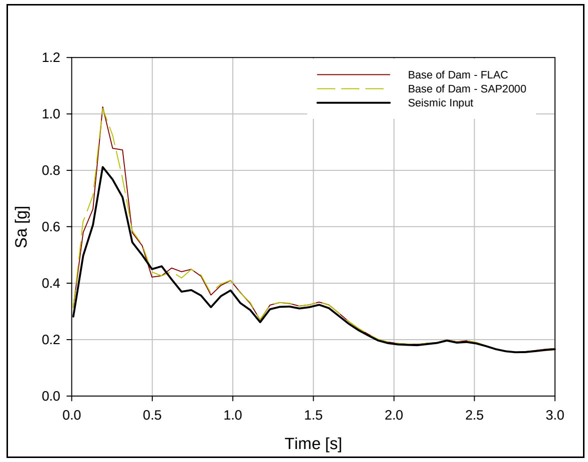

b) Control point 2. At base of dam

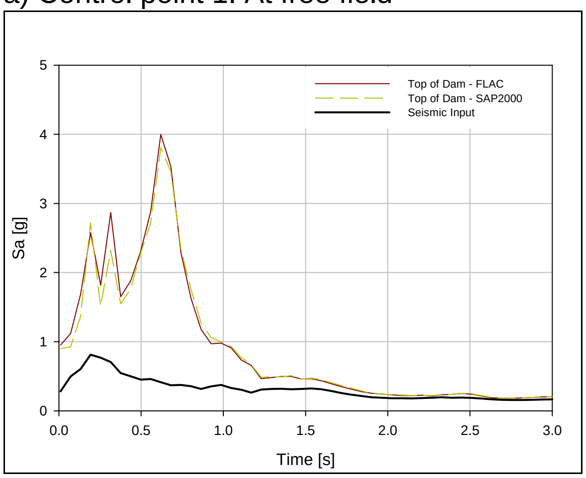

c) Control point 3. At top of dam

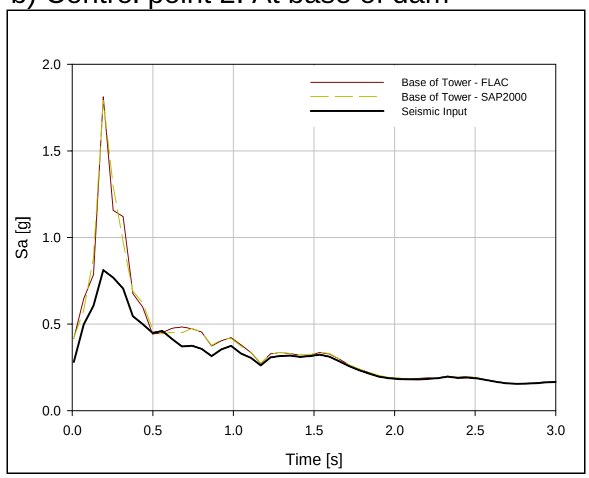

d) Control point 4. At base of tower

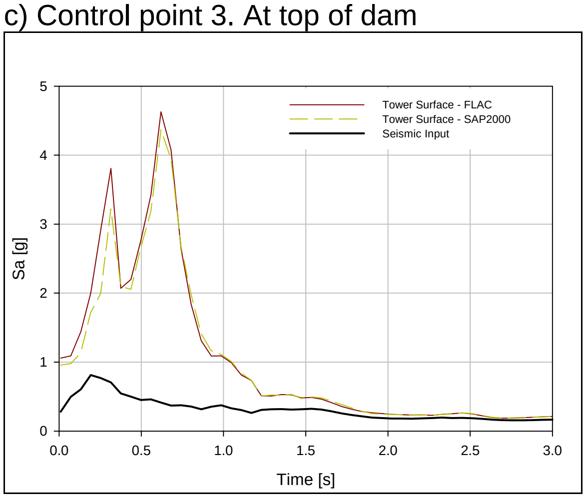

e) Control point 5. At tower surface

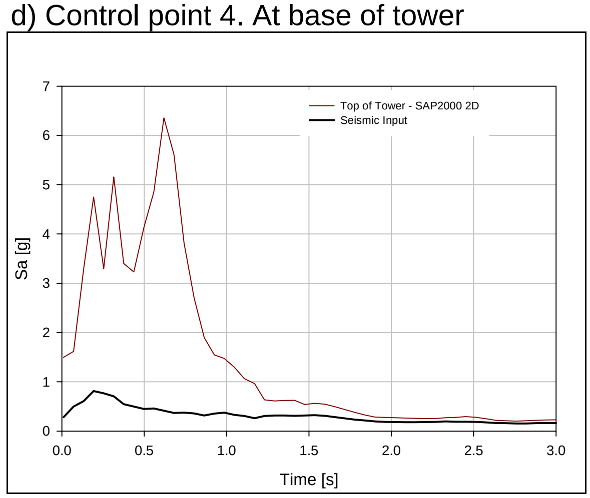

f) Control point 6. At top of tower

Figure 4-22 Pseudo Acceleration Response Spectra at Control Points for the 2D Models Including the Control Tower

The first five natural periods of the dam-tower system computed using the FEM model (SAP2000) are presented in Table 4-10. They are helpful to analyze the results of the response spectra (for Control Points 3, 5 and 6).

Table 4-10 Natural Periods of the 2D SAP2000 FEM Model Including the Control Tower

Mode Number	Period [s]	Modal Participating Mass Ratio
1	0.657	0.3443
2	0.387	0.0042
3	0.367	0.0068
4	0.357	0.0042
5	0.316	0.1095

Figure 4-22 shows that the response spectra have significant peaks at the first two and three fundamental periods. At these periods, the spectrum for the points at the top of the dam and tower surface show peaks with amplifications between 3 to 6 compared to the peak of the input motion spectrum (at the bedrock). These high amplification factors may decrease if a non-linear analysis is performed. For the remaining points of analysis, the amplification factor is about 1.25 at the period where the original spectrum presents the highest peak.

4.6.2.4 Vibration Mode Shapes Using SAP2000

The first five vibration modes computed for the 2D model that includes the control tower are presented in Figure 4-23 to Figure 4-27. According to the modal participating ratios listed in Table 4-10, the first and fifth mode will contribute the most to the response of the dam to horizontal ground motion. Note that the part of the control tower that emerges from the dam mostly deflects as a rigid body, i.e. there is lateral motion of the tower but to a large extent due to the deformations of the dam.

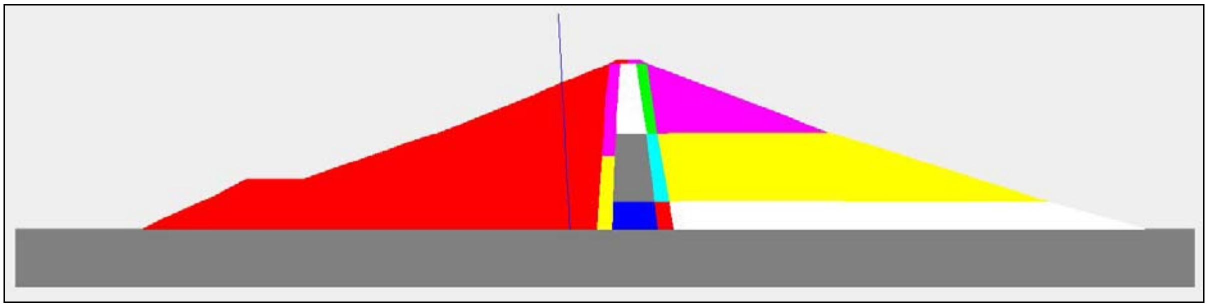

Figure 4-23 First Vibration Mode Shape of the 2D Model Including the Control Tower

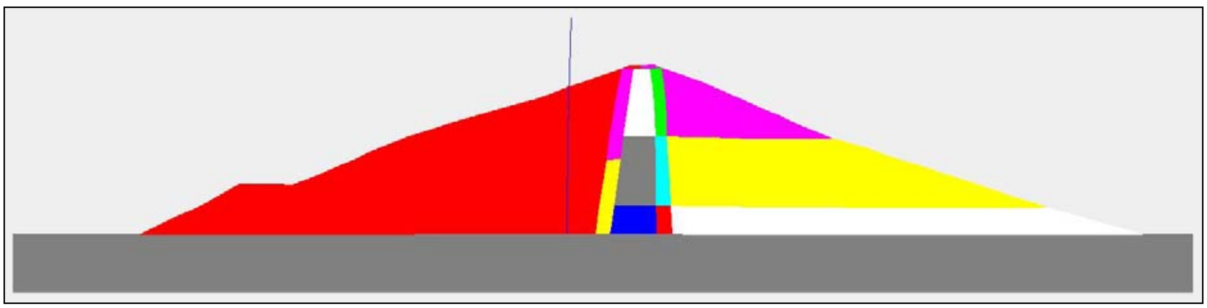

Figure 4-24 Second Vibration Mode Shape of the 2D Model Including the Control Tower

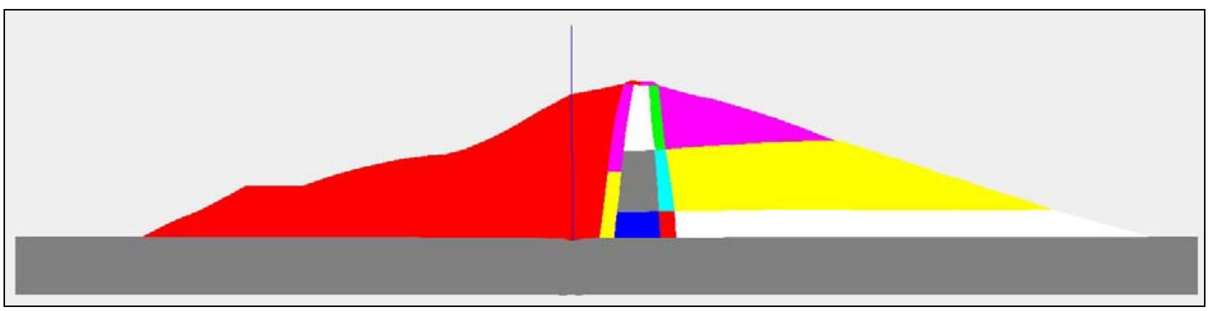

Figure 4-25 Third Vibration Mode Shape of the 2D Model Including the Control Tower

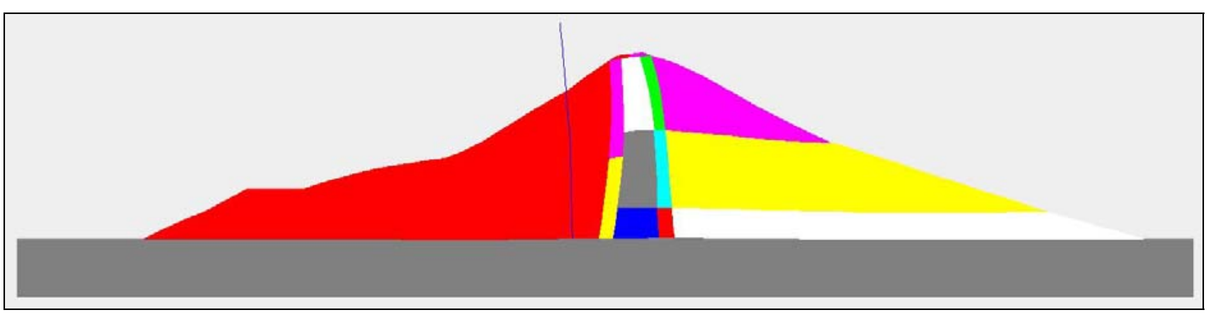

Figure 4-26 Fourth Vibration Mode Shape of the 2D Model Including the Control Tower

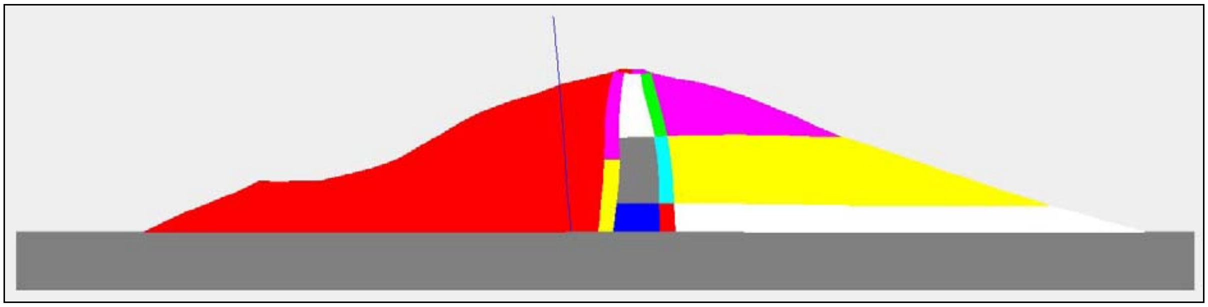

Figure 4-27 Fifth Vibration Mode Shape of the 2D Model Including the Control Tower

4.6.2.5 Comparison of Reactions at the Base of the Control Tower

For this study, one of the most important response quantities is the base reactions acting on the tower, since it provides information for retrofit evaluations and because it can be used for comparison with previous studies.

The time histories of the shear force acting at the base of the control tower are presented in Figure 4-28 for the two approaches used. The time histories obtained using FEM and EFDM are practically identical. The magnitudes of the maximum shear force obtained with FLAC2D and SAP2000 were also found to be very similar, as shown on Table 4-11 also presents values for the maximum bending moment at the base of the tower.

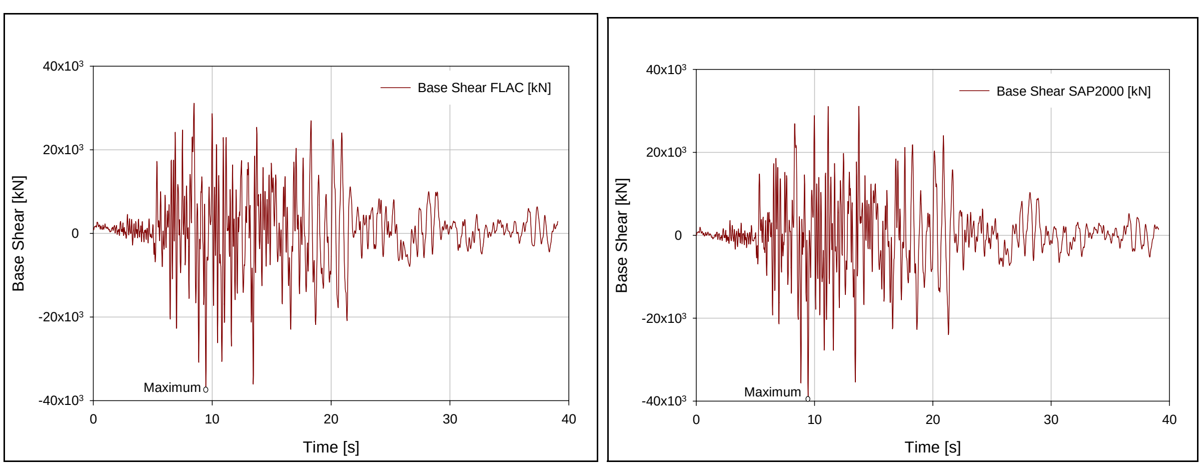

a) Finite Difference method – FLAC 2D b) Finite Element Method -SAP2000

Figure 4-28 Base Shear Acting on the Control Tower Using 2D Analyses

Table 4-11 Maximum Reactions Acting on the Control Tower Using 2D Analyses

Method of Analysis	Maximum Base Shear [kN]	Time of Occurrence [s]	Maximum Bending Moment [kN-m]	Time of Occurrence [s]
2D FEM – SAP2000	39826	9.46	8427	18.64
2D EFDM – FLAC2D	37565	9.48	53	8.8

It is important to examine the maximum shear forces acting along the shaft of the control tower and the shear force distribution when the maximum base shear occurs. These two diagrams are presented in Figure 4-29 and Figure 4-30, respectively. Results presented correspond only to the SAP2000 FE methodology. Note that if the sign of the shear forces is ignored in Figure 4-30, the two diagrams look similar. This implies that the maximum shear forces occur along the shaft occur at about the same time than the maximum base shear force.

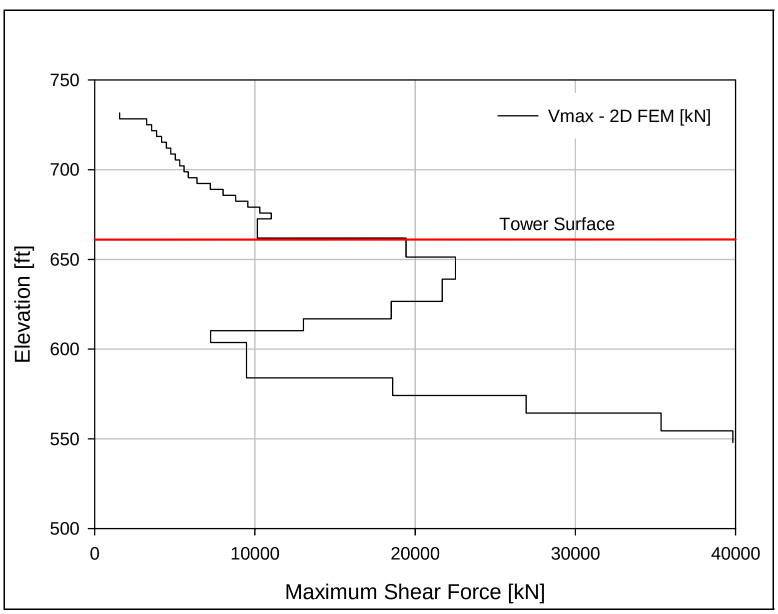

Figure 4-29 Maximum Base Shear Force Acting Along the Control Tower Using 2D Analyses

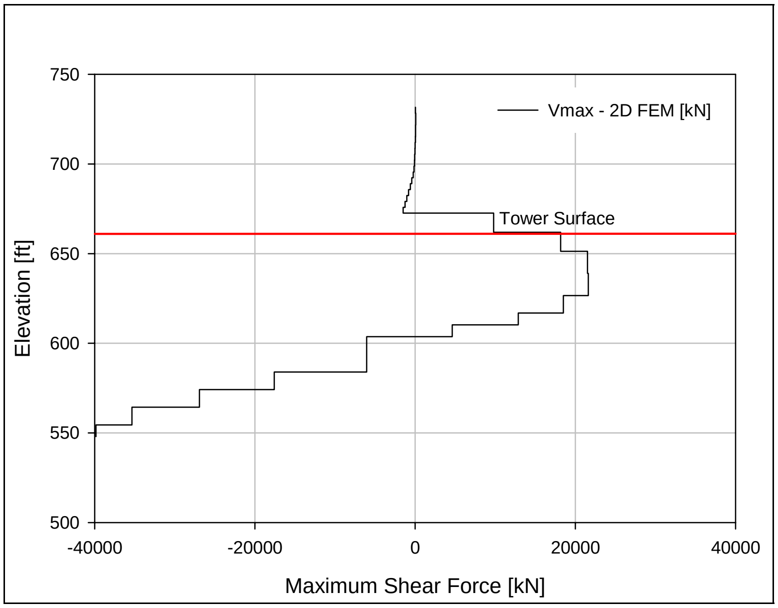

Figure 4-30 Shear Force Distribution When the Maximum Base Shear Force Occurs

A similar comparison of the maximum bending moment acting along the shaft of the control tower, and the bending moment distribution when the maximum bending moment at the base occurs is presented in Figure 4-31 and Figure 4-32, respectively.

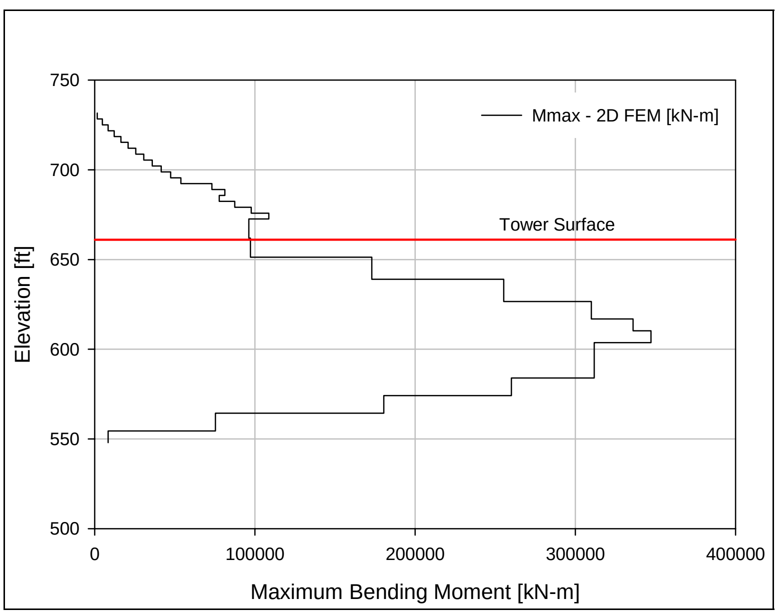

Figure 4-31 Maximum Bending Moment Acting Along the Control Tower Using 2D Analyses

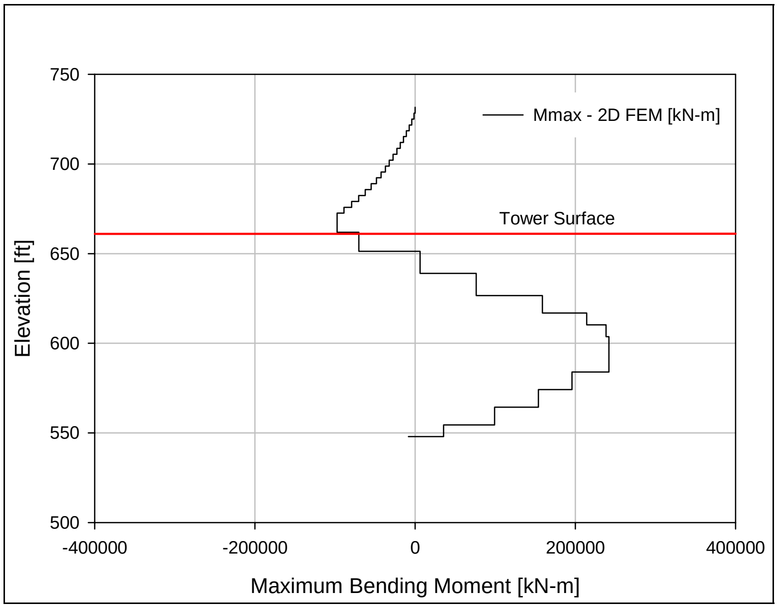

Figure 4-32 Bending Moment Distribution When the Maximum Bending Moment at the Base Occurs

4.6.3 DSSI Analyses for 2D Models of the Dam Including the Control Tower and the Intake Pipe

This section presents results obtained from 2D models that include both the control tower and the underlying intake pipe that traverses the full width of the dam. An important consideration in the analyses was the connection between the control tower and the intake pipe. This connection was considered as rigid because the gates regulating the discharge are located at this point and it is vital that they remain operational after an earthquake hits the dam. Hence the joint node of the control tower and the intake pipe was modeled with full compatibility of their degrees of freedom (i.e. no restraint was applied at the control tower-intake pipe connection node). In both types of numerical methods the control tower was represented using the methodology described in section 4.2.2, and the intake pipe was modeled using the approach described in section 4.2.3. The displacements and accelerations time histories and the pseudo acceleration response spectra obtained at the six selected control points are presented in the following sections. For comparison purposes, the results are presented together with those obtained from models that included the control tower only. By doing so, one can evaluate the influence of the discharge pipe on the seismic response of the dam and the tower.

Figure 4-33 shows the finite element model developed in SAP2000.

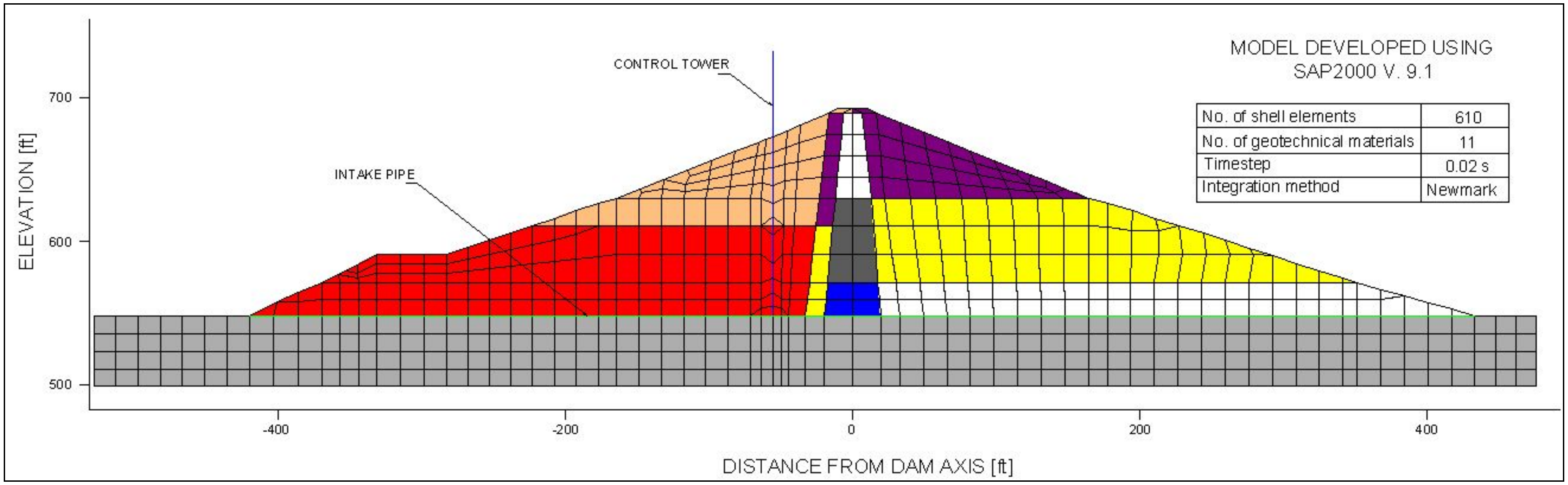

Figure 4-33 Finite Element Model Including the Control Tower and the Intake Pipe

4.6.3.1 Comparison of Displacement Time Histories

Figure 4-34 shows the relative displacement time histories of at the control points obtained using the FEM and EFDM and including the intake pipe in the model. The displacements obtained without including the intake pipe in the model are also included in the plots.

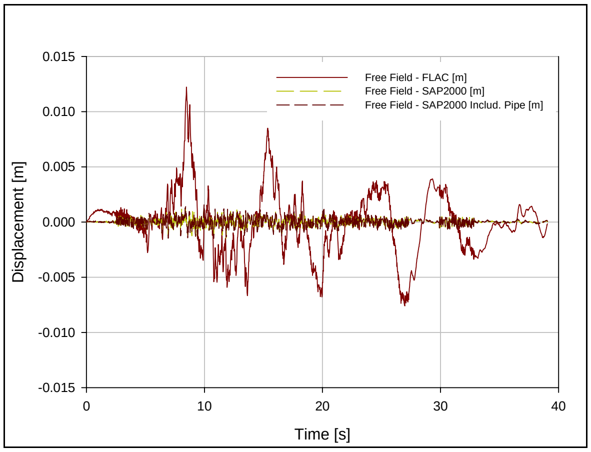

a) Control point 1. At free field

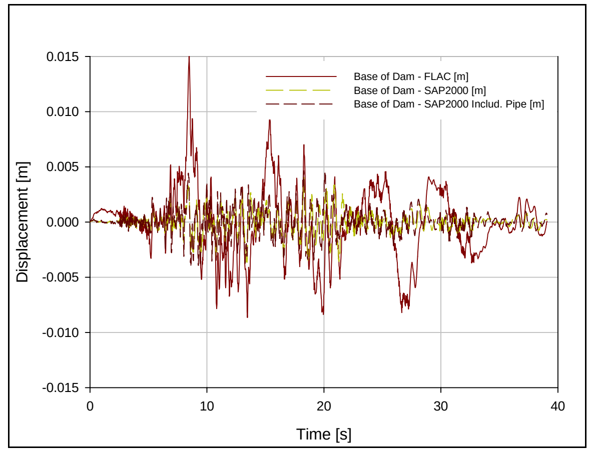

b) Control point 2. At base of dam

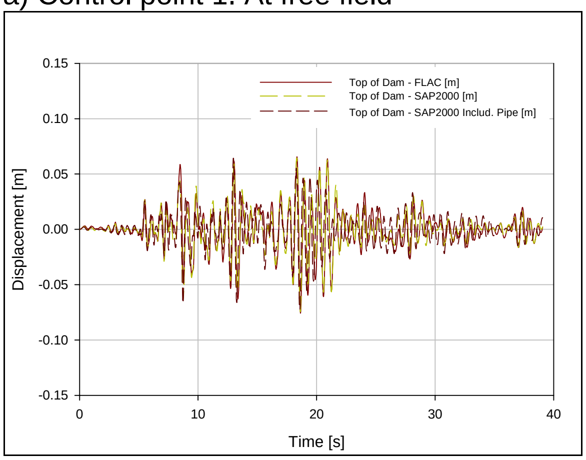

c) Control point 3. At top of dam

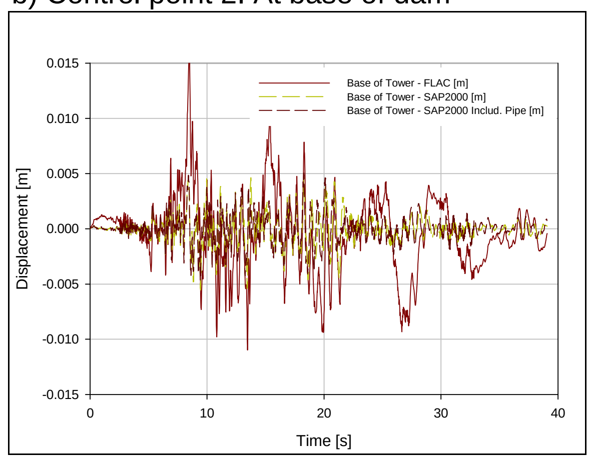

d) Control point 4. At base of tower

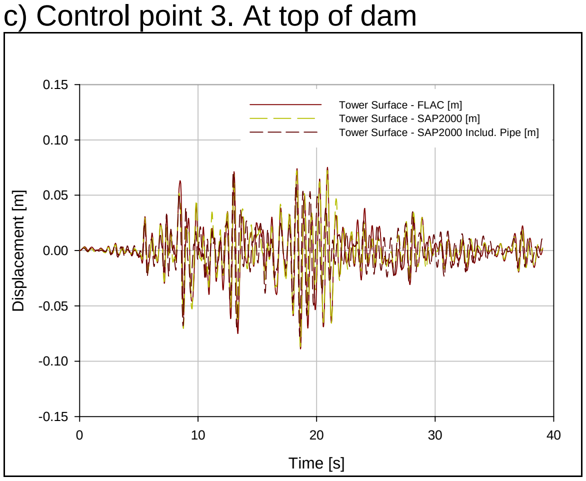

e) Control point 5. At tower surface

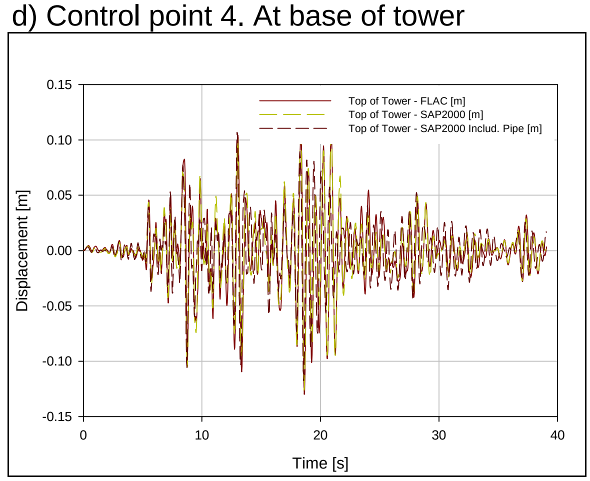

f) Control point 6. At top of tower

Figure 4-34 Displacement Time Histories at Control Points for the 2D Models Including the Control Tower and the Intake Pipe

The maximum displacement obtained using both methodologies for the top of the dam when including the tower and the intake pipe was computed as 0.074 m. This displacement is slightly less than 0.075 m which was obtained in the models without the intake pipe.

The maximum displacement computed for the point at the top of the tower was 0.126 m while at the same time at the point at the tower surface was 0.086 m. The maximum drift of this segment of the tower is:

$$Drift = \frac{0.126m - 0.086m}{18m} \times 100\% = 0.22\%$$

The maximum drift of 0.22% occurs at 18.58 s of the seismic input.

4.6.3.2 Comparison of Acceleration Histories

Figure 4-35 presents the acceleration time histories at the six control points of analysis using the FEM and EFDM including the intake pipe in the model, and compared with the results obtained without including the intake pipe.

As mentioned before, it may be difficult to appreciate the differences in these plots. Therefore, in the next section results are presented in terms of response spectra for a 5% of structural damping.

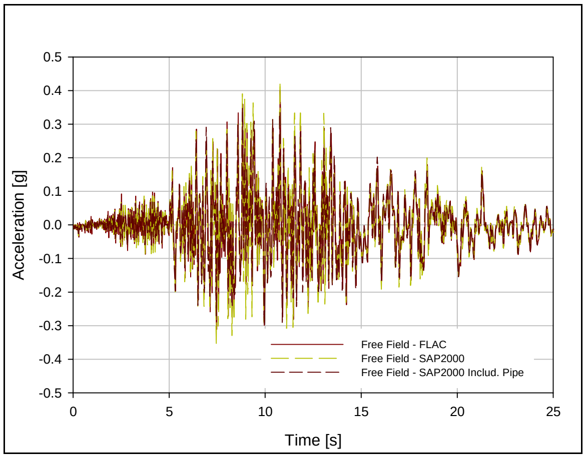

a) Control point 1. At free field

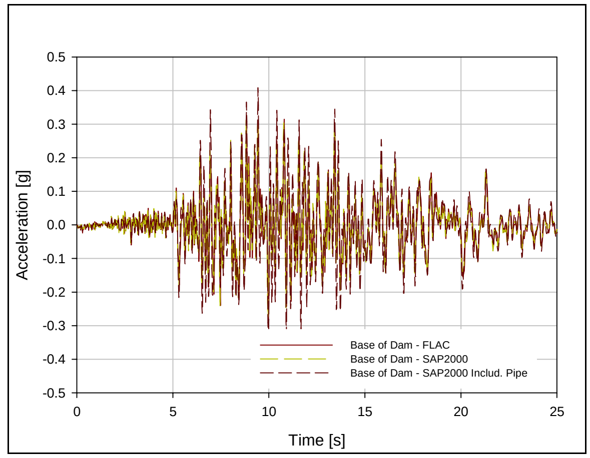

b) Control point 2. At base of dam

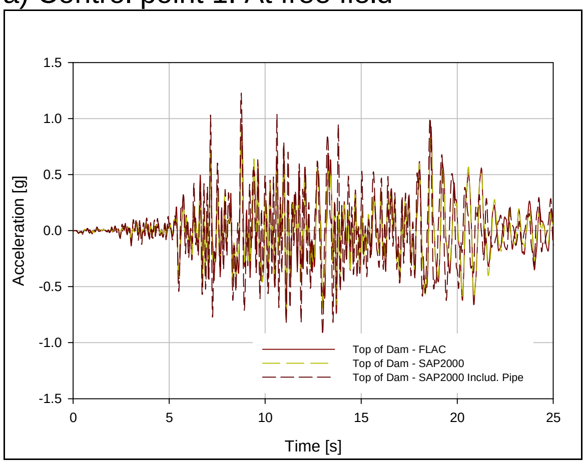

c) Control point 3. At top of dam

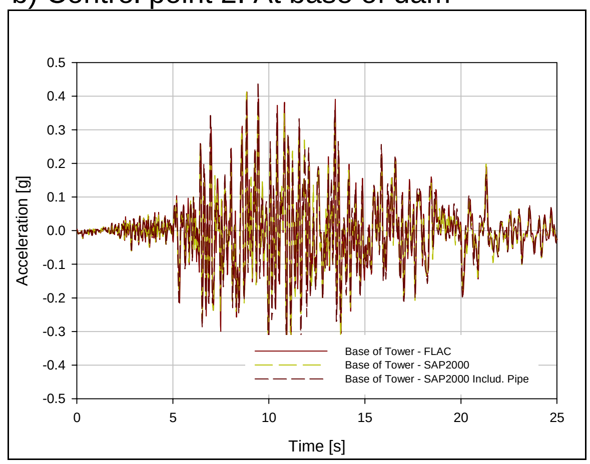

d) Control point 4. At base of tower

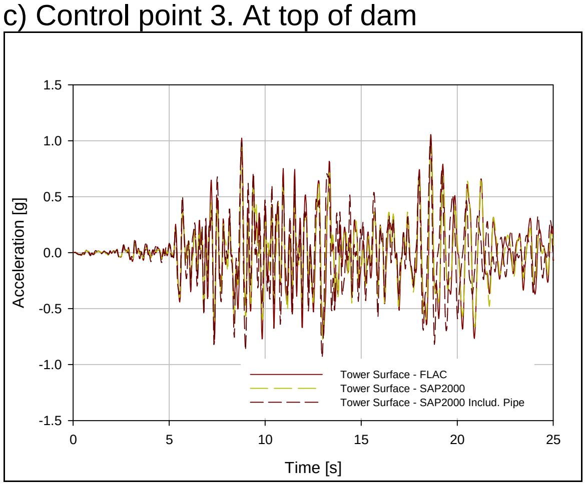

e) Control point 5. At tower surface

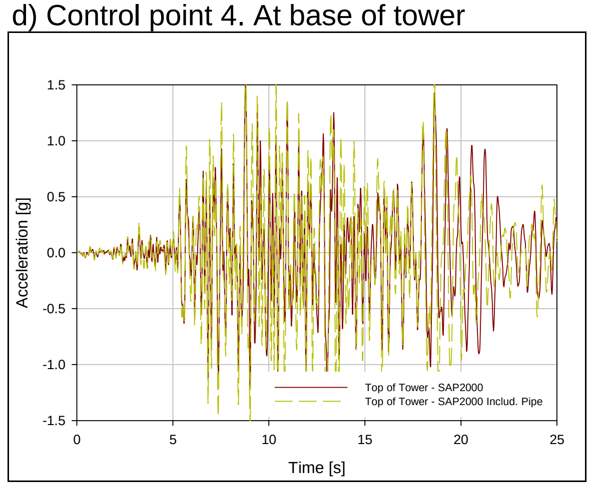

f) Control point 6. At top of tower

Figure 4-35 Acceleration Time Histories at Control Points for the 2D Models Including the Control Tower and the Intake Pipe

4.6.3.3 Comparison of Pseudo Acceleration Response Spectra

Figure 4-36 presents the pseudo acceleration response spectra at the six control points of analysis obtained using the FEM and EFDM methodologies that included both the tower and the intake pipe in the model. The spectra obtained without including the intake pipe are also shown for comparison.

The plots of Figure 4-36 show the spectrum of the input ground motion. The response spectra for Control Points 1, 2, and 4 are not affected much by the dam due to their location. Hence, tend to show one predominant peak in their response spectra that is closely related to the peak of the input ground motion spectrum. The response spectra for Control Points 3, 5, and 6 are affected by the natural periods of the dam-tower-pipe system.

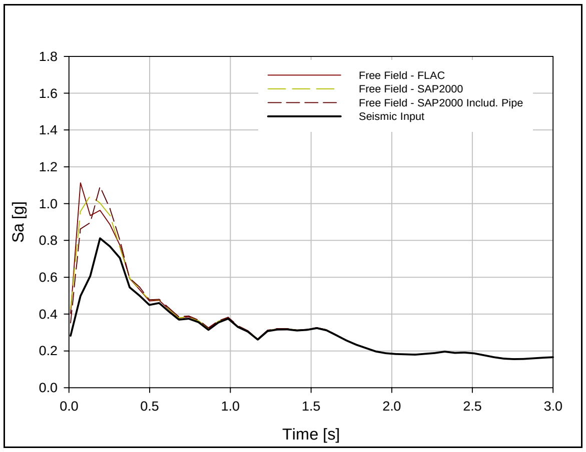

a) Control point 1. At free field

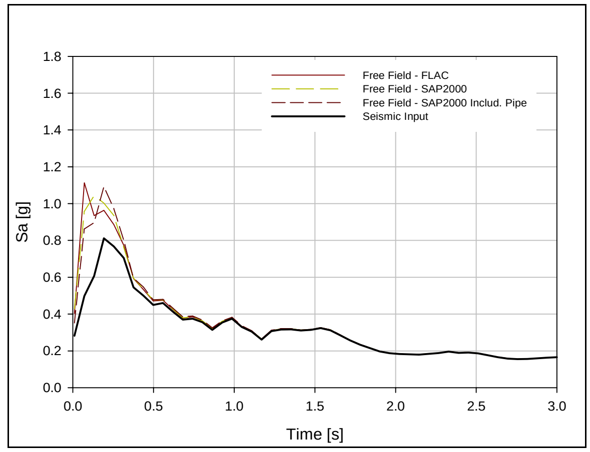

b) Control point 2. At base of dam

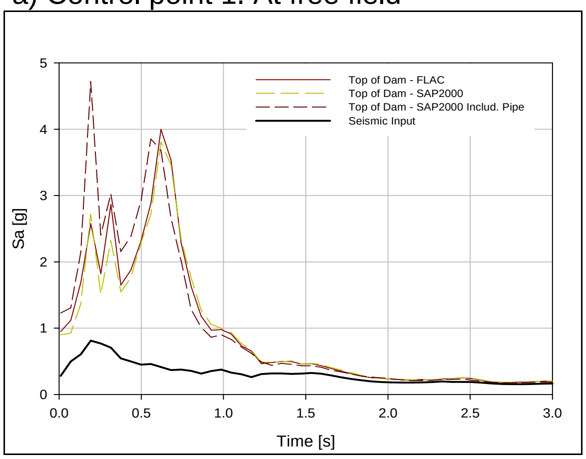

c) Control point 3. At top of dam

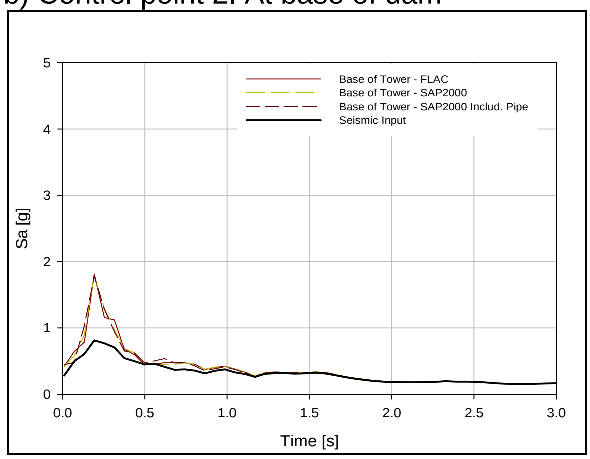

d) Control point 4. At base of tower

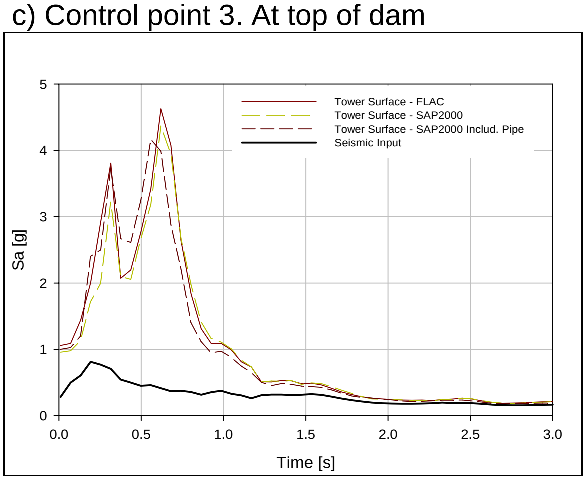

e) Control point 5. At tower surface

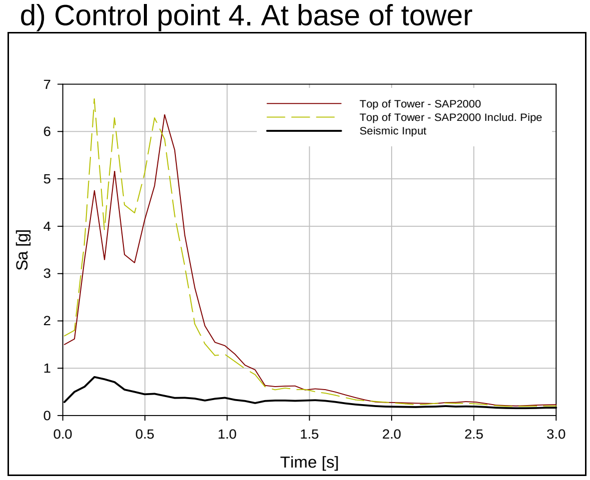

f) Control point 6. At top of tower

Figure 4-36 Pseudo Acceleration Response Spectra at Control Points for the 2D Models Including the Control Tower and the Intake Pipe

The magnitudes of the first five natural periods of the dam-tower0pipe system were computed with SAP2000 and are summarized in Table 4-12.

Comparison of the results from Table 4-12 and Table 4-10 indicate the presence of the pipe intake pipe has no significant impact on the periods.

Table 4-12 Natural Periods from the 2D SAP2000 FEM Model Including the Control Tower and the Intake Pipe

Mode Number	Period [s]	Modal Participating Mass Ratio
1	0.598	0.3001
2	0.384	0.0044
3	0.358	0.0092
4	0.354	0.0028
5	0.312	0.1069

In general, the spectra obtained are also not affected significantly by the addition of the intake pipe to the models. There are, however, small differences in the peaks of the response spectra at a period of about 0.3 s for the control points at the base of the dam and at the tower surface. Note that there are four natural periods at the period range between 0.3 and 0.38 s. Therefore, it is pointful to examine the base shear since the new conditions at the base of the tower and dam may modify the structures response. This will be done in a following section.

4.6.3.4 Vibration Modes Shapes Using SAP2000

As in the previous models, the first five vibration modes of the 2D models that include the control tower and the intake pipe were retrieved from the SAP2000 output. They are displayed in Figure 4-37 through Figure 4-41.

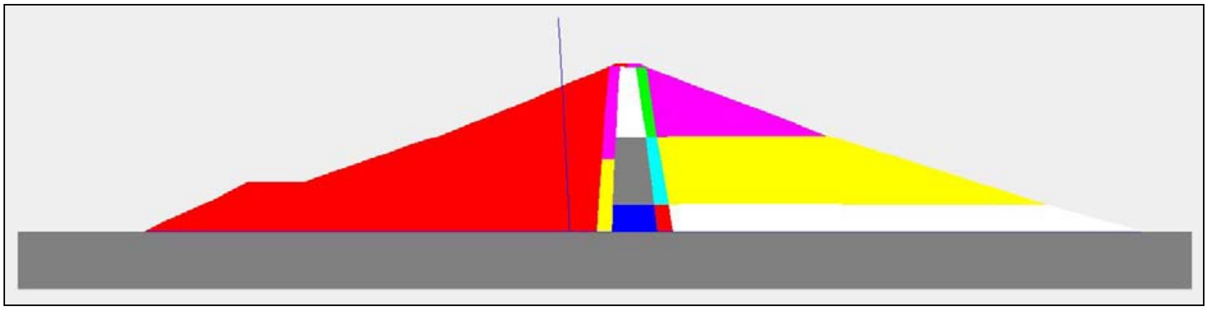

Figure 4-37 First Vibration Mode Shape of the 2D Model Including the Control Tower and the Intake Pipe

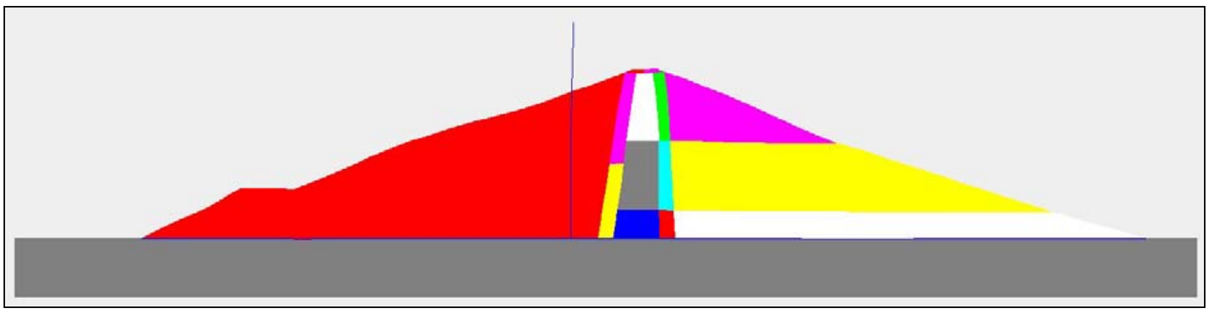

Figure 4-38 Second Vibration Mode Shape of the 2D Model Including the Control Tower and the Intake Pipe

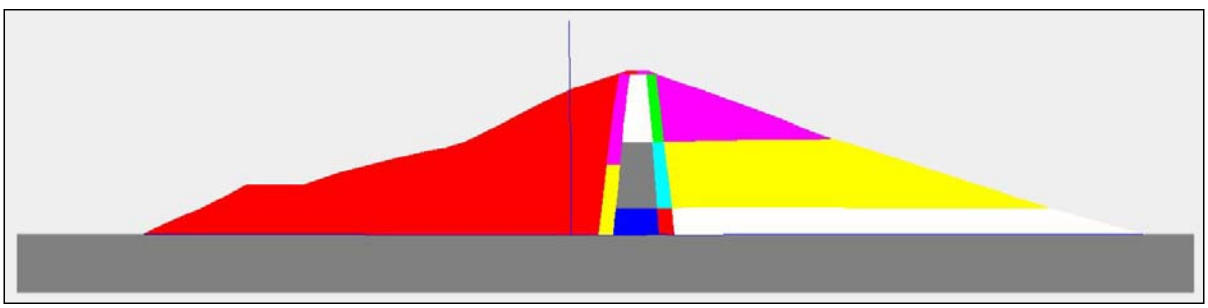

Figure 4-39 Third Vibration Mode Shape of the 2D Model Including the Control Tower and the Intake Pipe

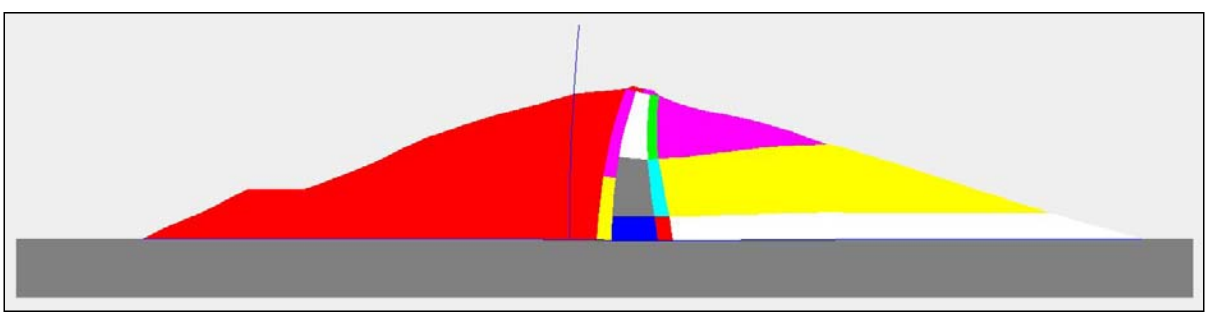

Figure 4-40 Fourth Vibration Mode Shape of the 2D Model Including the Control Tower and the Intake Pipe

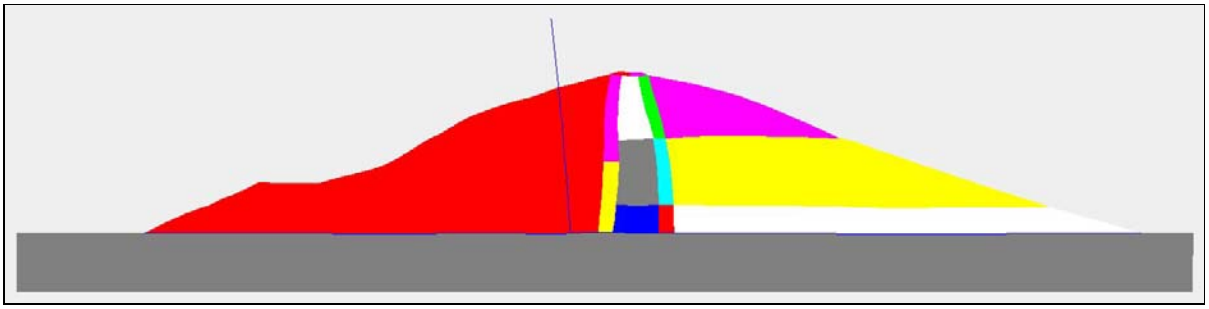

Figure 4-41 Fifth Vibration Mode Shape of the 2D Model Including the Control Tower and the Intake Pipe

4.6.3.5 Comparison of Reactions at the Tower Base Including the Intake Pipe

The time histories of the base shear force at the base of the tower computed using both types of models that include tower and intake pipe are presented in Figure 4-42.

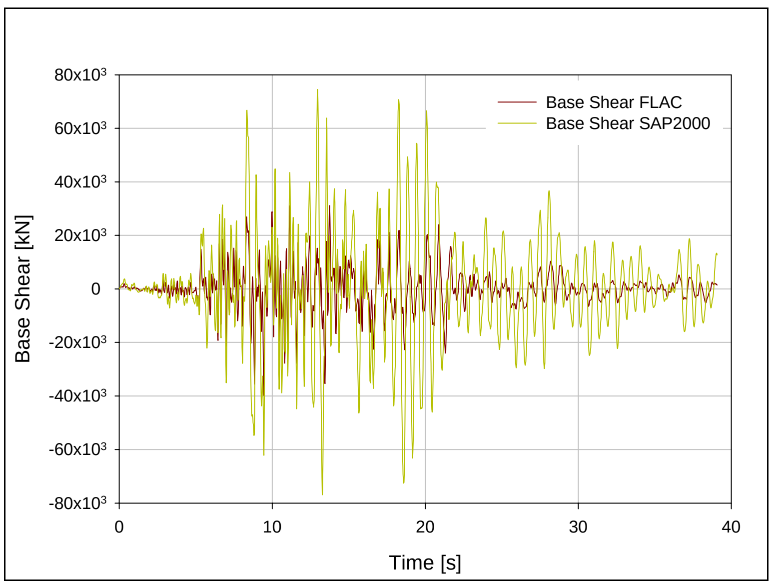

Figure 4-42 Base Shear Force Time Histories on the Control Tower for 2D Models That Include the Intake Pipe

The base shear time histories computed including the intake pipe in the FEM and that from the equivalent model without the intake pipe have similar variation. However, the peaks in the first case are higher mainly because the intake pipe modifies the conditions of the base of the control tower. The connection between the control tower and the intake pipe is very stiff, therefore reducing the rotation and displacement of the base of the tower. The maximum values of the base shear force and bending moment at the base of the control tower obtained using three methodologies are presented in Table 4-13.

Table 4-13 Maximum Reaction Values Acting on the Control Tower

Method of Analysis	Maximum Base Shear [kN]	Time of Occurrence [s]	Maximum Bending Moment [kN-m]	Time of Occurrence [s]
2D Including the Intake Pipe – SAP2000	76912	13.28	1416747	18.6
2D FEM – SAP2000	39826	9.46	8427	19.64
2D EFDM – FLAC2D	37565	9.48	53	8.8

It is also instructive to examine the maximum shear force acting along the shaft of the control tower, and the shear force distribution when the maximum base shear occurs. These two conditions are presented in Figure 4-43 and Figure 4-44, respectively.

Note that the shape of the distribution in Figure 4-44 is similar to that in Figure 4-43, except for the sign which is ignored when the maximum shear forces are plotted. This means that the maximum shear forces along the tower occur at a similar time that at the base.

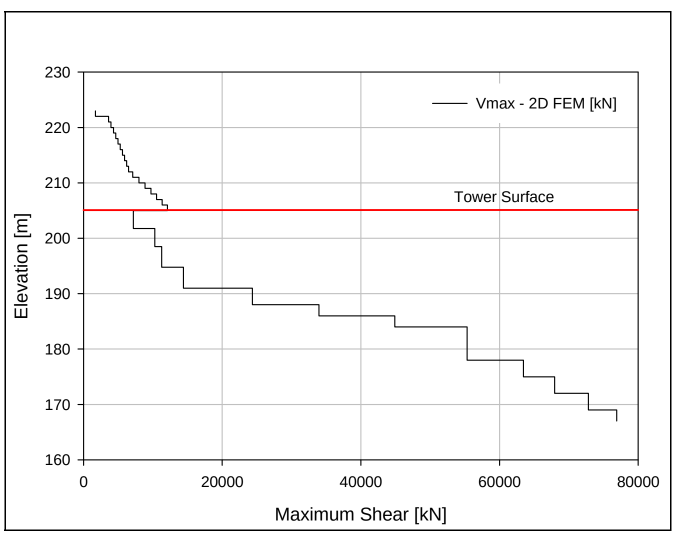

Figure 4-43 Maximum Shear Force Acting Along the Control Tower using 2D Analyses Including the Intake Pipe

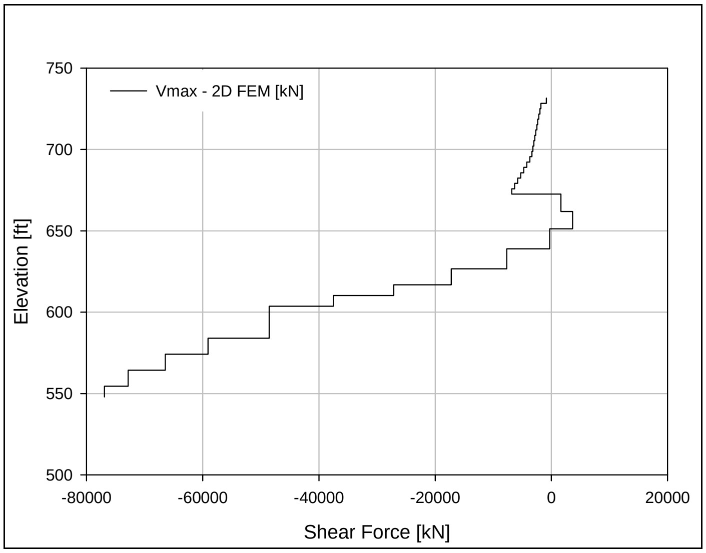

Figure 4-44 Shear Force Distribution When the Maximum Shear Force Occurs Including the Intake Pipe

As mentioned before, it is also important to consider the maximum bending moment acting along the shaft of the control tower, and the bending moment distribution when the maximum bending moment at the base occurs. These two plots are presented in Figure 4-45 and Figure 4-46, respectively.

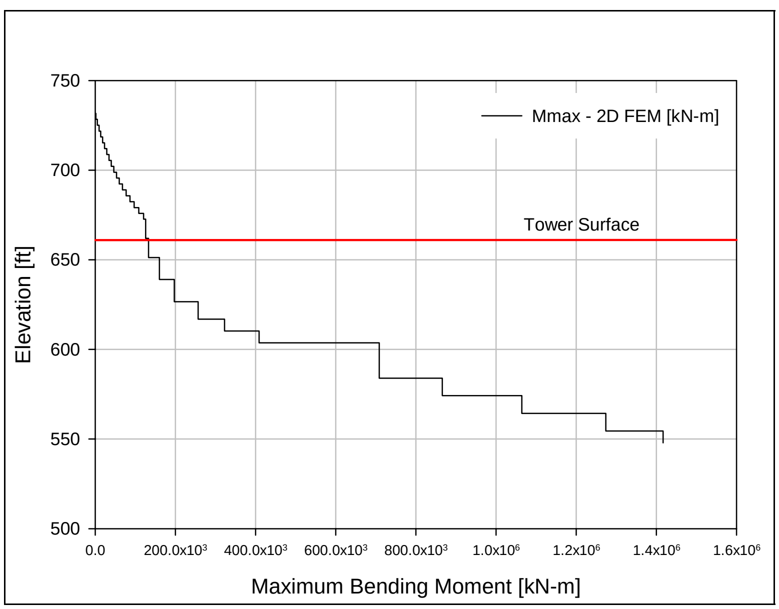

Figure 4-45 Maximum Bending Moment Acting Along the Control Tower Using 2D Analyses Including the Intake Pipe

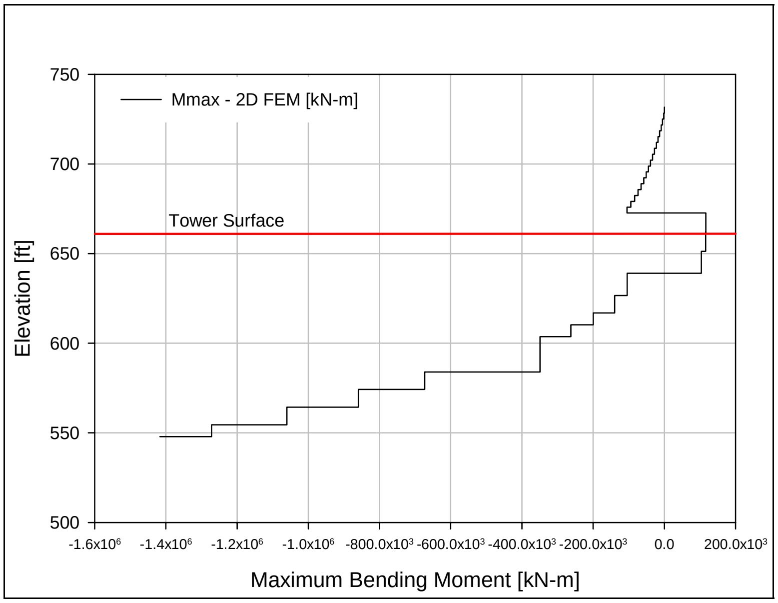

Figure 4-46 Bending Moment Distribution When the Maximum Bending Moment at the Base of the Control Tower Occurs Including the Intake Pipe

4.7 Results of the 2D DSSI Linear Equivalent Analysis

As described in Section 4.5 the linear equivalent method is considered one of the best practical approaches to incorporate the non linear behavior of soils under dynamic load conditions. Due to the difficulty of this type of analysis, it was only included for the 2D DSSI analysis of the dam including the control tower and the intake pipe. As mentioned in Section 4.5, first a 2D model without structures is analyzed using the linear equivalent method implemented in QUAKE/W, and then the results are used as input for a 2D model including the control tower and the intake pipe using SAP2000.

The use of additional software and numerical methods can add difficulty to the analyses of the complete set of results; therefore, the comparison of results is presented directly only in terms of the maximum base shear force and maximum bending moment at the base of the tower. These results are presented in section 4.7.3

4.7.1 Shear Strain Contours

The shear strain contours obtained using the computer program QUAKE/W and the equivalent linear method correspond to the shear strain required according to the G/G_{max}, and β versus γ curves for a satisfactory convergence of the results. These final values are the best estimate of the soil stiffness reduction and damping increase developed by the soil during the dynamic load. The shear strain contours obtained for the 2D model without structures are presented in Figure 4-47.

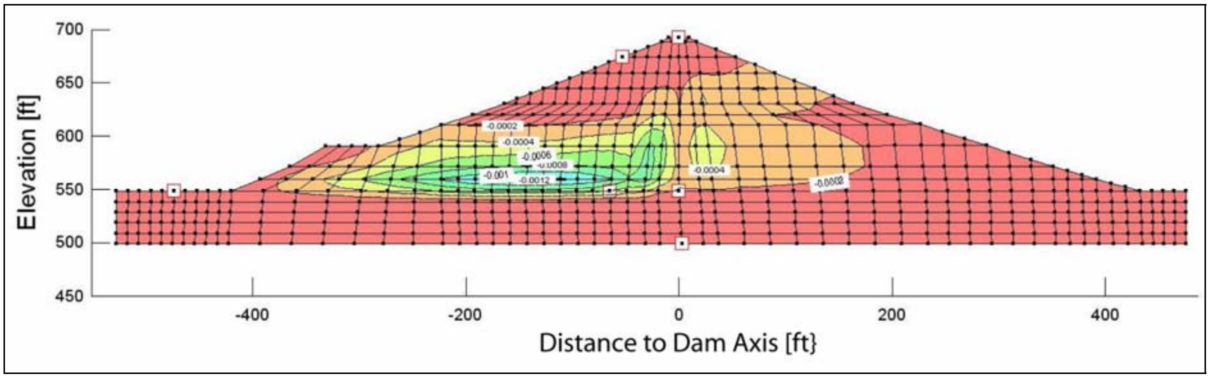

Figure 4-47 Shear Strain Contours from QUAKE/W 2D Model without Structures

Figure 4-47 indicates that the higher shear strain (0.0012) occurs at the base of the dam towards the upstream side. The model did not include the effect of the reservoir.

The shear strain values were used to establish zones of similar stiffness reduction. This simplified approach permitted incorporating somewhat the soil nonlinearity in the SAP2000 2D FEM model that included the control tower and the intake pipe. The zones of similar shear modulus reduction are discussed in the following section.

4.7.2 Shear Modulus Reduction

The shear strain contours presented in Figure 4-47 were used together with the G/G_{max} and β versus γ curves presented in Figure 4-9 to estimate zones with similar stiffness reduction. The resulting shear modulus reduction zones defined for the Success dam soils and the MCE earthquake are presented in Figure 4-48.

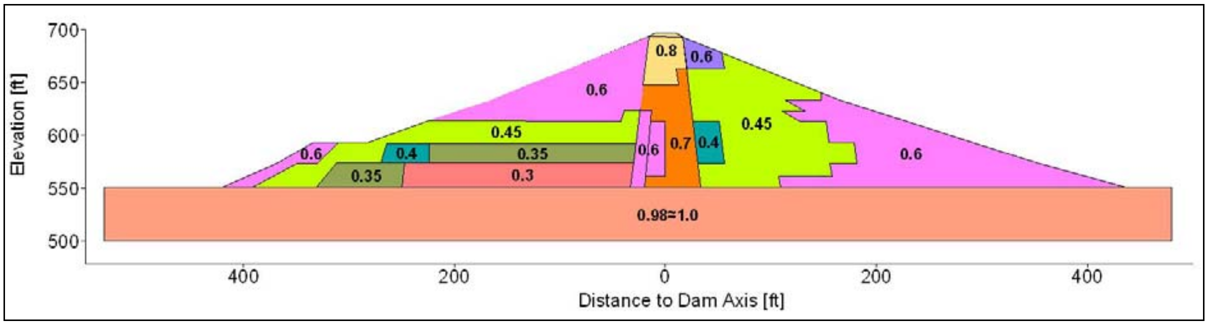

Figure 4-48 Shear Modulus Reduction Ratios From Linear Equivalent Analysis of a 2D Model without Structures

The reduction factors presented in Figure 4-48 were used to compute the new reduced shear modulus for each zone. These reduced shear modulus values were used as input to develop a 2D model using SAP2000 that included both the control tower and the intake pipe.

The results of this model, with reduced stiffness, are presented in the following section in terms of the maximum base shear force and the maximum bending moment at the base of the control tower.

4.7.3 Reactions at Control Tower Base

The time history of the shear force acting at the base of the control tower obtained with the reduced stiffness model is presented in Figure 4-49.

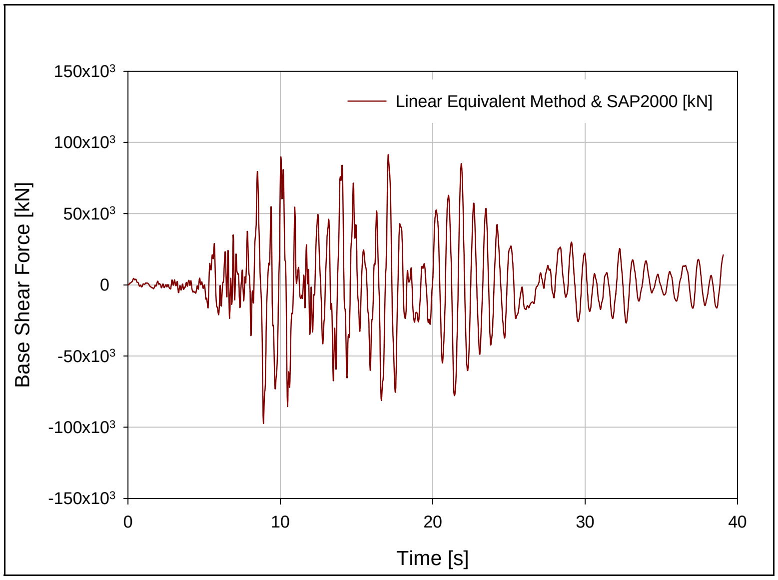

Figure 4-49 Base Shear at the base of the Control Tower Using 2D Model Including the Intake Pipe and the Linear Equivalent Method

The maximum base shear force and the maximum bending moment at the base of the control tower obtained using the above mentioned methodology are presented in Table 4-14.

Table 4-14 Maximum Base Shear Force and Bending Moment at the Base of the Control Tower Using 2D Model including the Intake Pipe and the Linear Equivalent Method

Method of Analysis	Maximum Base Shear Force [kN]	Time of occurrence [s]	Maximum Moment at Control Tower Base [kN-m]	Time of occurrence [s]
2D SAP2000 – LEM	97320	8.88	1702628	17.12

The maximum shear force envelope along the shaft of the control tower, and the shear force distribution when the maximum base shear occurs are presented in Figure 4-50 and Figure 4-51, respectively.

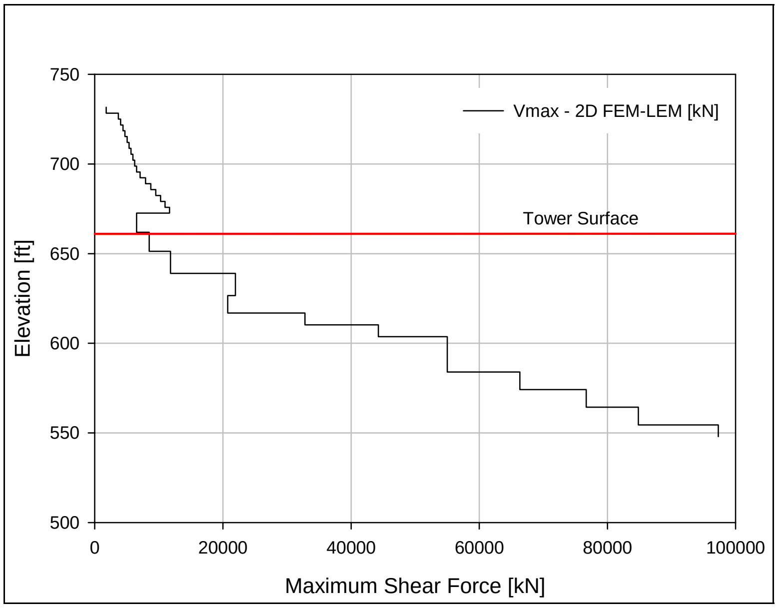

Figure 4-50 Maximum Shear Force Acting Along the Control Tower Using 3D Analyses

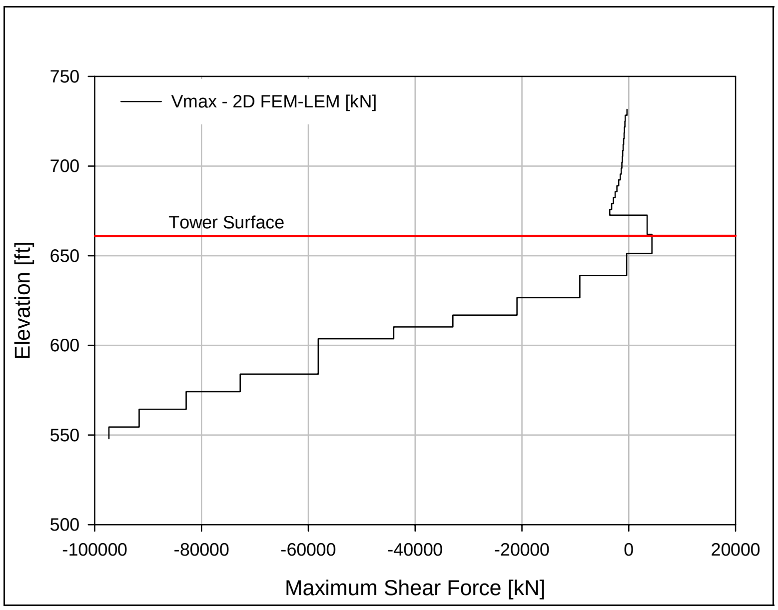

Figure 4-51 Shear Force Distribution When the Maximum Shear Occurs using 3D Analyses

Similarly, the maximum bending moment envelope along the shaft of the control tower, and the bending moment distribution when the maximum bending moment at the base of the control tower occurs are presented in Figure 4-52 and Figure 4-53, respectively.

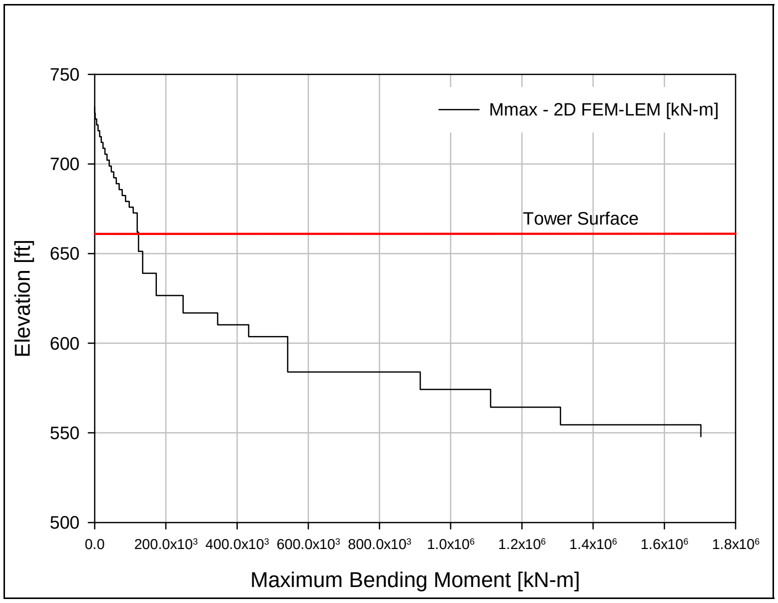

Figure 4-52 Maximum Bending Moment Acting Along the Control Tower Using 3D Analyses

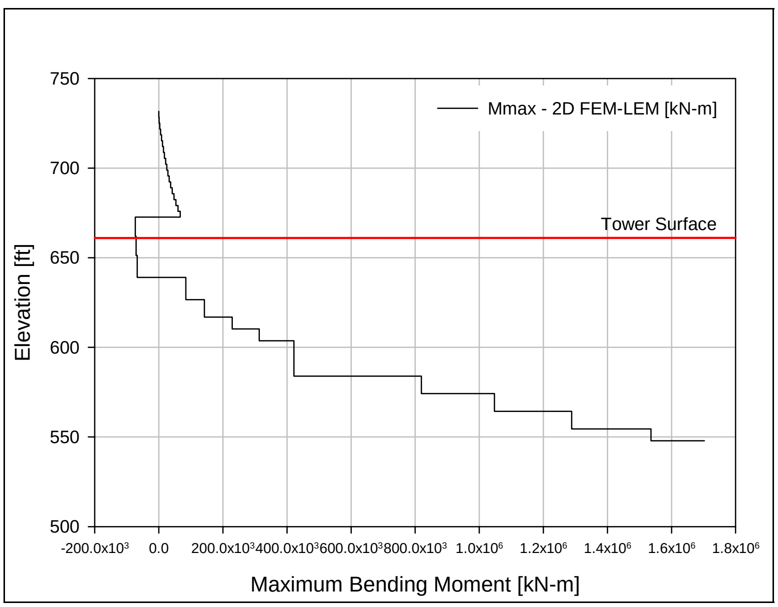

Figure 4-53 Bending Moment Distribution When the Maximum Bending Moment at the Base of the Control Tower Occurs Using 3D Analyses

5 THREE DIMENSIONAL DSSI ANALYSES

Two three-dimensional models were developed to evaluate 3D present in the dynamic soil structure interaction problem of the embedded tower. The first 3D model includes the control tower only, while the second 3D model includes both the control tower and the intake pipe. For simplicity, the 3D models were linear elastic and used the same material properties values as those used in the 2D models. The main difference in the 3D models is the direct representation of the structures (tower and discharge pipe) which did not have to be converted to equivalent 2D representations. As discussed earlier, this is one of the main sources of uncertainty in the 2D models (for the ones presented in this thesis or published earlier). All 3D analyses were carried out using only the FEM software SAP2000 due to time considerations and ease of use.

5.1 Dam Modeling Information

As mentioned earlier, the case of the seismic response of the dam in which the representative section used for the model includes structures with short extent along the perpendicular axis out of the plane on a simplified 2D model has some limitations. The most important limitation is the fact that it is necessary in a 2D model to combine plane strain elements representing the assumed infinitely long dam, with plane stress elements commonly used to model structures. The other limitation is that this 2D model cannot account for the dissipation of the seismic input energy in the longitudinal (out-of-plane) direction. There are techniques proposed to take into account the effect of the three dimensional radiation damping. In some cases it can be partially accounted for by using dashpots on every node or zone of the 2D model so they can represent the dissipation of the radiating waves in the out-of-plane direction. Nevertheless, these assumptions or simplifications are completely avoided when a full 3D model is used. However, since 3D FE models are also bounded in the longitudinal direction, the radiation damping is only approximately accounted for.

However, by sufficiently extending the model in the out-of-plane direction, one can minimize the artificial wave reflections and thus reasonably represent the radiation damping.

The soil properties, the seismic input, and the distribution of the finite elements in the dam cross section plane are the same as those used for the 2D models. Only an extrusion of the area elements over the out-of-plane direction was performed until a 80 m deep model was obtained. The procedure followed to define the practical width of the model is presented in section 5.2 of this chapter. The extrusion was accomplished using 20 elements with a 4 m length each. Figure 5-1 presents the 3D model and the geotechnical zones used in the analyses.

The following boundary conditions were applied:

- All the nodes at the base of the model were fixed. The seismic input was applied at the base as a time history of accelerations in the horizontal direction normal to the dam longitudinal axis (the same MCE record was used).
- All the nodes in the vertical faces of the model located at the dam foundation were only restrained against vertical movement.

The 3D FEM model had the following main characteristics:

- 12200 solid elements
- 30 frame elements
- 14172 nodes
- 11 types of geotechnical materials
- Time step 0.02 s

- Damping formulation: Rayleigh method. Critical damping ratio = 5% at the response in the first natural period.

- Integration method: Newmark with gamma = 0.5 and beta =0.25, also called the trapezoidal rule.

A modal analysis was performed only to evaluate the fundamental periods corresponding to the first five vibration modes.

The seismic response of the 3D model was obtained using a time history analysis. A modal analysis would have required an important number of modes in order to be representative of the true response of the model, and therefore a longer time of computational resources. In addition, the combination of the response of all the modes adds some uncertainty to the final results, as this is avoided by using a time history analysis.

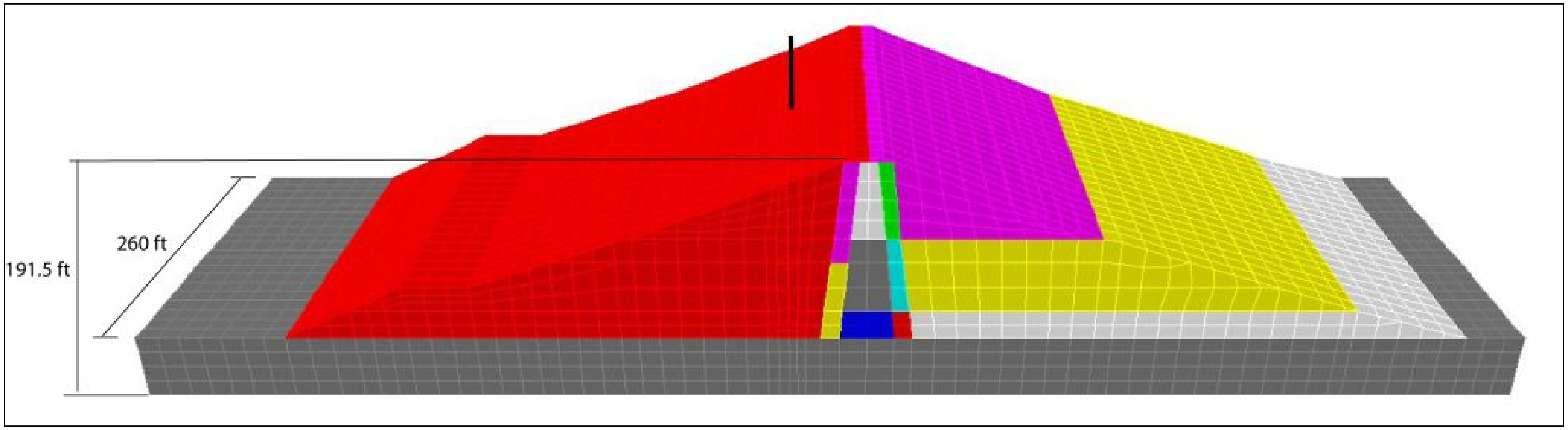

Figure 5-1 3D Finite Element Method Model Including the Control Tower

The same control points used for the 2D models were used for the 3D models. This allowed easy comparison of results among the different models (2D and 3D). The control points are located on the plane of the control tower, to be consistent with the previous analyses. Figure 5-2 shows the location of the control points of analysis.

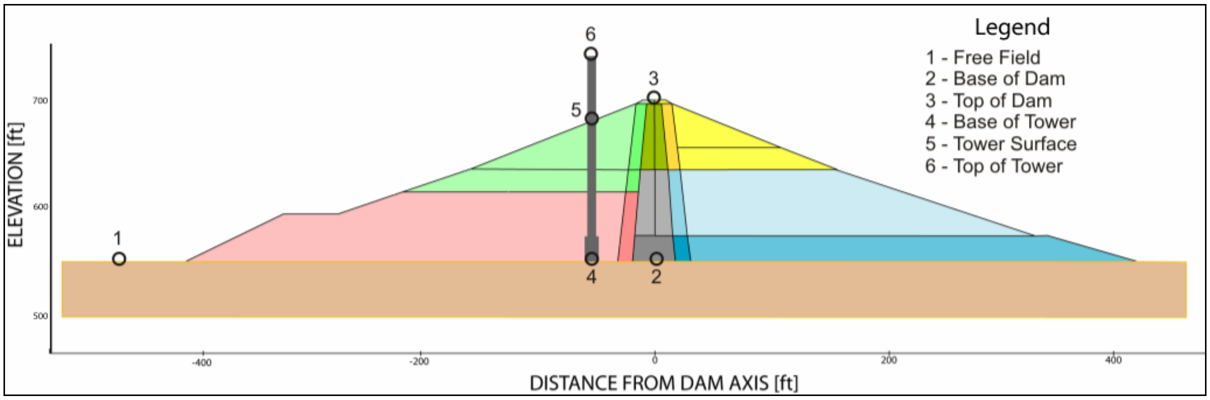

Figure 5-2 Control Points of Analysis for Comparison of Results

The material properties used to model the dam and structures were discussed in Chapter 3.

5.2 Definition of the Optimum Depth of the 3D Model

The 3D model is analyzed under dynamic conditions. In dynamic modal analyses, it is a generally accepted matter that the first mode is usually the most important because it usually controls the seismic response of the majority of systems. The dynamic analyses carried out in this study are time history analyses.

The selection of the optimum depth of the 3D model was based on assessing the convergence of the first natural period of the model and on practical consideration (i.e. running time and size of the model). The convergence of the first natural period was considered optimum when the increase of the depth of the model resulted in less than 0.5% change in the magnitude of the period. A model was defined as of practical use when the computation time was less than 24 hours, and when the size of the memory required to store the results was less than 30 Giga Bytes (GB).

After several trials the optimum depth of the model was defined as 262 ft (80 m). this depth resulted in a running time of about 1 hour and a size of the results file of about 27 GB. The Figure 5-3 through Figure 5-6 show different 3D models used to evaluate the above mentioned factors. Figure 5-7 shows the convergence of the first natural period of the 3D model.

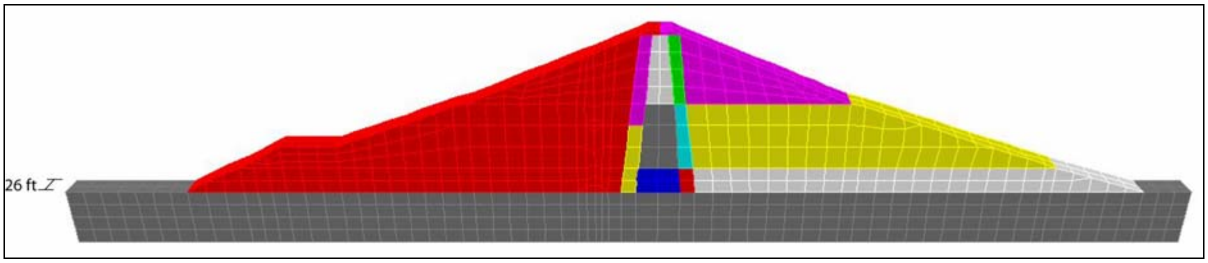

Figure 5-3 3D Model – 26 ft (8 m) Depth

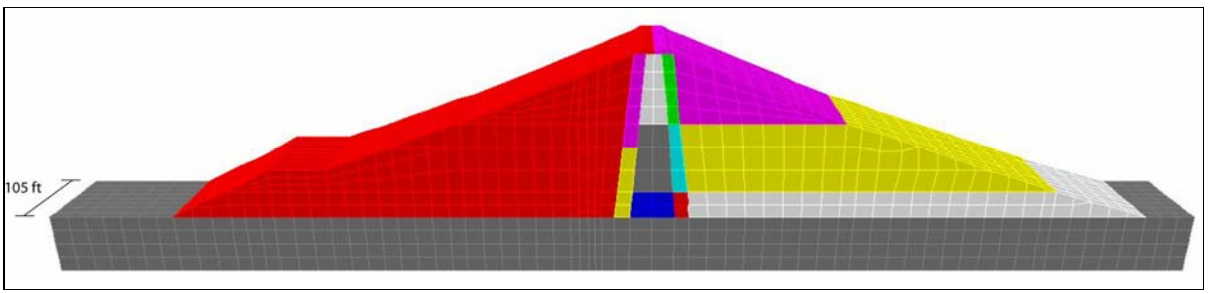

Figure 5-4 3D Model – 105 ft (32 m) Depth

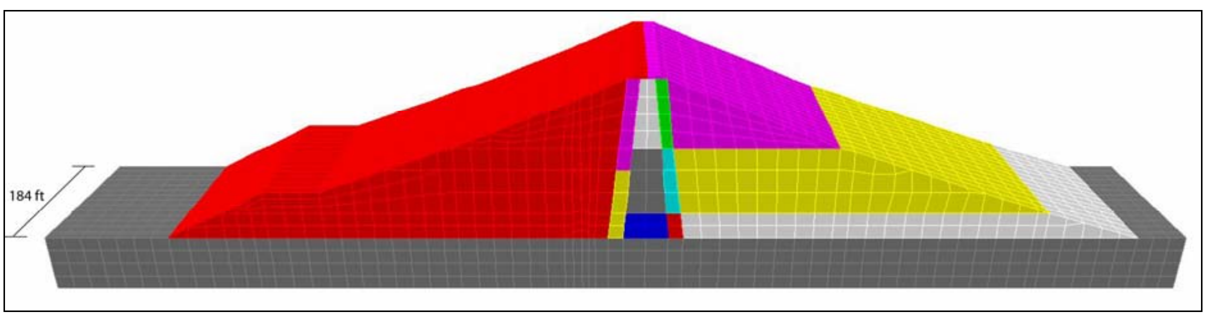

Figure 5-5 3D Model – 184 ft (56 m) Depth

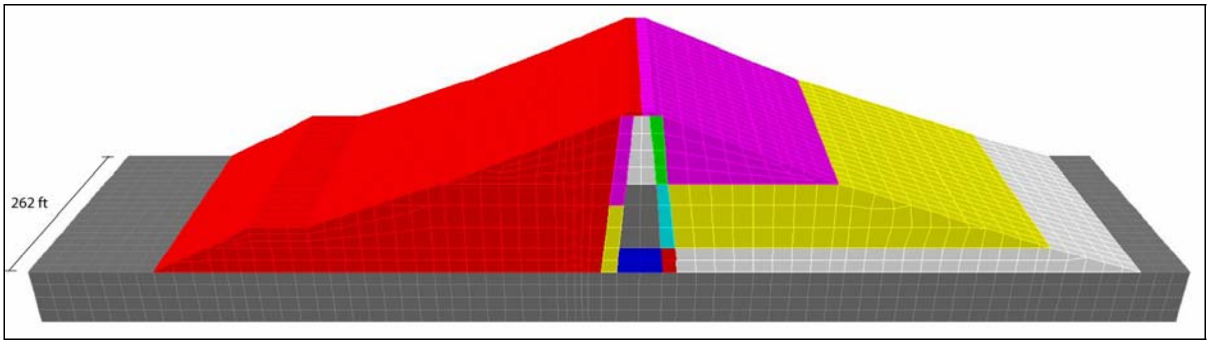

Figure 5-6 3D Model – 262 ft (80 m) Depth

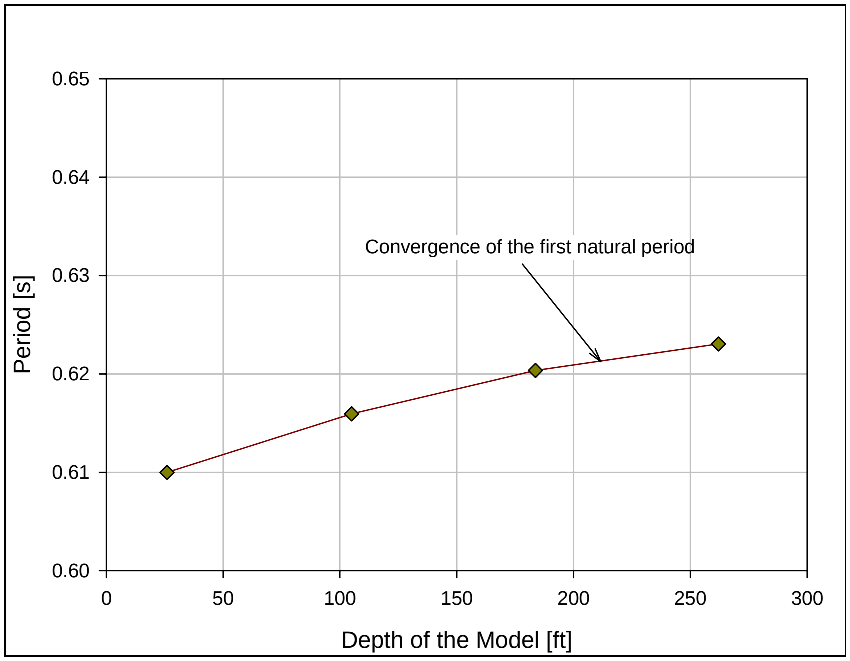

Figure 5-7 Convergence of the First Natural Period

Table 5-1 lists the first natural period for the different 3D models depths shown on Figure 5-3 through Figure 5-6, and the percentage of change with the depth of the model.

Table 5-1 Convergence of the First Natural Period

3D Model Depth [ft]	First Natural Period [s]	Change [%]
105	0.6159	0.9732
183.7	0.6203	0.7169
262	0.6230	0.4337

5.3 Results of the 3D DSSI Linear Analyses

This section presents the results for two 3D models analyzed using SAP2000 (FEM). The first model includes only the control tower, the second model includes the control tower and the intake pipe.

5.3.1 DSSI Analyses for a 3D Model of the Dam Including the Control Tower

The results are presented in terms of relative displacement and absolute acceleration time histories, and pseudo acceleration response spectra calculated at the six control points of analysis previously defined. Additionally, the shear force at the base of the control tower is presented. Where possible, results of the 2D models are presented, so that the three dimensional effects can be evaluated.

5.3.1.1 Comparison of Displacement Time Histories

Figure 5-8 presents the relative displacement time histories obtained using the 3D model for the six control points. This figure shows SAP2000 results obtained from both 3D and 2D models. This model includes the control tower only. As it is evident from these figures, there are no important differences in terms of the history of displacements calculated with the two approaches. The maximum displacement computed from the 3D model at the top of the dam was 0.075 m. This is in very good agreement with the value obtained with the 2D FEM model of 0.074 m.

The 3D model yields a maximum displacement at the Top of the Tower point of 0.131 m and a displacement at the Tower Surface point of 0.088 m at the same time. The corresponding maximum drift of the part of the tower above the embedment is:

$$Drift = \frac{0.131m - 0.088m}{18m} \times 100\% = 0.24\%$$

This maximum drift of the tower occurred 18.60 s after the beginning of the seismic motion.

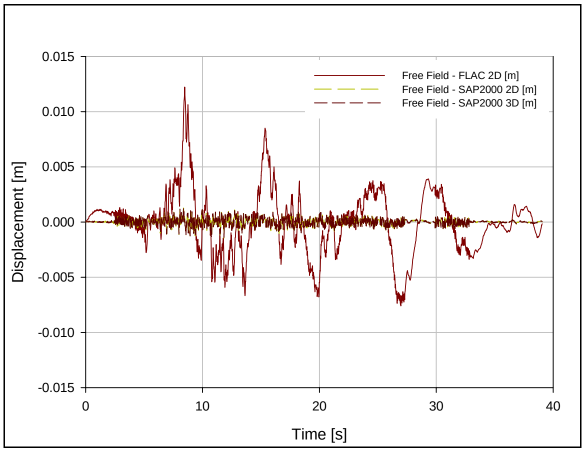

a) Control point 1. At free field

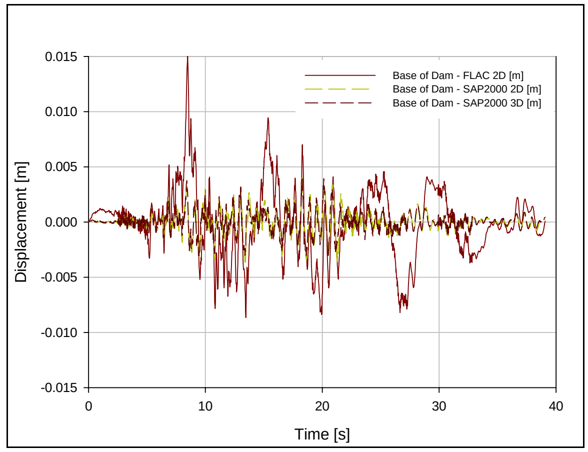

b) Control point 2. At base of dam

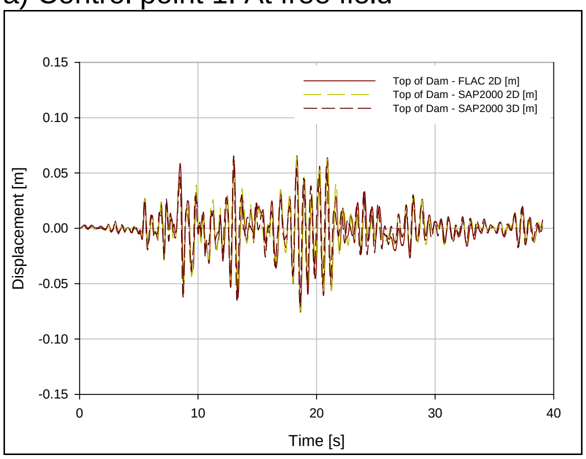

c) Control point 3. At top of dam

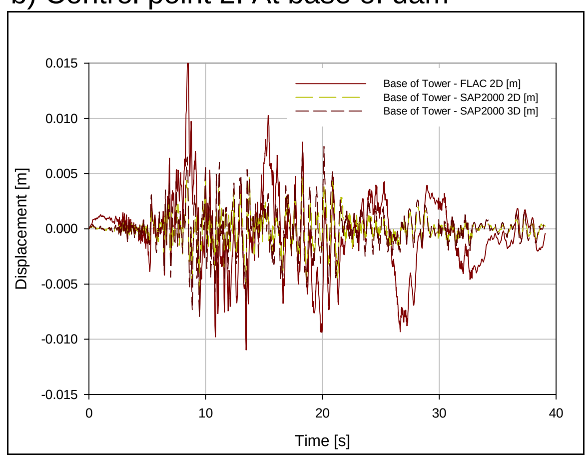

d) Control point 4. At base of tower

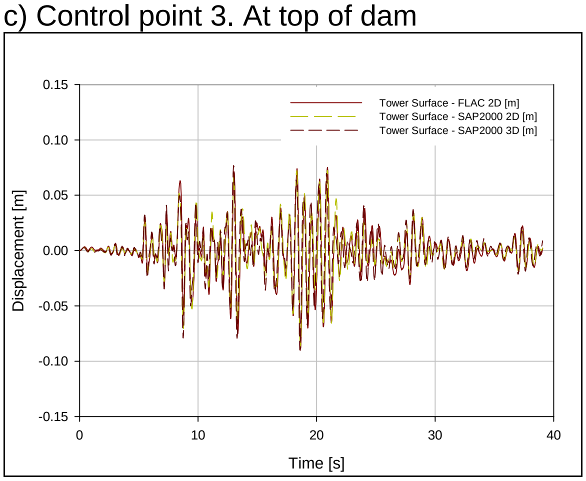

e) Control point 5. At tower surface

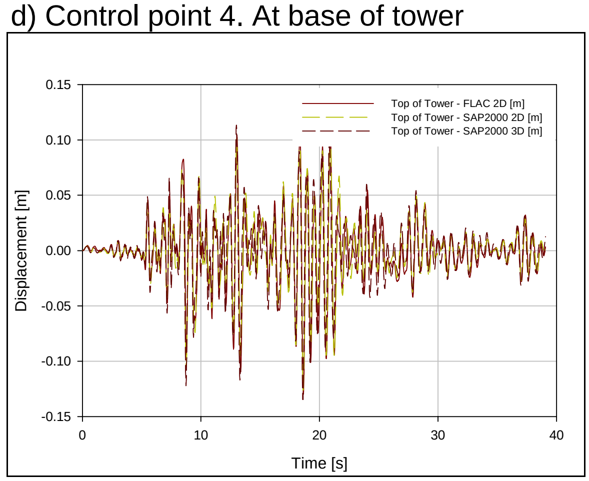

f) Control point 6. At top of tower

Figure 5-8 Displacement Time Histories at Control Points for 3D and 2D Models Including the Control Tower

5.3.1.2 Comparison of Acceleration Time Histories

Figure 5-9 presents the absolute acceleration time histories obtained using the 3D model for the six control points. To appreciate better the results, only the first 25 s of the accelerograms are displayed. For comparison purposes, the results from the SAP2000 2D model are also shown. Both models only include the control tower. Results shown in this figure indicate good agreement between 2D and 3D models using SAP2000.

The following section presents results in terms of response spectra for 5% structural damping ratio calculates using the accelerograms in Figure 5-9.

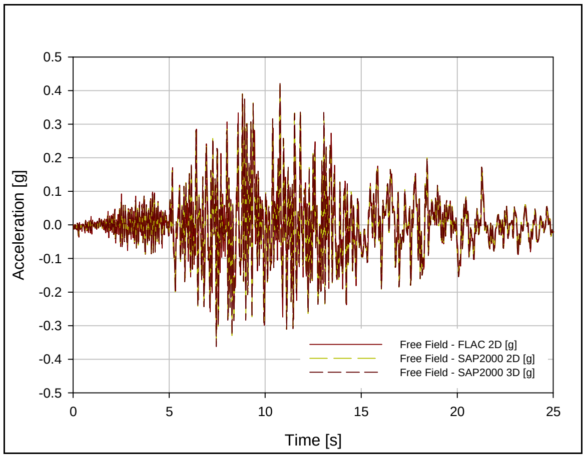

a) Control point 1. At free field

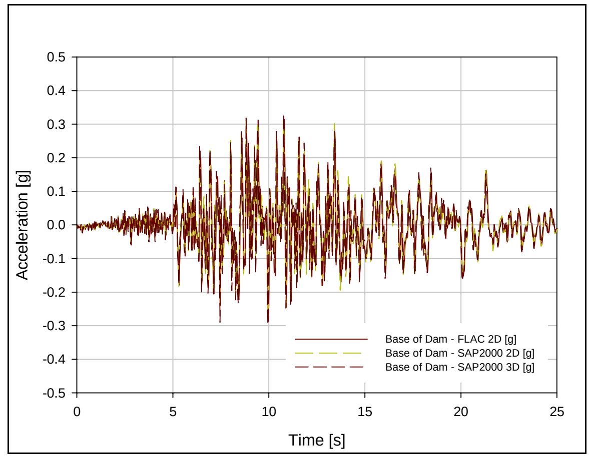

b) Control point 2. At base of dam

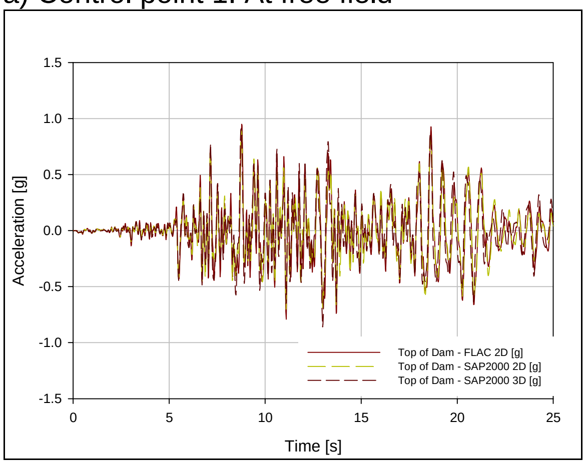

c) Control point 3. At top of dam

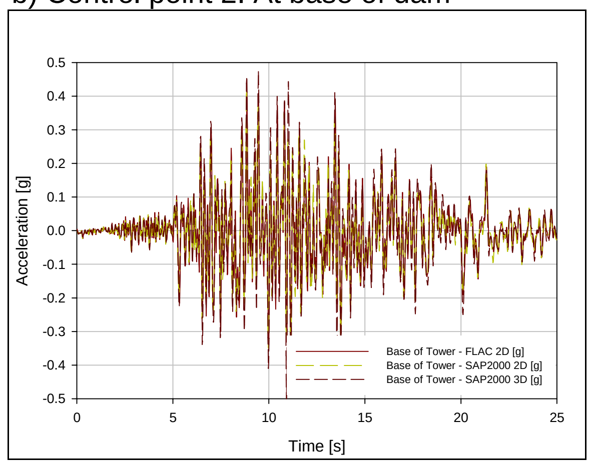

d) Control point 4. At base of tower

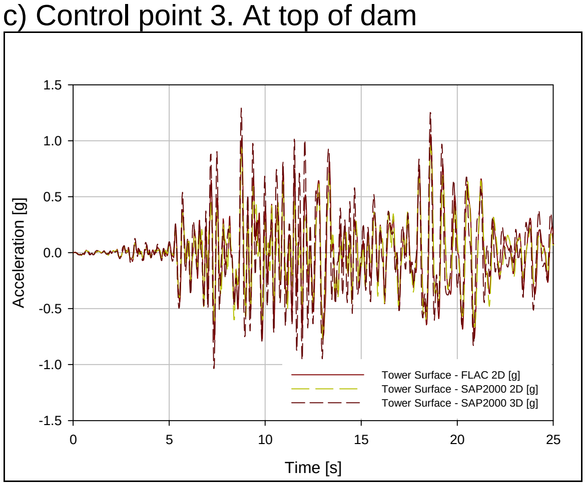

e) Control point 5. At tower surface

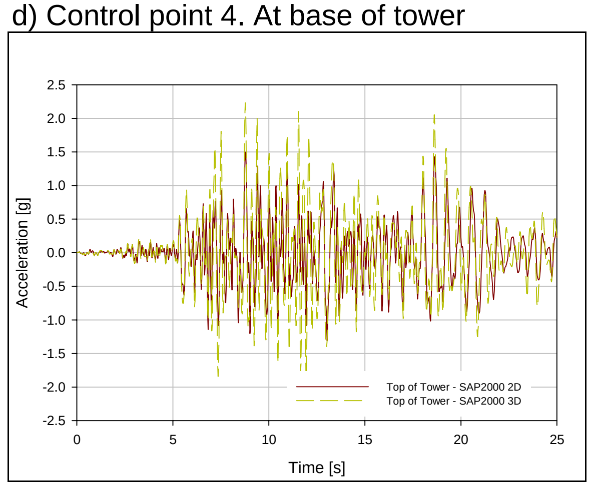

f) Control point 6. At top of tower

Figure 5-9 Acceleration Time Histories at Control Points for 3D and 2D Models Including the Control Tower and Without the Intake Pipe

5.3.1.3 Comparison of Pseudo Acceleration Response Spectra

Figure 5-10 shows the pseudo acceleration response spectra for the six control points selected for the analyses. Each plot presents results from the SAP2000 2D and 3D models that only include the control tower. The plots also include the response spectra for the input ground motions.

For comparison purposes and to observe the amplification the response spectrum of the original accelerogram applied at the base of the foundation is also included in the plots. As expected, the largest amplification of the original response spectrum occurs at the lower three natural periods of the system. At these points the amplification factors vary from 3 to 6. The natural periods of the dam-foundation-tower system are provided in the next section.

The results presented in Figure 5-10 show close agreement between the 2D and 3D models for Control Points 1 through 4 which are away from the control tower. Large differences are observed for Control Point 5 and 6 at the surface and top of the tower, respectively. The large differences are observed at a period close to the natural period of the input ground motion. The 3D models result in spectral values at this period that are between 1.5 to almost 2 times higher than the values for the corresponding 2D models.

In general, one can say that the shape of the spectra obtained with the three different methods, i.e. the 3D and 2D models of SAP2000 and the 2D model of FLAC, are quite similar. There are some differences in the peak at the lowest period for the spectra at the point where the tower emerges from the dam, the 3D model predicting higher values.

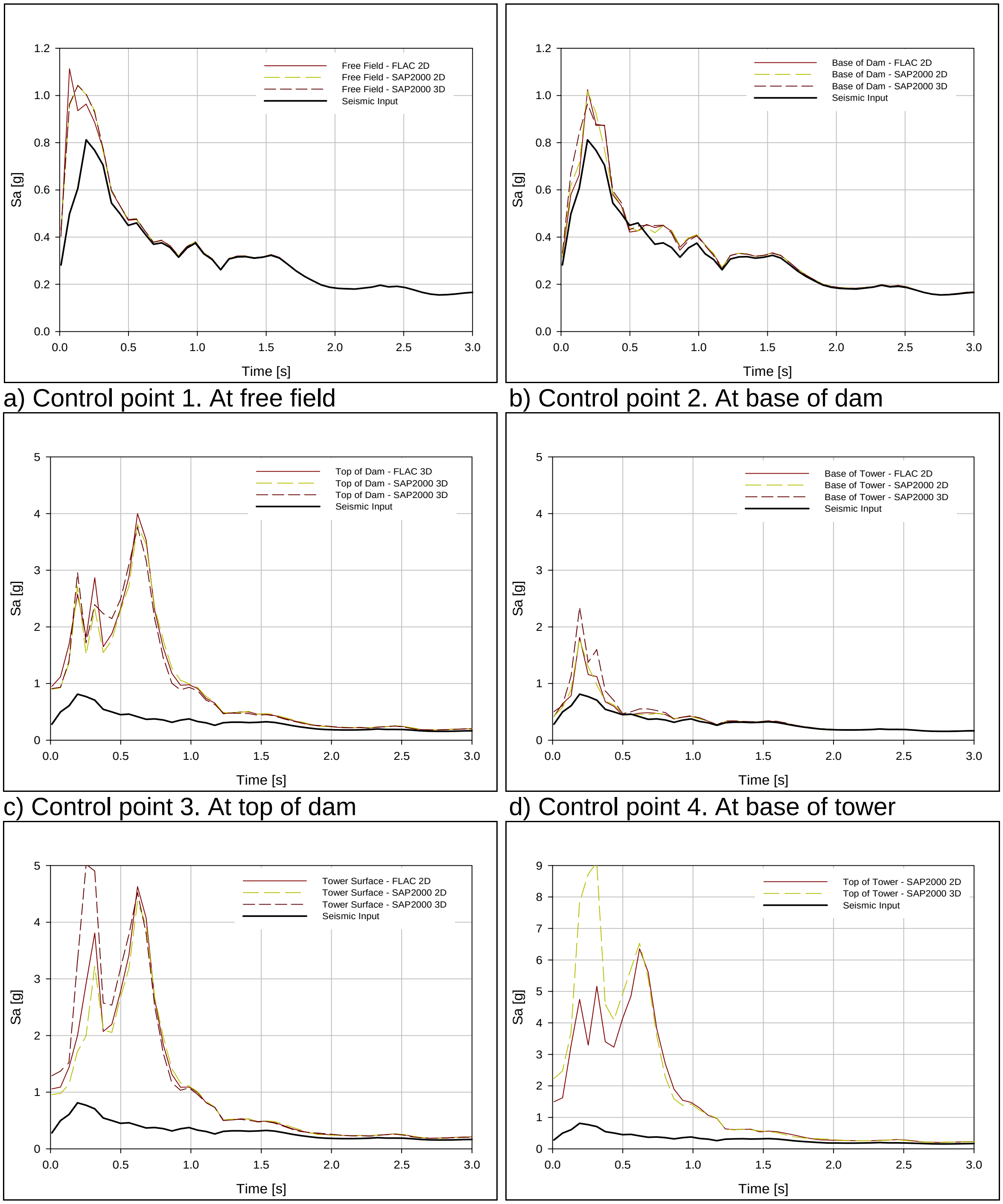

a) Control point 1. At free field

b) Control point 2. At base of dam

c) Control point 3. At top of dam

d) Control point 4. At base of tower

e) Control point 5. At tower surface

f) Control point 6. At top of tower

Figure 5-10 Pseudo Acceleration Response Spectra at Control Points for 3D and 2D Models Including the Control Tower and Without the Intake Pipe

5.3.1.4 Natural Periods of the 3D Dam-Foundation-Tower System

The first five natural periods for the dam-foundation-tower system were computed using the 3D FE Sap2000 model and are summarized in Table 5-2. The comparison of the periods of the 2D and 3D model is based on the mode shapes of each model. Therefore, the empty cells in the column of the 2D model indicate that the corresponding 3D vibration mode does not have a corresponding one in the 2D model, for instance it may be an out-of-plane mode.

Table 5-2 Natural Periods of the Dam-Foundation System Including the Control Tower and without the Intake Pipe. From the SAP2000 3D Model

Mode Number	3D Model Period [s]	Modal Participating Mass Ratio	2D Model Period [s]
1	0.627	0.3569	0.657
2	0.479	1.894E-12	-
3	0.384	0.0015	0.367
4	0.363	0.0133	0.357
5	0.341	4955E-12	-

In general, the natural periods for the 3D model are slightly longer than for the 2D model, except for the first natural period. Note that the new vibration modes in the 3D model have very low modal mass participating ratio, which means that practically they will no contribute to the seismic response for a horizontal ground motion acting normal to the dam axis.

5.3.1.5 Vibration Modes Shapes Using SAP2000

To facilitate the comparison with the 2D results, the lower vibration mode shapes of the 3D model were retrieved from the SAP2000 output. The first five vibration modes shapes of the 3D model including the control tower are presented in Figure 5-11 through Figure 5-15.

It may not be easy to visualize the overall shape of the 3D modes in planar plots. In the computer program, due to its capabilities for animation and rotation of the point of view, it is much easier to grasp the nature of the modes. Nevertheless, it can be seen that the second mode has a strong rotational motion around a vertical axis, and thus this mode does not show up in the 2D model. The fifth mode is associated again with a rotational motion around the vertical axis but the rotation is not the uniform on the entire depth of the dam.

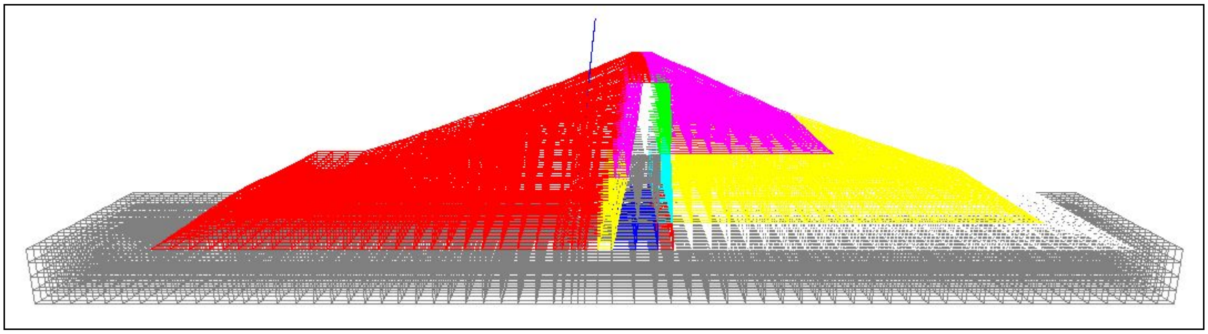

Figure 5-11 First Vibration Mode Shape of the 3D Model Including the Control Tower

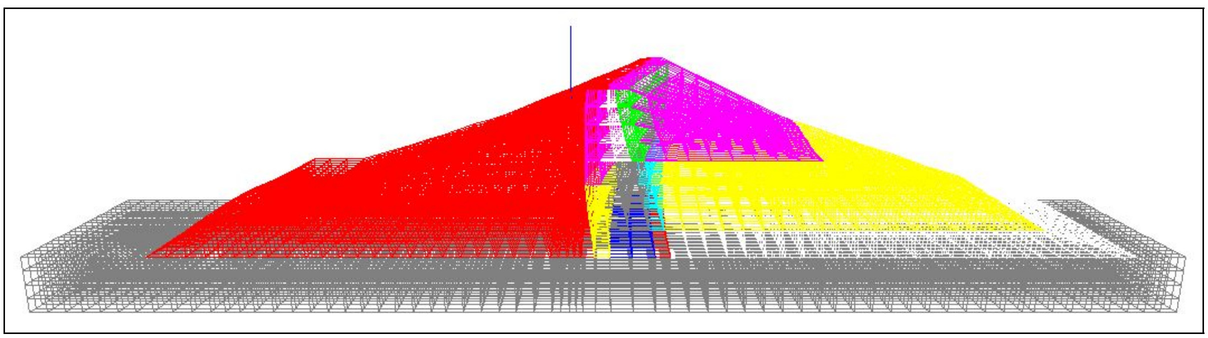

Figure 5-12 Second Vibration Mode Shape of the 3D Model Including the Control Tower

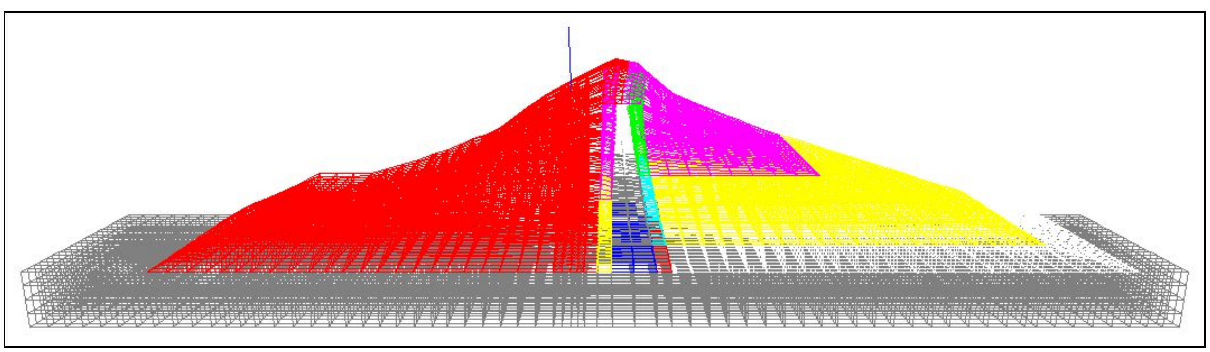

Figure 5-13 Third Vibration Mode Shape of the 3D Model Including the Control Tower

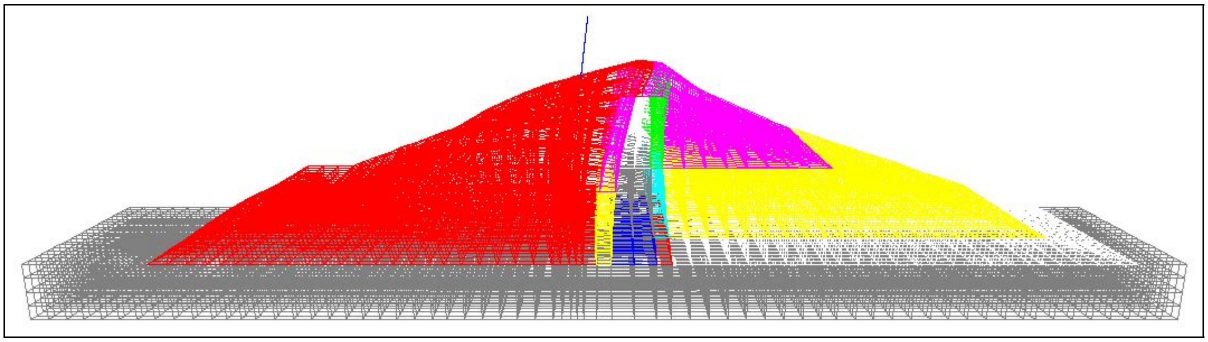

Figure 5-14 Fourth Vibration Mode Shape of the 3D Model Including the Control Tower

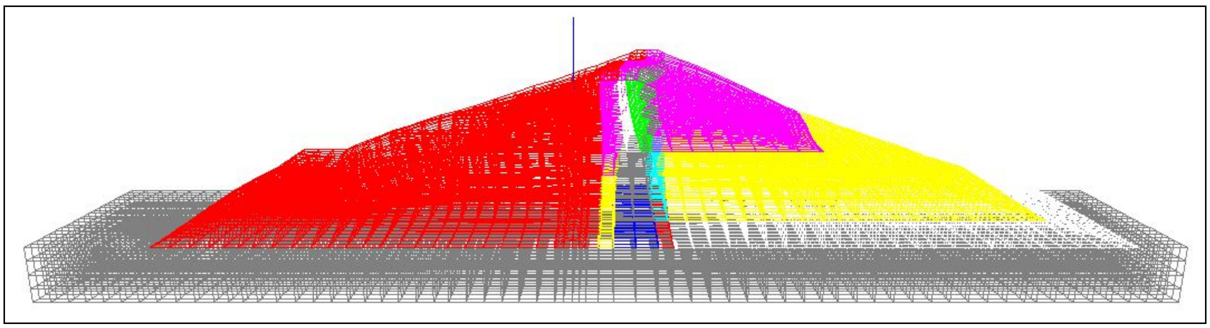

Figure 5-15 Fifth Vibration Mode Shape of the 3D Model Including the Control Tower

5.3.1.6 Reactions at the Base of the Control Tower

The time history of the shear force acting on the base of the control tower is shown in Figure 5-16.

The shear force component shown acts in the cross–sectional plane perpendicular to the longitudinal axis of the dam. For comparison purposes, the results from the Sap2000 2D model are also show.

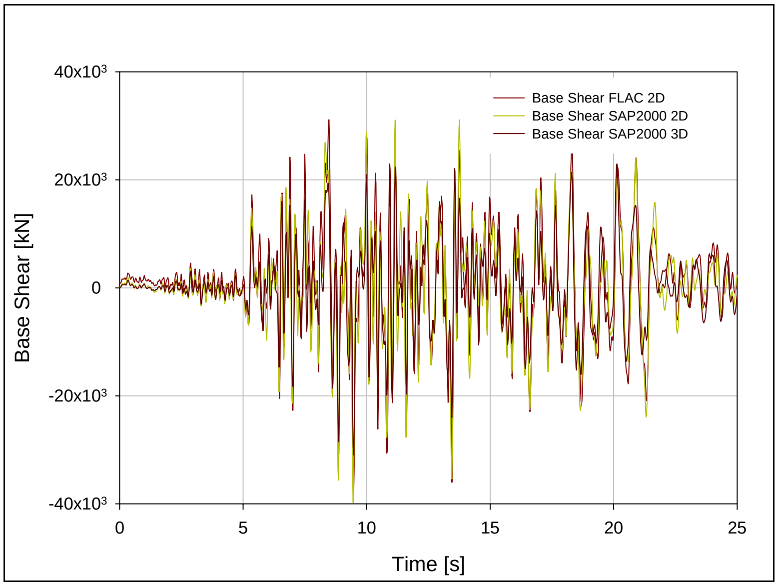

Figure 5-16 Base Shear Force Acting on the Control Tower Using 3D and 2D Models

In general, the traces of the time histories of the base shear force computed using 3D and 2D models are consistent. However, there are differences in the peak values. The maximum values obtained using the above mentioned methodologies are presented in Table 5-3.

Table 5-3 Maximum Reaction Values Acting on the Control Tower Using 3D and 2D Model without the Intake Pipe

Method of Analysis	Maximum Base Shear Force [kN]	Time of Occurrence [s]	Maximum Bending Moment [kN-m]	Time of Occurrence [s]
3D FEM – SAP2000	30988	9.48	0	0
2D FEM – SAP2000	39826	9.46	8427	19.64
2D EFDM – FLAC2D	37565	9.48	53	8.8

It is also interesting the distribution of the maximum shear force acting along the shaft of the control tower, and the shear force distribution at the instant when the maximum base shear occurs. These two shear diagrams are presented in Figure 5-17 and Figure 5-18, respectively.

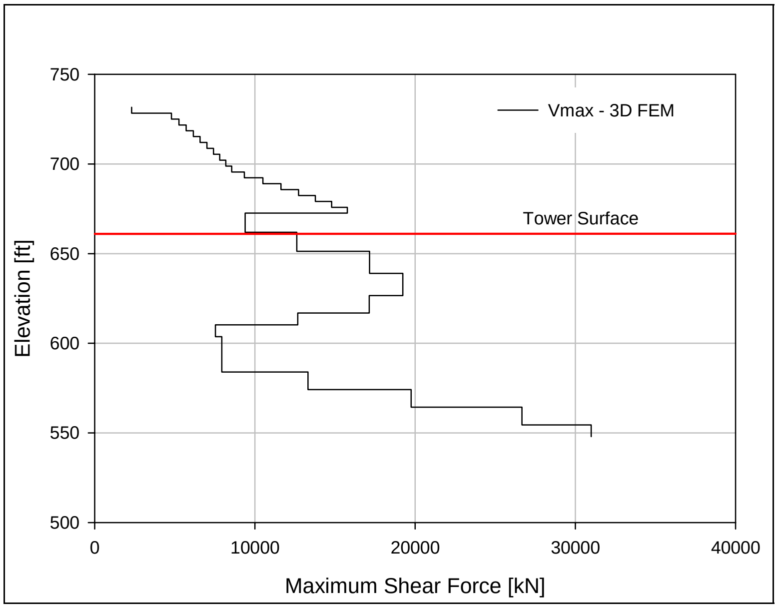

Figure 5-17 Maximum Shear Force Acting Along the Control Tower Using 3D Analysis

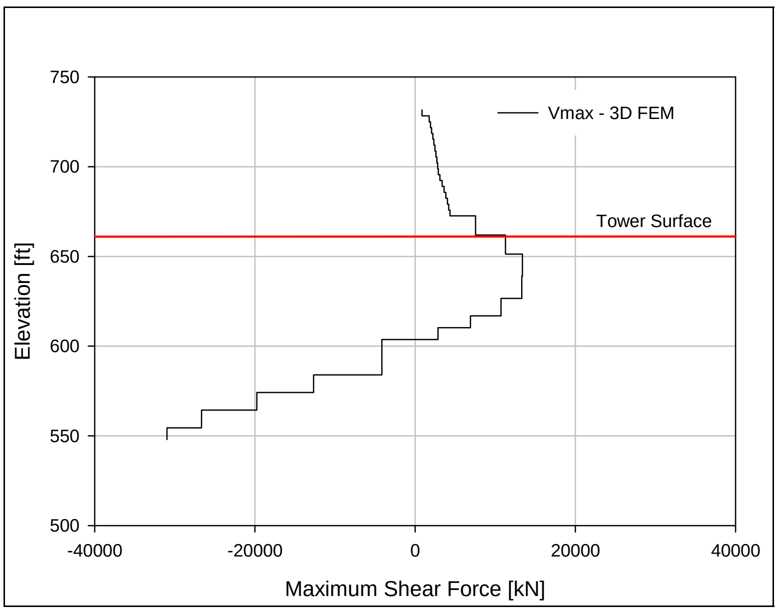

Figure 5-18 Shear Force Distribution when the Maximum Shear Force Occurs Using 3D Analysis

It is also interesting to consider the maximum bending moment acting along the shaft of the control tower. This bending moment diagram is presented in Figure 5-19.

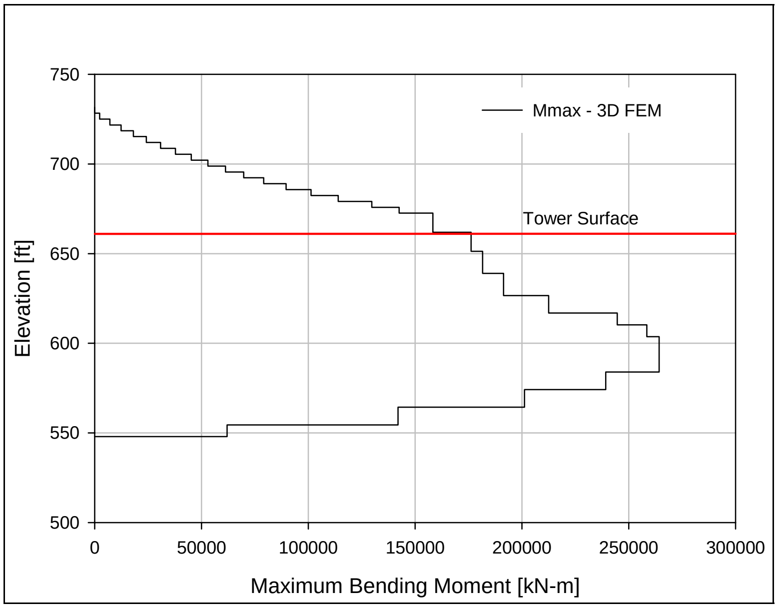

Figure 5-19 Maximum Bending Moment Acting Along the Control Tower Using 3D Analysis

5.3.2 DSSI Analysis for a 3D Model of the Dam Including the Control Tower and the Intake Pipe

The 3D FE model previously developed was modified to include the intake pipe that crosses the dam at its bottom. The pipe modifies the displacement and rotation conditions at the base of the tower, thus it is expected to have an effect on the seismic response of the tower. This is the most detailed model developed and thus it is considered to be the most representative of the true conditions at the Success Dam.

5.3.2.1 Details of the Structural Model for the Intake Pipe

The 3D model that includes the pipe has the same longitudinal extension as in the previous 3D model. Figure 5-20 presents the 3D FE model that includes the conduit crossing the dam.

The boundary conditions are also the same as in the previous model::

- All nodes at the base are fixed. The seismic input is applied at these nodes as a horizontal acceleration time history.

- The nodes in the four vertical faces of the model (i.e. the foundation soils) are restrained only in the vertical direction.

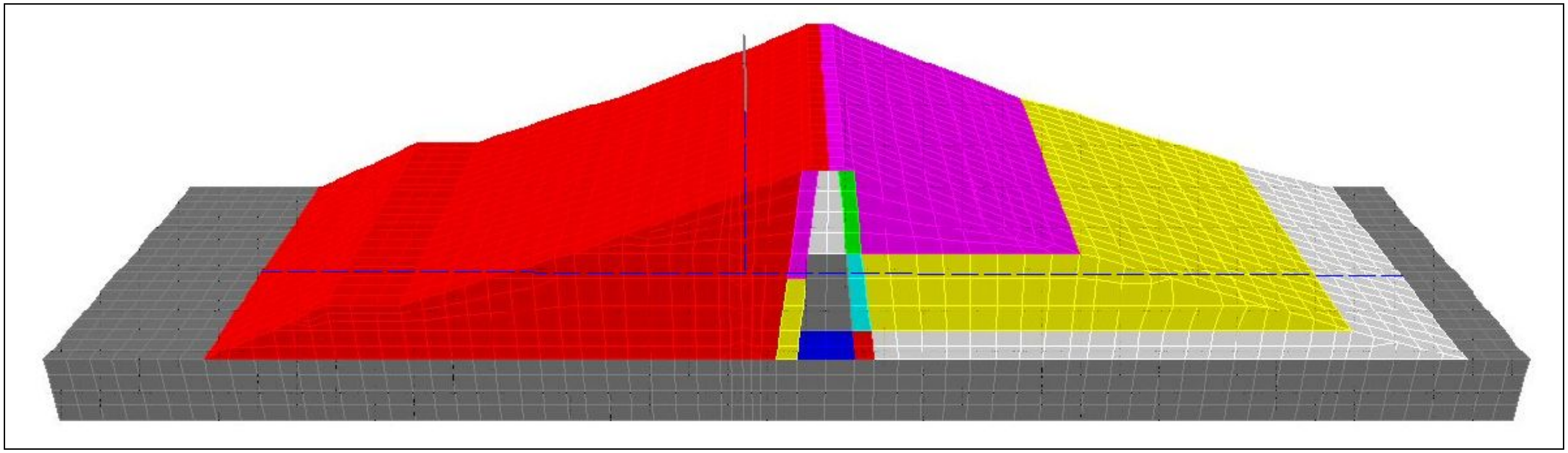

Figure 5-20 3D Finite Element Method Model Including the Control Tower and the Intake Pipe

The 3D FEM model that includes the discharge pipe has the following main characteristics:

- 12200 solid elements
- 87 frame elements
- 14172 nodes
- 11 types of geotechnical materials
- Time step: 0.02 s
- Damping formulation: Rayleigh method. Critical damping ratio = 5% at the response in the first natural period.
- Integration method: Newmark with gamma = 0.5 and beta =0.25, also called the trapezoidal rule.

A modal analysis was performed only to evaluate the fundamental periods corresponding to the first five vibration modes.

The same six control points were used for this set of analyses. As shown in Figure 4-11, these points are located over the plane of the control tower, in order to be consistent with the 2D models.

The results are presented in terms of relative displacement and absolute acceleration time histories, and pseudo acceleration response spectra calculated at the points of analysis previously selected. In addition, the shear force and moment at the base of the control tower are presented. When presenting the new results, those previously obtained with the two-dimensional are also included, so that the three dimensional effects can be evaluated.

5.3.2.2 Comparison of Displacement Time Histories

Figure 5-21 presents the relative displacements time histories for the six control points obtained using the 3D and 2D models that include both the control tower and the intake pipe. The plots in this figure indicate that there are no important differences in terms of the history of displacements. The maximum displacement computed at the top of the dam using the 3D model was 0.0017 m., which is a lower than the value obtained from the 2D models using FEM and EFDM.

The maximum displacement of the point at the top of the tower was 0.0045 m while at the point at the tower surface was 0.06 m at the same instant of time. The maximum drift of this section of the tower is:

$$Drift = \frac{0.06m - 0.0045m}{18m} \times 100\% = 0.31\%$$

This maximum drift occurs at 18.58 s of the seismic motion.

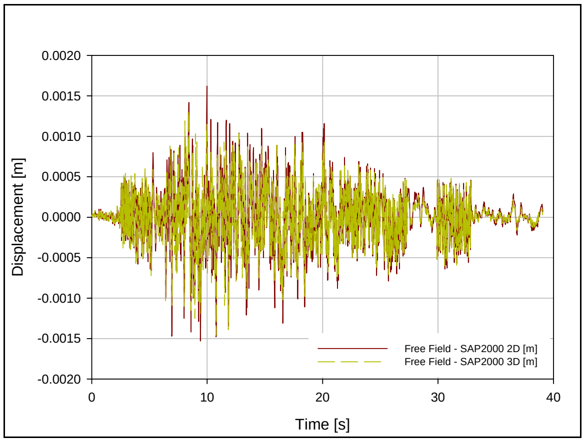

a) Control point 1. Free Field

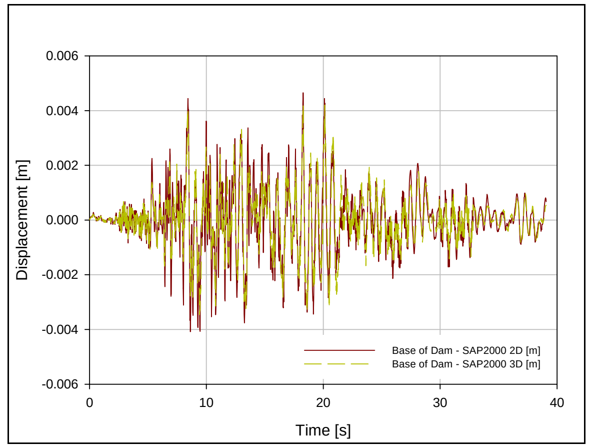

b) Control point 2. At base of dam

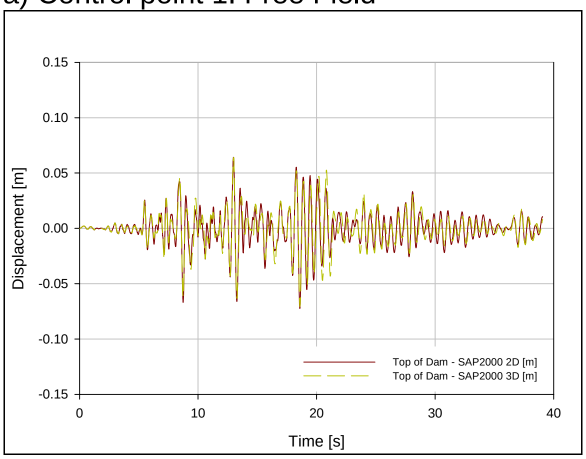

c) Control point 3. At top of dam

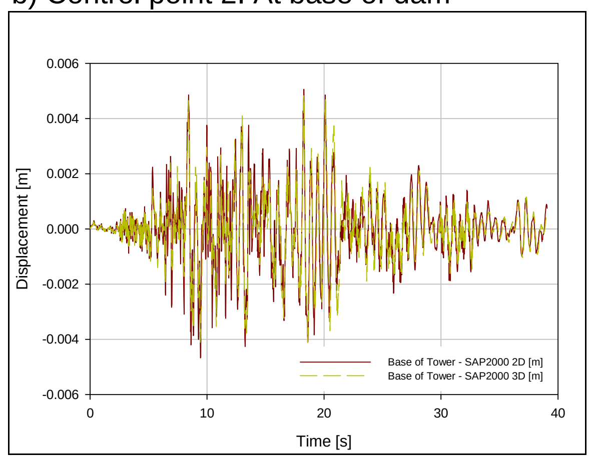

d) Control point 4. At base of tower

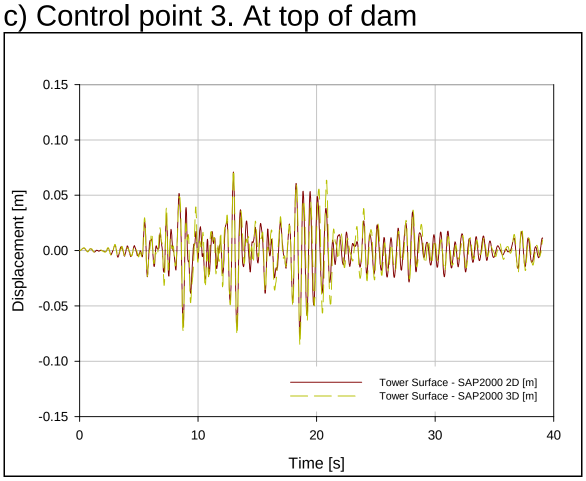

e) Control point 5. At tower surface

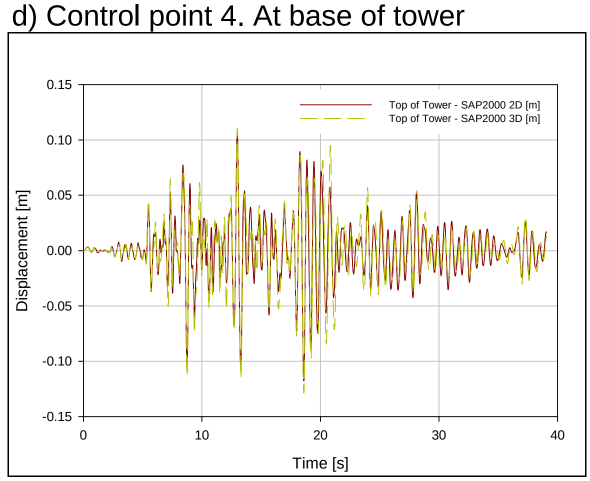

f) Control point 6. At top of tower

Figure 5-21 Displacement Time Histories at Control Points for 3D and 2D Models Including the Control Tower and the Intake Pipe

5.3.2.3 Comparison of Acceleration Time Histories

Figure 5-22 presents the acceleration time histories at the six control points of analysis. The plots presented correspond to the 2D and 3D SAP2000 models that include both the tower and intake pipe. The results obtained with the 2D and 3D models look similar, but some differences are observed in the peak values. For instance, at the top of the dam the 2D model of SAP2000 predicts a maximum value of 1.229 g whereas the peak acceleration according to the 3D model is 0.902 g. These differences will be more evident when the accelerograms in Figure 5-22 are used to calculate the response spectra.

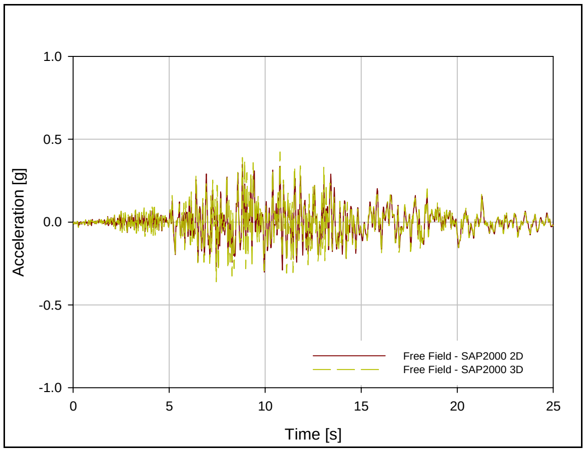

a) Control point 1. At free field

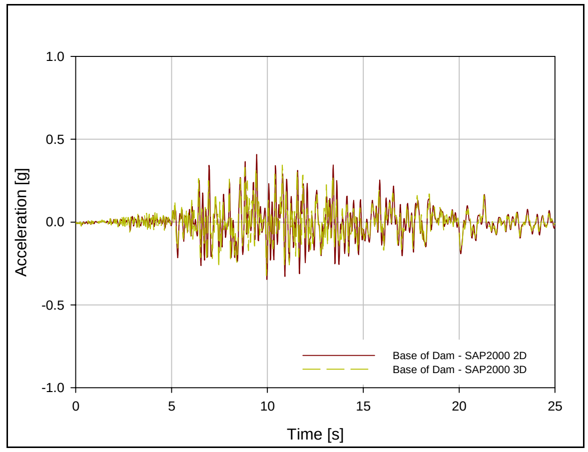

b) Control point 2. At base of dam

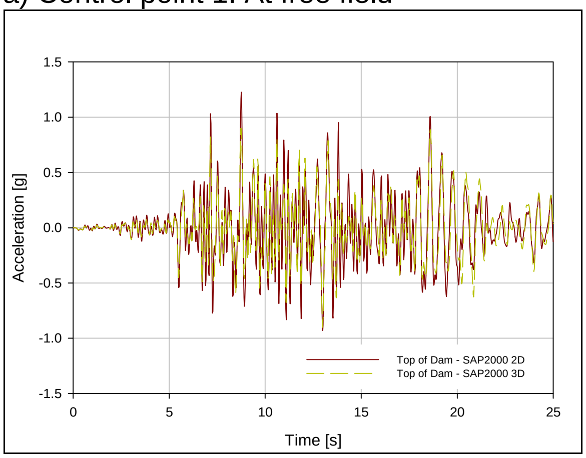

c) Control point 3. At top of dam

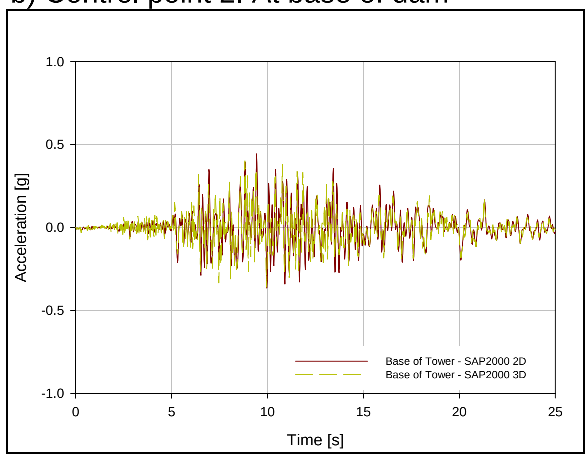

d) Control point 4. At base of tower

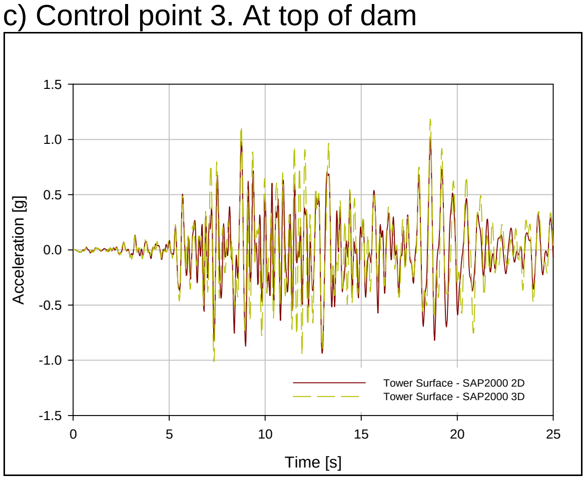

e) Control point 5. At tower surface

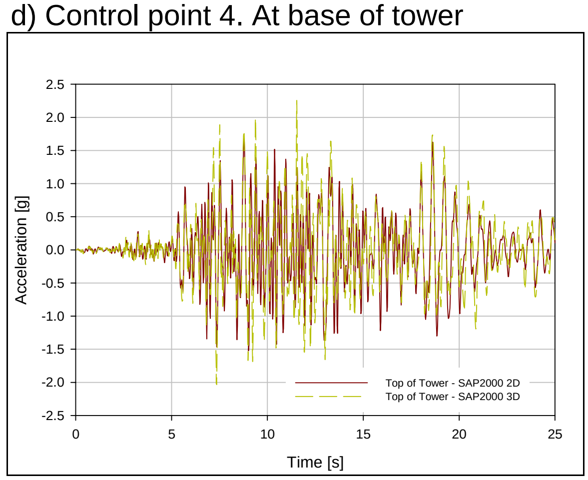

f) Control point 6. At top of tower

Figure 5-22 Acceleration Time Histories at Control Points for 3D and 2D Models Including the Control Tower

5.3.2.4 Comparison of Pseudo Acceleration Response Spectra

Figure 5-23 presents pseudo acceleration response spectra at the six control points of analysis. Six sets of plots show results from the 3D and 2D models that include the control tower and the intake pipe.

Relatively good agreement between the 2D and 3D model is observed for Control Points 1, 3, and 4. The remaining three control points show noticeable differences particularly for periods near the predominant period of the seismic input motion. For Control Point 2, the 2D model predicts a spectral peak at the predominant period of the input motion about 1.6 times higher than the one predicted by the 3D model. The opposite trend is observed for Control Points 5 and 5 which are located near the control tower. For these points the 3D SAP2000 model predicts spectral values at the predominant period of the input motion that are 20 to 30% higher than the values predicted with the 2D SAP2000 models.

Figure 5-23 shows a marked influence in the response of the dam of the lower natural periods, especially at the tower surface (Control Point 5) and the top of dam (Control Point 3). The amplification of the seismic input at the point below of the dam is very low when compared to the amplification located in the surface.

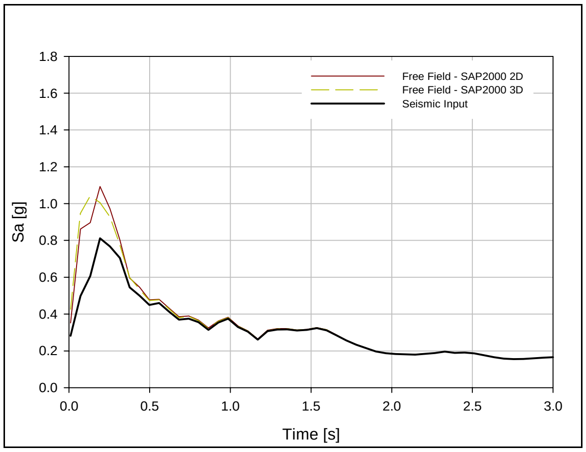

a) Control point 1. At free field

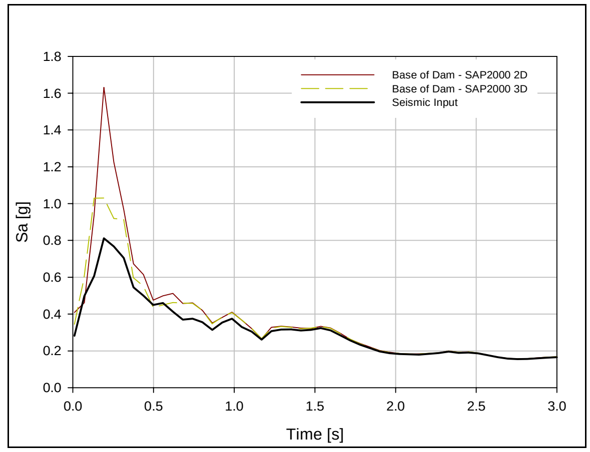

b) Control point 2. At base of dam

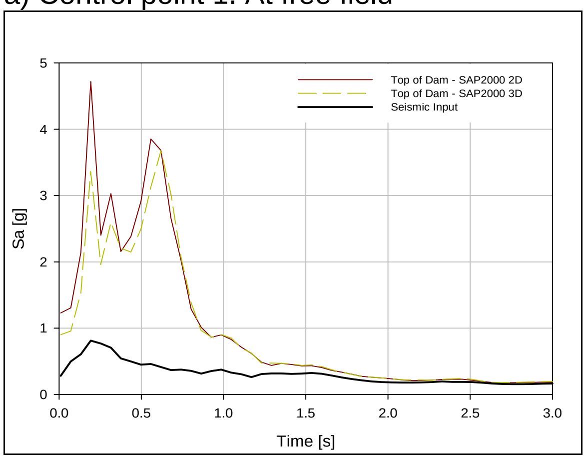

c) Control point 3. At top of dam

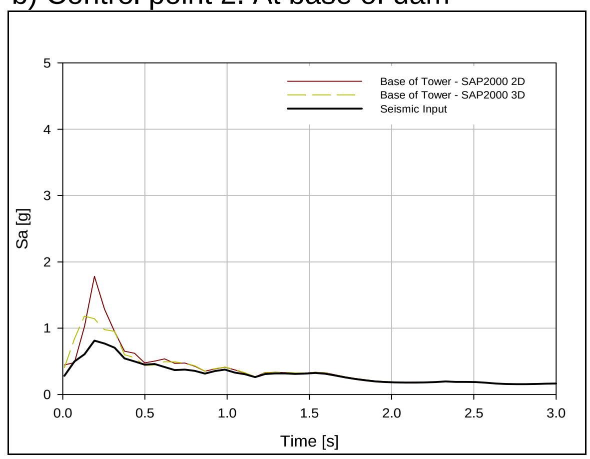

d) Control point 4. At base of tower

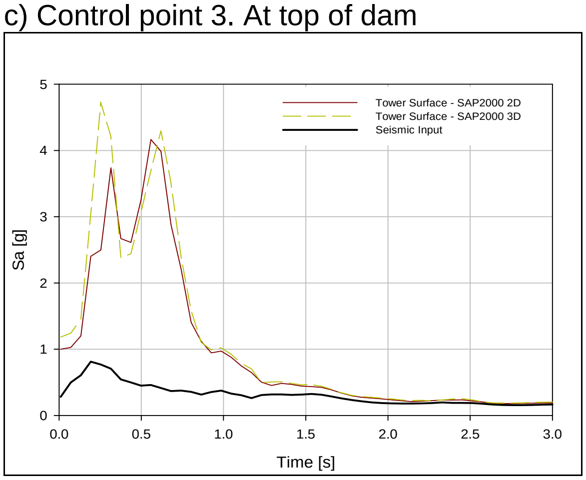

e) Control point 5. At tower surface

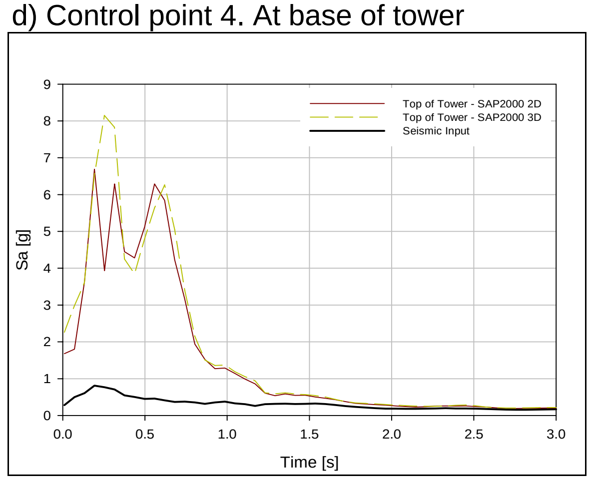

f) Control point 6. At top of tower

Figure 5-23 Pseudo Acceleration Response Spectra at Control Points for 3D and 2D Models Including the Control Tower and the Intake Pipe

5.3.2.5 Natural Periods of the 3D Dam-Foundation-Tower-Pipe System

The first five periods for the 3D dam-foundation-tower-pipe system were computed using the 3D FEM SAP2000 model, and are summarized in Table 5-4. The table also includes in the fourth column the natural periods calculated with the 2D model created in SAP2000. Some cells in the fourth column are labeled to indicate that there is no corresponding mode of vibration in the 2D model.

In general, the natural periods for the 3D model are longer than the corresponding values obtained from the 2D model. Modes 3 and 5 for the 3D model have a very low mass participation ratio and they involve motions that do not contribute much to the seismic response of the dam.

Table 5-4 Natural Periods of the Dam-Foundation System Including the Control Tower and Intake Pipe

Period Number	3D Model Period [s]	Modal Participating Mass Ratio	2D Model Period [s]
1	0.622	0.3577	0.598
2	0.479	1.211E-12	-
3	0.381	0.0002551	0.358
4	0.353	0.0149	0.354
5	0.341	6.736E-12	-

Comparing the periods in Table 5-2 and Table 5-4 of the models with and without the discharge pipe, one can conclude that the presence of the pipe has very small effects on the natural periods. In addition, the second and fifth mode have very small participating mass ratio, which means that they will not contribute to the response due to the horizontal ground motion applied at the base.

5.3.2.6 Vibration Modes Shapes Using SAP2000

The first five vibration modes shapes of the 3D model including the control tower and the intake pipe are presented in Figure 5-24 through Figure 5-28.

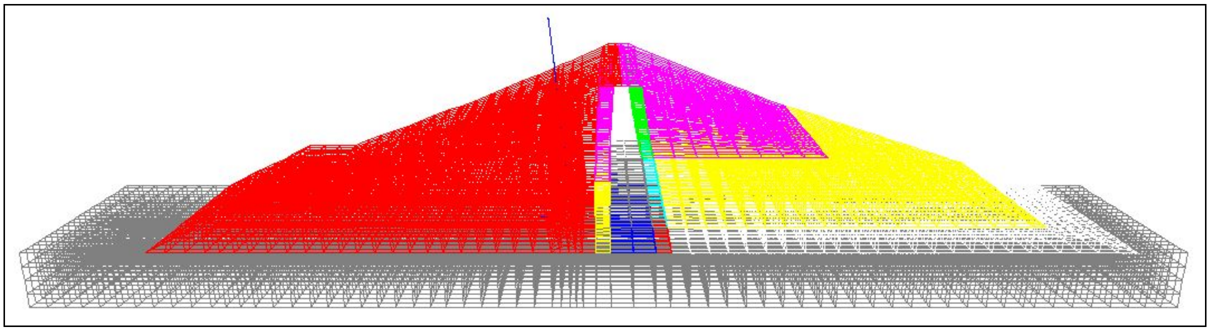

Figure 5-24 First Vibration Mode Shape of the 3D Model Including the Control Tower and the Intake Pipe

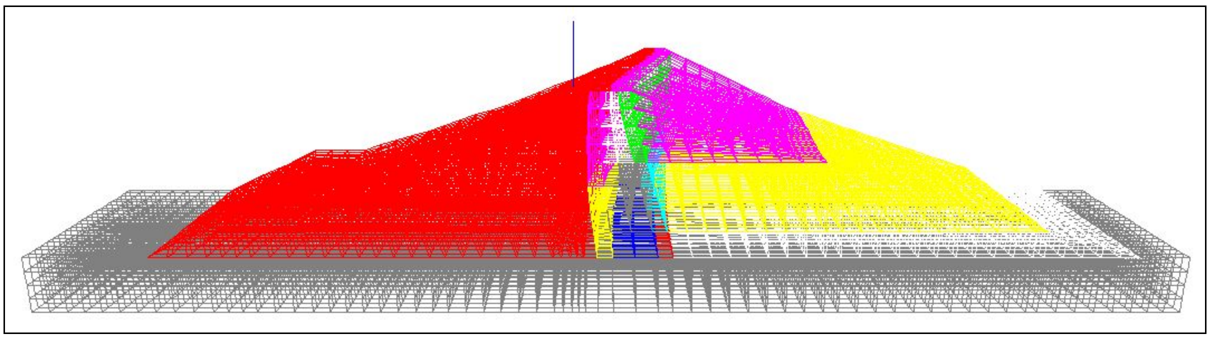

Figure 5-25 Second Vibration Mode Shape of the 3D Model Including the Control Tower and the Intake Pipe

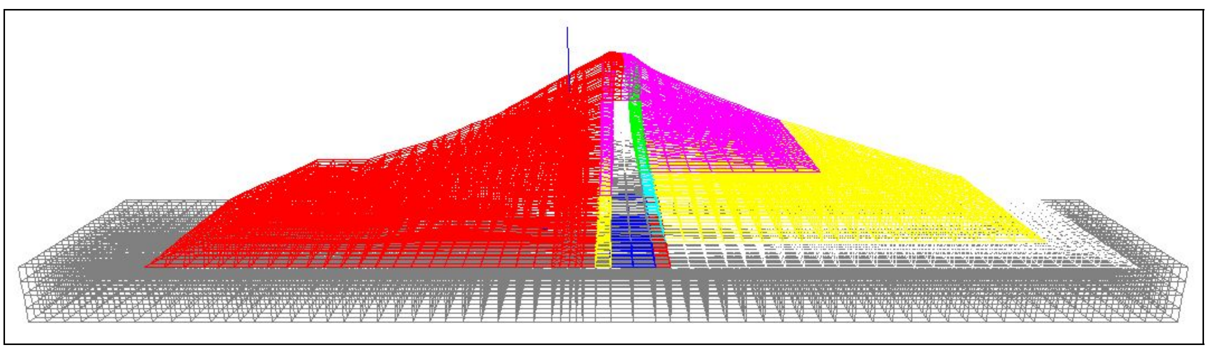

Figure 5-26 Third Vibration Mode Shape of the 3D Model Including the Control Tower and the Intake Pipe

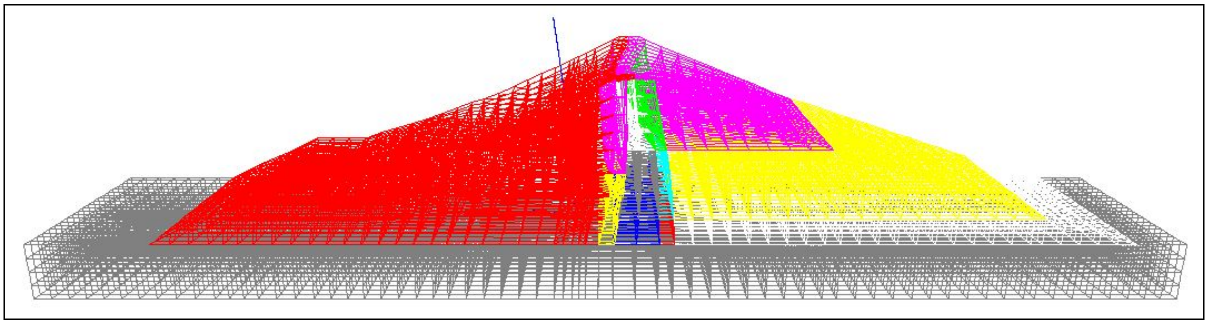

Figure 5-27 Fourth Vibration Mode Shape of the 3D Model Including the Control Tower and the Intake Pipe

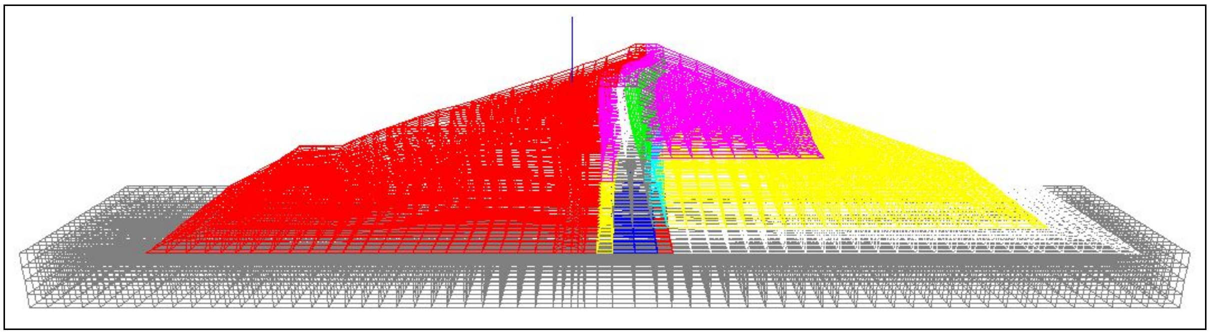

Figure 5-28 Fifth Vibration Mode Shape of the 3D Model Including the Control Tower and the Intake Pipe

5.3.2.7 Reactions at Control Tower Base

The time variation of the shear force at the base of the tower obtained from the 3D model is presented in Figure 5-29. The shear force for the 2D model is also included in the same figure. The base shear time history was clipped at 30 s to better appreciate the time variation.

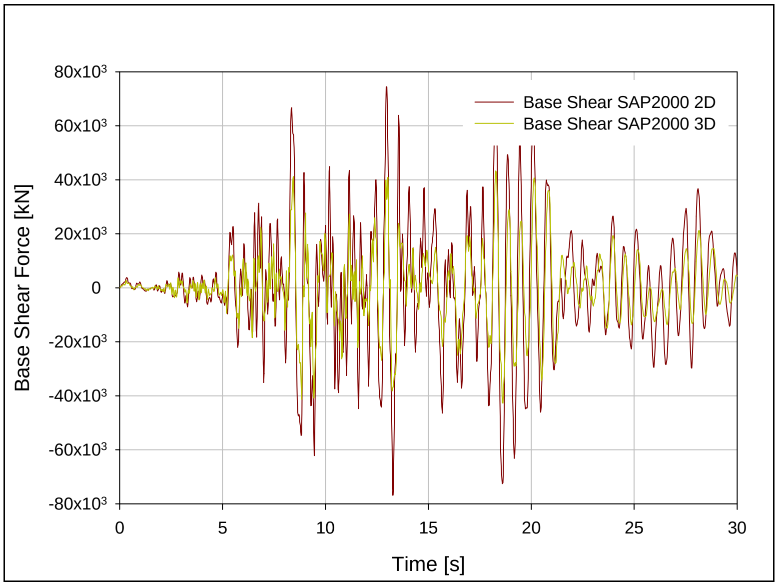

Figure 5-29 Base Shear Force Acting at the Base of the Control Tower in 3D and 2D Models Including the Intake Pipe

The traces of the time histories computed using the 3D and 2D models are similar, however the maximum shear force value predicted with the 2D model is 77% higher than the one from the 3D model. Similarly, the maximum basal bending moment predicted with the 2D modes is 47% lower than the predicted using the 2D mode. The maximum base shear force and the maximum bending moment at the base of the tower using the two methodologies are presented in Table 5-5.

Table 5-5 Maximum Base Shear Force and Maximum Bending Moment at the Base of the Control Tower Using 3D and 2D Model Including the Intake Pipe

Method of Analysis	Maximum Base Shear Force [kN]	Time of Occurrence [s]	Maximum Bending Moment [kN-m]	Time of Occurrence [s]
3D with Intake Pipe – SAP2000	43261	18.28	668074	18.6
2D with Intake Pipe – SAP2000	76912	13.28	1416747	18.6

The observed reduction in the basal shear force and moment of the control tower may be due to the radiation damping effects in the 3D model. This result may serve as an important reason in favor of using 3D models for these type of structures.

However, the problem requires additional research to reach more definite conclusions.

Table 5-6 presents the maximum shear force and bending moment at the base of the tower obtained using the 3D models with and without the intake pipe. Note that there is a 40% increase in the base shear when the discharge pipe is included in the model. The bending moment now is non-zero given that the presence of the pipe provides a partially fixed condition.

Table 5-6 Maximum Base Reaction Values Obtained Using 3D Models

Method of Analysis	Maximum Base Shear Force [kN]	Time of occurrence [s]	Maximum Bending Moment [kN-m]	Time of occurrence [s]
FEM Model without Intake Pipe	30988	9.48	0	-
FEM Model with Intake Pipe	43261	18.28	668074	18.6

Diagrams showing the variation of the maximum shear force acting along the shaft of the control tower and the shear force distribution at the time when the maximum base shear occurs are presented in Figure 5-30 and Figure 5-31, respectively.

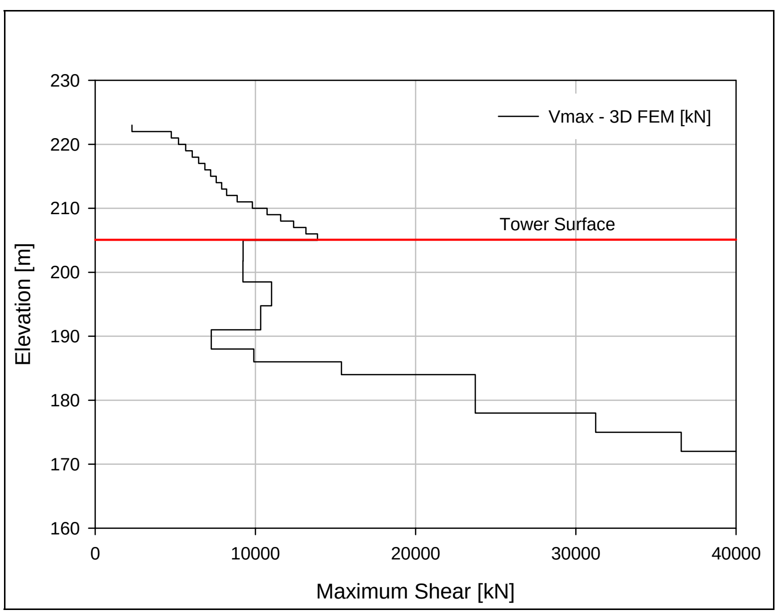

Figure 5-30 Maximum Base Shear Force Acting Along the Control Tower Using 3D Analysis Including the Intake Pipe

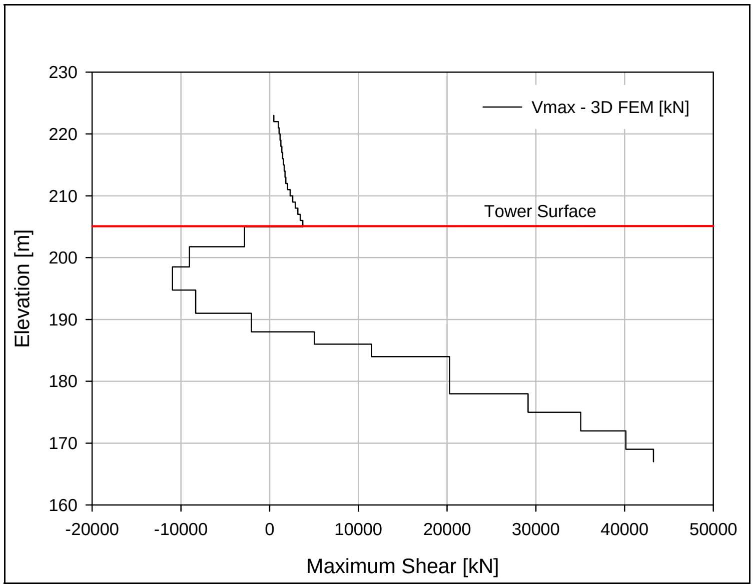

Figure 5-31 Shear Force Distribution When the Maximum Base Shear Occurs Using 3D Analysis Including the Intake Pipe

Similarly, the variation of the maximum bending moment acting along the shaft of the control tower, and the bending moment distribution when the maximum bending moment at the base of the control tower occurs are presented in Figure 5-32 and Figure 5-33, respectively.

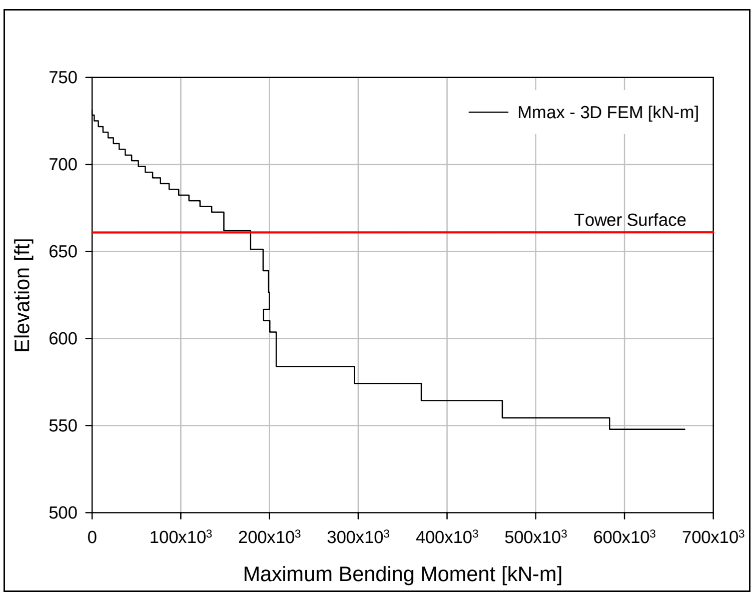

Figure 5-32 Maximum Bending Moment Acting Along the Control Tower Using 3D Analysis Including the Intake Pipe

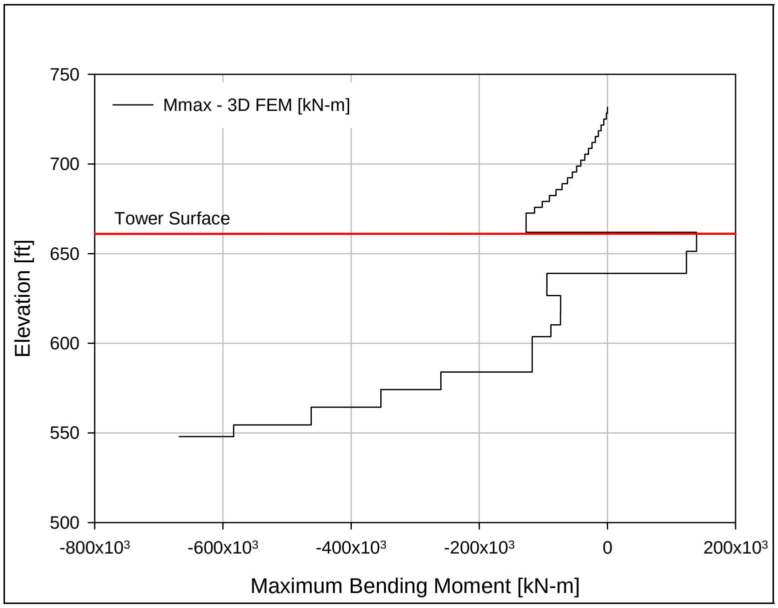

Figure 5-33 Bending Moment Distribution When the Maximum Bending Moment at the Base of the Control Tower Occurs Using 3D Analysis Including the Intake Pipe

6 ANALYSIS OF RESULTS

The first section of this chapter presents a sensitivity analysis carried out to evaluate the influence of varying soil parameters such as stiffness and Poisson's ratio on the basal reactions at the control tower. The second section of this chapter presents a summary of the results obtained using the different models. The summary of results presented in this chapter is provided in terms of the maximum base shear force and maximum moment at the base of the tower. The third section of this chapter presents the variation of the maximum acceleration computed along the embedded part of the control tower. The last section of this chapter presents a comparison of the results obtained in this study with the results from previous studies.

6.1 Sensitivity Analysis

Sensitivity analyses was carried out varying the stiffness (i.e. maximum shear modulus), and the Poisson's ratio. The maximum shear modulus G_{max} was varied ±40% and ±20% for the dam soils and ±10% for the rock foundation. The Poisson's ratio was varied from 0.30 to 0.45 for the complete model. The results of the sensitivity analysis are presented in terms of maximum base shear force, maximum moment at the base of the control tower, drift of the free stand section of the tower, and maximum acceleration at the point where the embedment of the tower starts (i.e. Control Point 5).

6.1.1 Variation of the Maximum Base Shear Force

The impact of varying the stiffness of the soil materials by 0.6, 0.8, 1.0, 1.2, and, 1.4 of its baseline values on the maximum basal shear force is presented in Figure 6-1. in general, this figure shows higher basal shear forces are predicted when lower stiffness values are assigned to the soils in the different models. The largest impact was observed for the 2D SAP2000 model that included the tower and the intake pipe, where the maximum basal shear force for a 0.6 stiffness relative stiffness was 37 %

higher than the value computed for the baseline value. Similarly, the sensitivity to stiffness of the 3D models is 40 %

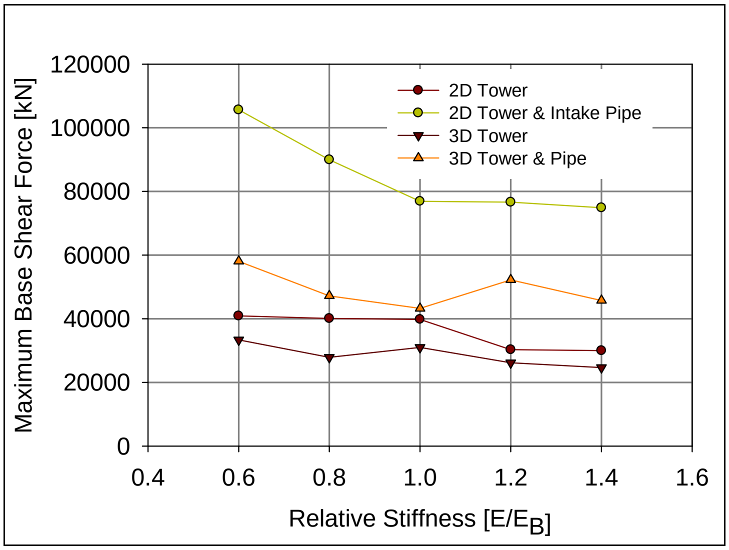

Figure 6-1 Base Shear Force - Stiffness Sensitivity Analysis

The results of the sensitivity analyses for the basal shear force in terms of the Poisson's ratio are presented in Figure 6-2.

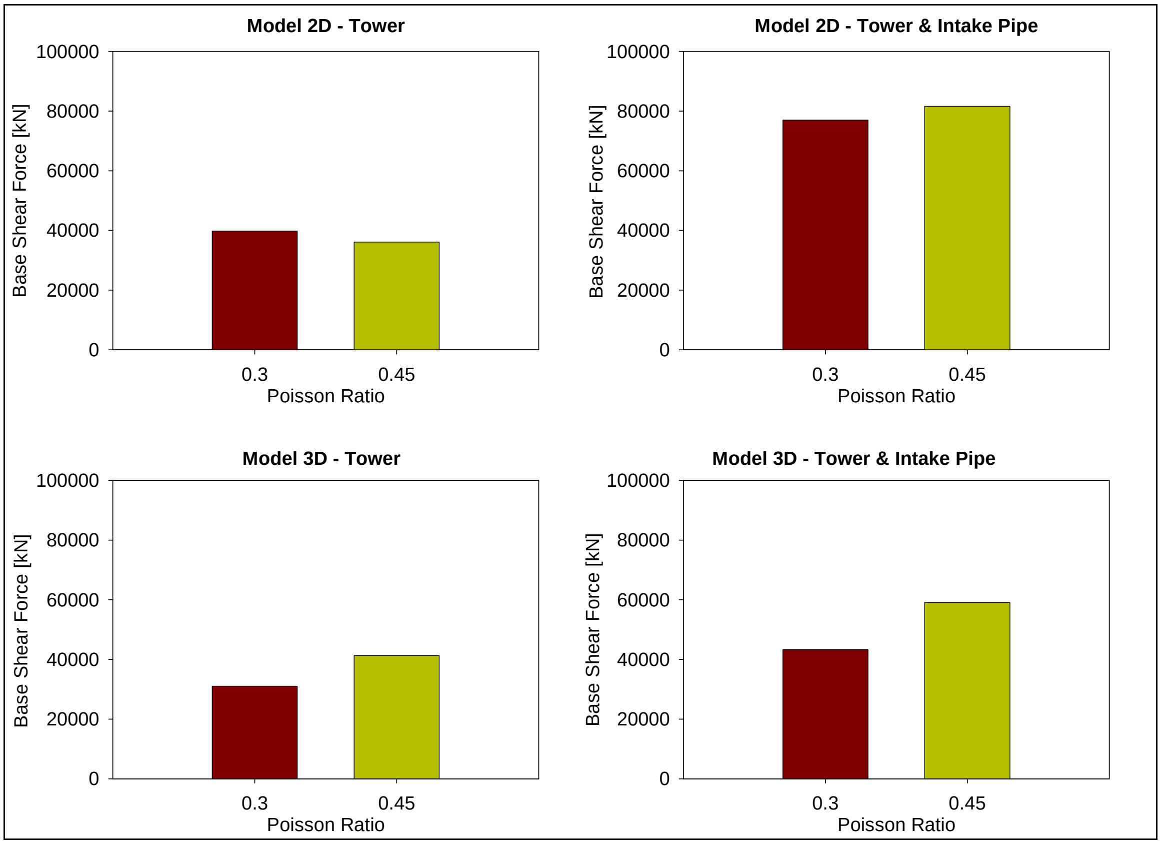

Figure 6-2 Base Shear Force – Poisson's Ratio Sensitivity Analysis

In general, the increment of the Poisson's ratio from 0.30 to 0.45 raises the maximum base shear force from 2 to 40% depending on the type of model. The 2% increase was found for the 2D SAP2000 model including the intake pipe, while the 40% increase was found for the 3D SAP2000 model including the intake pipe.

6.1.2 Variation of the Maximum Moment at the Base of the Tower

The influence on the maximum basal bending moment of the tower to soil stiffness variation is shown in Figure 6-3. The soil stiffness was varied from 60 % to 140 % of the baseline values.

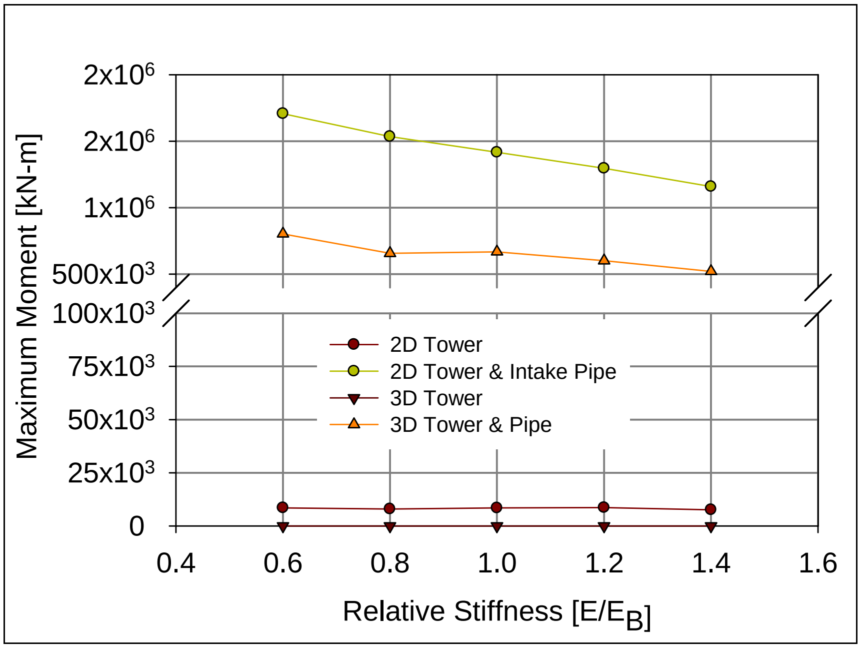

Figure 6-3 Maximum Bending Moment at the Base of Control Tower - Stiffness Sensitivity Analysis

Figure 6-3 shows a tendency of decreasing basal moments as the soil stiffness increases. This tendency was more pronounced for the 2D SAP2000 model that included the intake pipe. The 2D and 3D models without the intake pipe had little sensitivity to soil stiffness variations.

The moment at the base of the control tower for the 3D model without intake pipe is zero because this point can rotate in the model.

The influence of varying the Poisson's ratio on the maximum basal bending moment is shown in Figure 6-4.

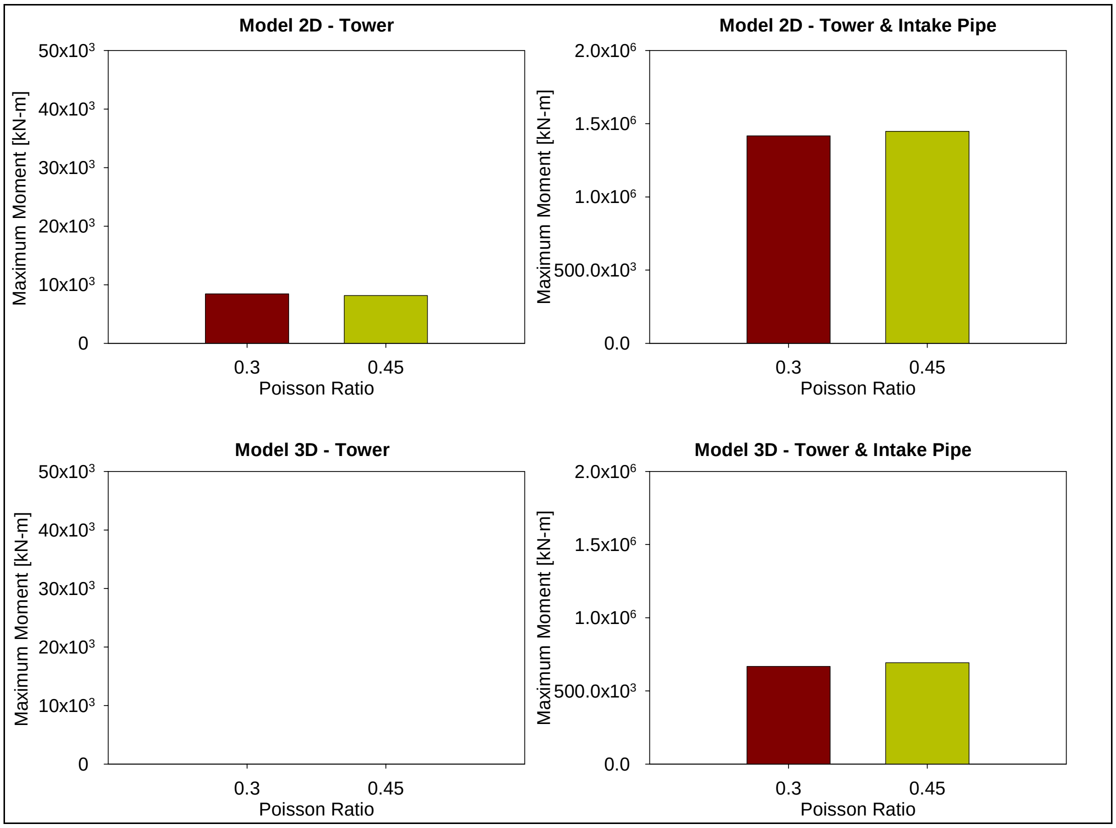

Figure 6-4 Maximum Bending Moment at the Base of the Control Tower – Poisson's Ratio Sensitivity Analysis

The increment of the Poisson's ratio from 0.30 to 0.45 has practically no effect on the maximum moment at the base of the control tower.

6.1.3 Variation of the Maximum Drift of the Free Stand Section of the Tower

The influence of stiffness variation on the computed maximum drift of the exposed portion of the tower is shown in Figure 6-5.

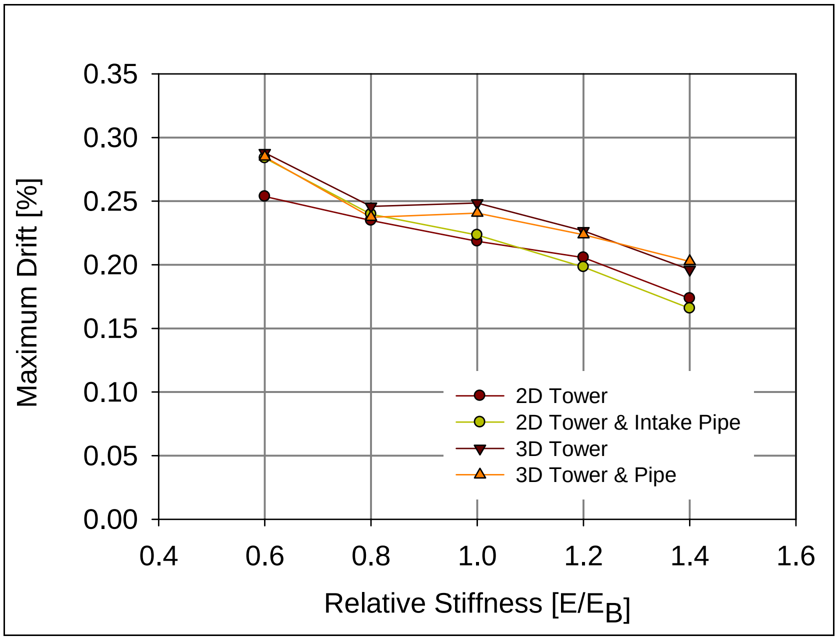

Figure 6-5 Maximum Drift at the Free Stand Section of the Control Tower - Stiffness Sensitivity Analysis

Figure 6-5 shows a general tendency of decreasing drift as the soil stiffness increased. On average a decrease of about 20 % was observed for a 40 % increase in soil stiffness.

The influence of Poisson’s ratio variation on the maximum drift of the tower is presented in Figure 6-6.

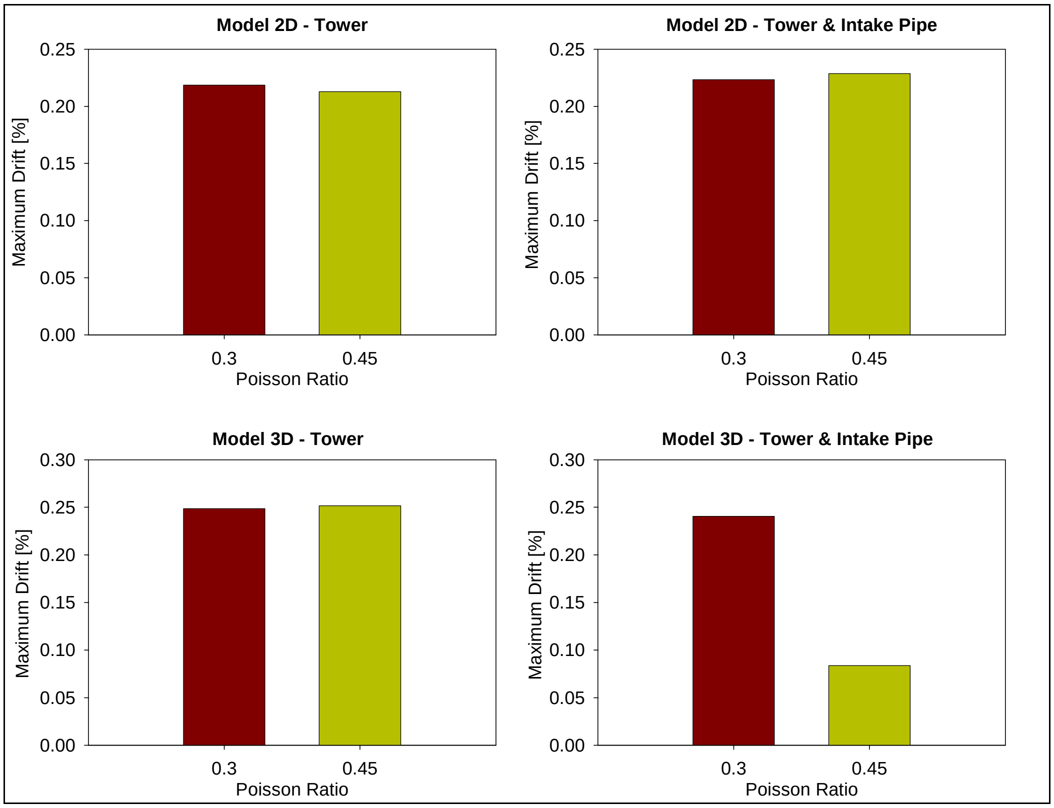

Figure 6-6 Maximum Moment at the Base of the Control Tower – Poisson's Ratio Sensitivity Analysis

An increase on the Poisson's ratio has practically no effect on the maximum drift computed on the models, except for the 3D model that includes the intake pipe. For the 3D model with the intake pipe the drift reduces by about 62 % when the Poisson's ratio is increased from 0.3 to 0.45. This change results in a stiffer response of the tower.

6.1.4 Variation of the Maximum Acceleration at Tower Surface Point

Variation of computed maximum accelerations at the tower surface point (Control Point 5) as the soil stiffness varies is shown in Figure 6-7.

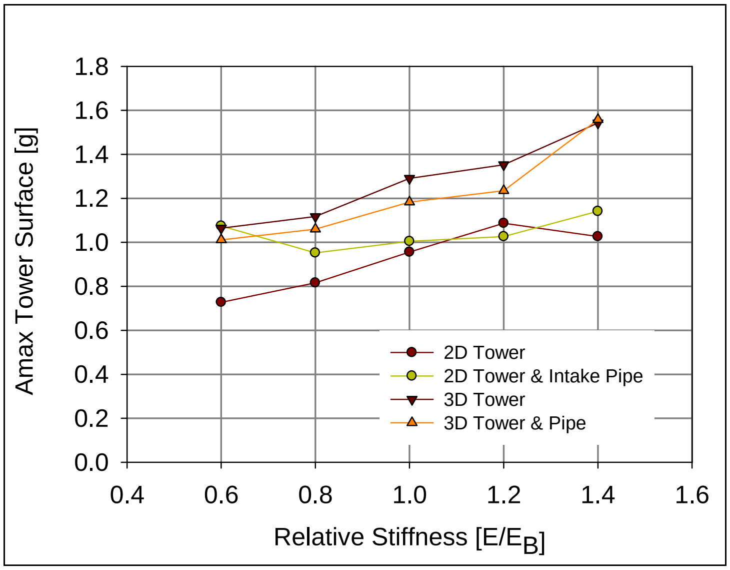

Figure 6-7 Maximum Acceleration at Tower Surface Point - Stiffness Sensitivity Analysis

In general, Figure 6-7 shows a tendency of increasing the maximum acceleration as the soil stiffness increases. The impact was greatest in the 3D model, and the least in the 2D model with the intake pipe.

The influence of varying Poisson’s ratio is presented in Figure 6-8.

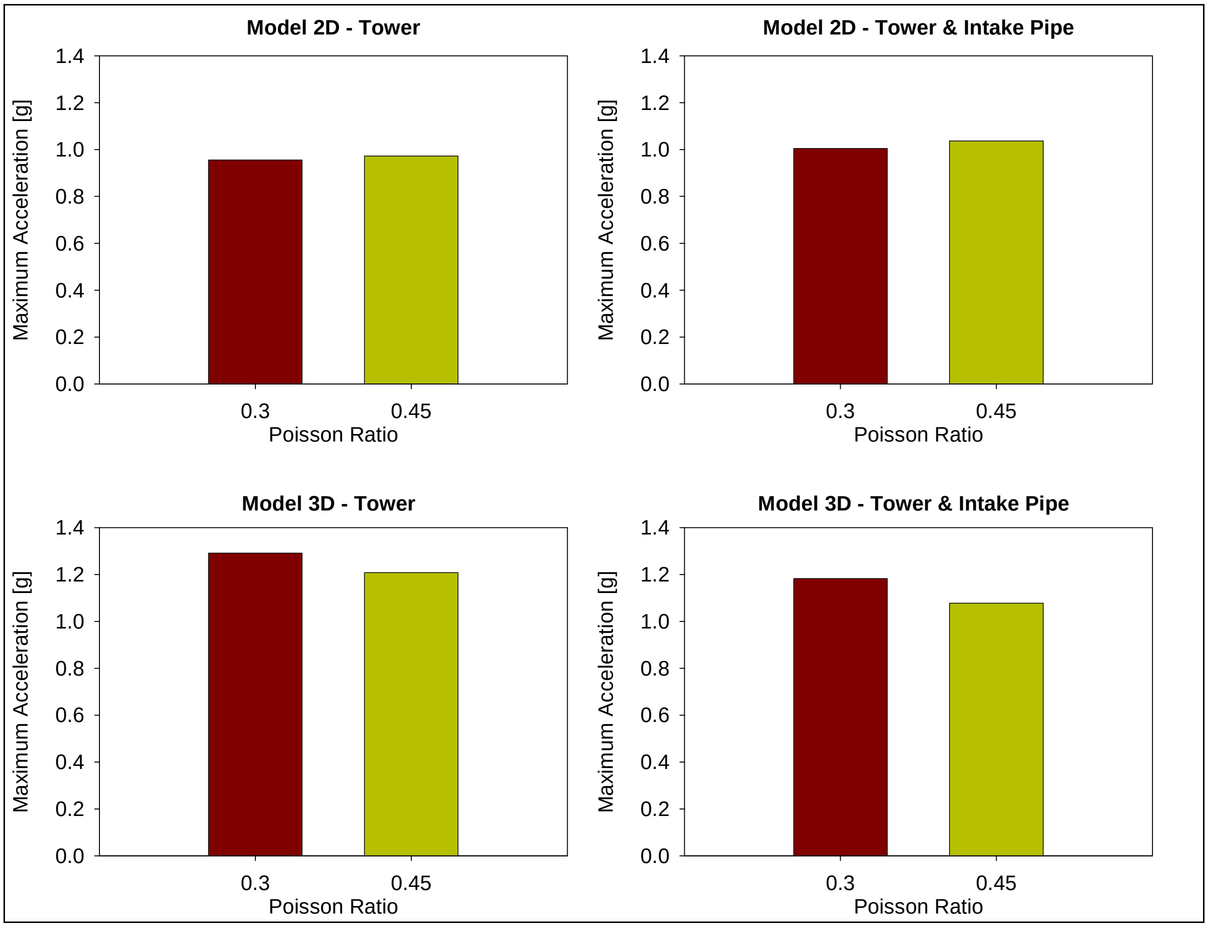

Figure 6-8 Maximum Acceleration at Tower Surface Point – Poisson's Ratio Sensitivity Analysis

The increase in the Poisson's ratio value has practically no effect on the maximum acceleration at the tower surface point for 2D models, while for 3D models a reduction of the maximum acceleration of about 7% was observed when the Poisson's ratio was increased.

6.2 Summary of Results

The maximum base shear force and the maximum bending moment at the base of the control tower for all the analyses carried out in this project are summarized in Table 6-1.

Table 6-1 Summary of Base Shear Force Obtained by 2D and 3D Models

Model Type	Seismic Input	Material Properties	V_{max} [kN]	M_{max} [kN]
2D FLAC tower only	Modified Taft Figure 4-4	Baseline values	37565	53
2D SAP2000 tower only	Modified Taft Figure 4-4	Base Line values	39826	8427
2D SAP2000 tower only	Modified Taft Figure 4-4	Soil properties: 60% Baseline Foundation properties: 90% Baseline	40932	8492
2D SAP2000 tower only	Modified Taft Figure 4-4	Soil properties: 140% Baseline Foundation properties: 110% Baseline	30356	7581
2D SAP2000 with intake pipe	Modified Taft Figure 4-4	Baseline values	76912	1416747
2D SAP2000 with intake	Modified Taft Figure 4-4	Soil properties: 60% Baseline Foundation properties: 90% Baseline	105668	1707973
2D SAP2000 with intake pipe	Modified Taft Figure 4-4	Soil properties: 140% Baseline Foundation properties: 110% Baseline	74911	1158476
2D QUAKE/W & SAP2000 with intake. Linear Equivalent Method	Modified Taft Figure 4-4	QUAKE/W with Base Line values. SAP2000 with reduced stiffness values	97320	1702628
3D SAP2000 tower only	Modified Taft Figure 4-4	Base Line values	30988	0
3D SAP2000 tower only	Modified Taft Figure 4-4	Soil properties: 60% Baseline Foundation properties: 90% Baseline	33326	0
3D SAP2000 tower only	Modified Taft Figure 4-4	Soil properties: 140% Baseline Foundation properties: 110% Baseline	24662	0

Table 6-1 Summary of Base Shear Force Obtained by 2D and 3D Models

Model Type	Seismic Input	Material Properties	V_{max} [kN]	M_{max} [kN]
3D SAP2000 with intake pipe	Modified Taft Figure 4-4	Baseline values	43261	668074
3D SAP2000 with intake pipe	Modified Taft Figure 4-4	Soil properties: 60% Baseline Foundation properties: 90% Baseline	58070	803170
3D SAP2000 with intake pipe	Modified Taft Figure 4-4	Soil properties: 140% Baseline Foundation properties: 110% Baseline	45759	520757

The 3D DSSI models resulted in reduced basal reactions at the tower. For the models with no intake pipe, the maximum base shear force obtained with 3D models was 78% of the values from 2D models. The reduction in reactions due to 3D effects is significant and the analyses presented in this study suggest they must be included in DSSI analyses of embedded structures in order to obtain reliable estimates.

Another important consideration required to obtain realistic estimates of the basal reactions is the inclusion of the intake pipe. This pipe adds horizontal and rotational rigidity to the base of the tower and results in increased base reaction values. For the base shear force the maximum values obtained were 95% higher for the 2D SAP2000 models, and 39% higher for the 3D SAP2000 models. Both analyses were linear elastic. The importance of using numerical models that represent the problem in a realistic way is highlighted with these results.

6.3 Maximum Acceleration along the Embedded Section of the Control Tower

The variation of the maximum acceleration along the embedded section of the control tower is presented in Figure 6-9.

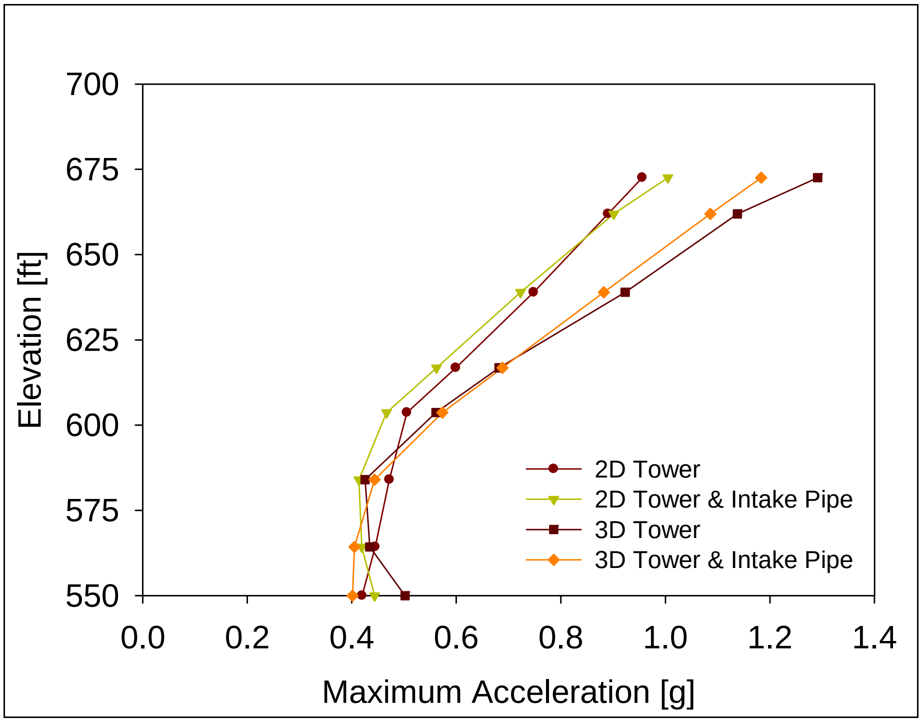

Figure 6-9 variation of the Maximum Acceleration along the Embedded Section of the Control Tower

The results presented in Figure 6-9 correspond to the baseline properties and SAP2000 analysis using 2D and 3D models with and without the intake pipe. The accelerations shown are for nodes in the model in contact with the tower-soil interface.

6.4 Comparison of Results with Previous Studies

In terms of comparison of basal reaction values at the control tower obtained by others, we find that all values obtained in this study are higher than those obtained by Cocco (2004). The differences with values obtained using the CSM method are expected and can be attributed in part to the differences in the numerical methodologies. However, the differences with the SAP2000 analyses is somewhat surprising given that this method used the same numerical approach as the 2D SAP2000 case that does not include the intake pipe. Cocco (2004) used the same input motion but obtained values about half of those obtained in this study. Even sensitivity analyses of material properties of 40% do not help explain the differences in the results.

Comparison of the results with those reported by CSI (1981) reveals a large discrepancy. The CSI (1981) maximum base shear force at the control tower is 318% higher than the highest value obtained in this study (i.e. the value obtained with the 2D FEM model with intake pipe). The CSI study is believed to have used the same seismic input, however the pseudo acceleration spectrum provided in their report seems to suggest a higher seismic excitation may have been used.

Finally, a comparison was also made with the unpublished results from a private consulting firm on behalf of the USACOE. The analyses were reportedly carried out using FLAC2D and the results were provided by a personal communication (Matheu 2004). The maximum base shear force from this study is 13% higher than the value obtained with the FLAC2D analyses that included the intake pipe in the present study.

The result of maximum shear force obtained from an additional analysis not presented in the previous sections is included in this comparison. The additional analysis consisted in a SAP2000-2D model (with no intake pipe) with the node at the base of the tower restricted to any rotation. This is believed to represent better the rotation restriction provided by the embedment environment at the base of the tower.

The comparison of all basal shear computations is presented in Figure 6-10. This figure presents a bar diagram that also includes variation bars for the stiffness sensitivity analysis. This figure also includes results by other authors.

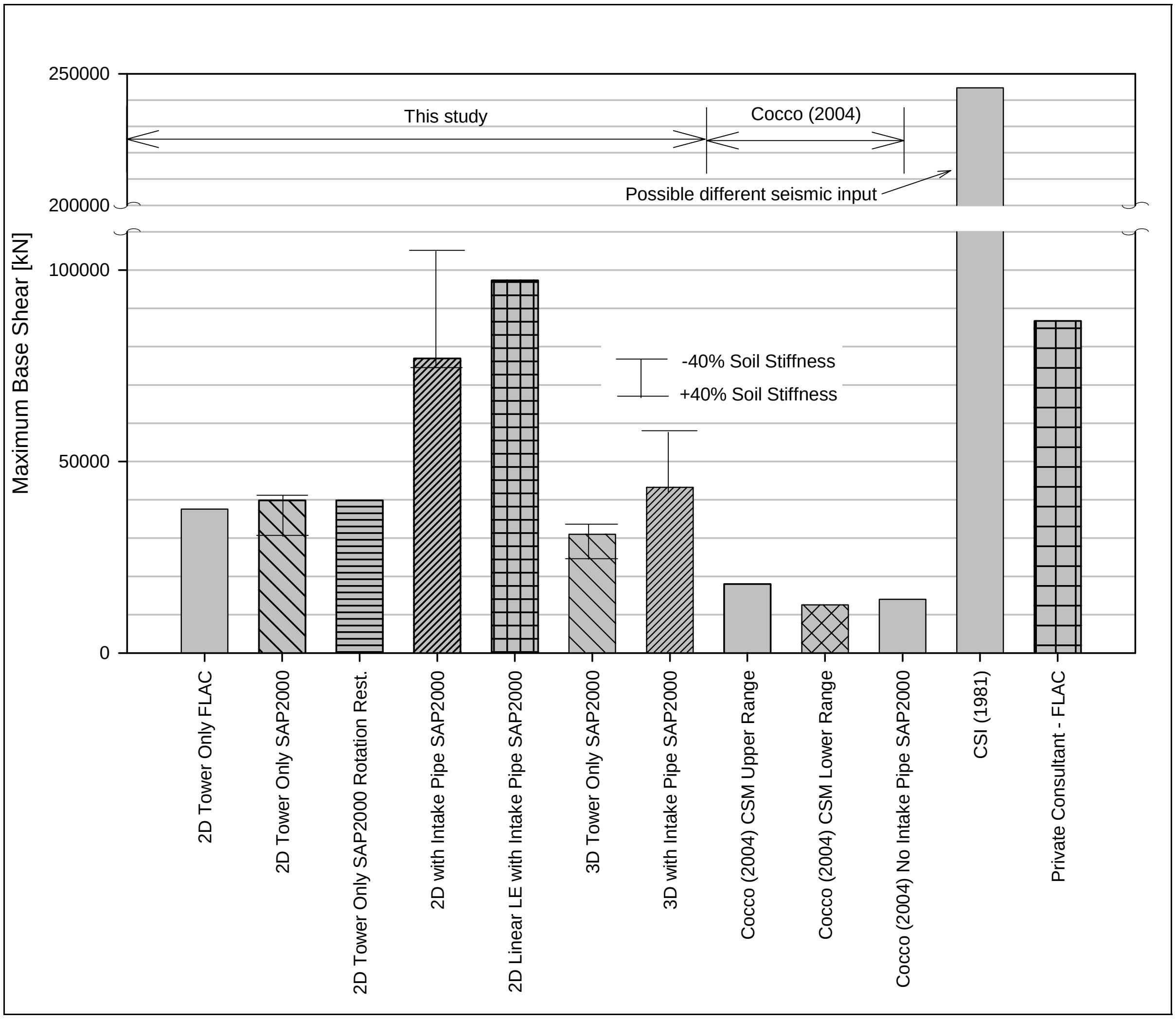

Figure 6-10 Comparison of Maximum Base Shear Force Values

A reduction in soil stiffness of 40% with respect to the baseline values used for the linear elastic analyses resulted in an increase of 2.7% and 7.5% for the base shear force using 2D and 3D finite element method models, respectively. An increase in soil stiffness of 40% resulted in a decrease of the maximum base shear force by 23% and 19% for the 2D and 3D finite element method models, respectively.

The importance of including 3D effects is highlighted in this figure. Shear forces decreased up to 44 % when the intake tower is included. Soil nonlinearity incorporated in the form of reduced equivalent linear values results in base shear force about 26 % higher than those computed using linear elastic models.

Similarly, the comparison of results in terms of the maximum bending moment is presented in Figure 6-11 in the form of variation bars. This figure also presents the results obtained by previous studies.

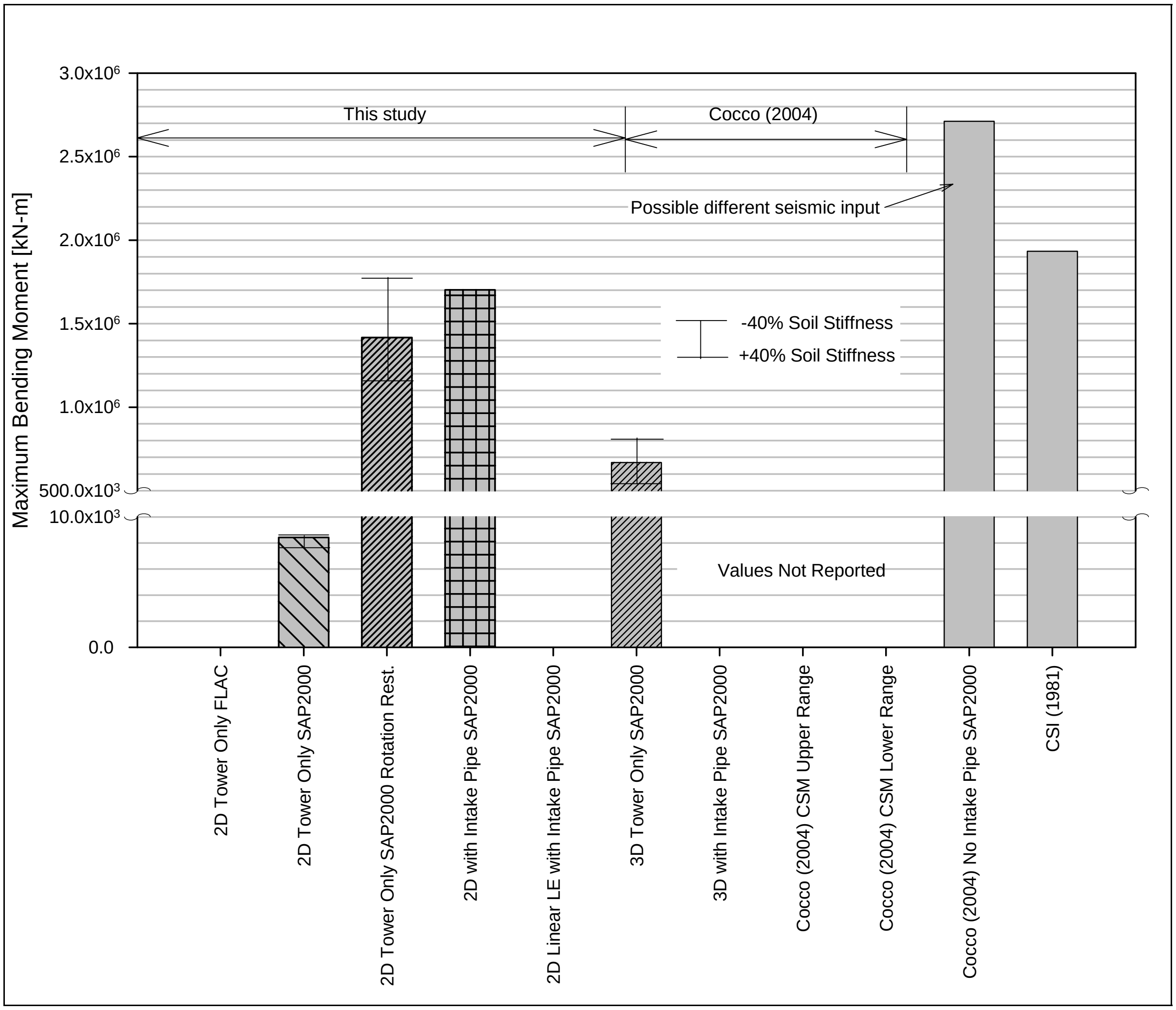

Figure 6-11 Comparison of Maximum Bending Moment Values

3D models resulted in lower basal moment values for the tower. However, the correct representation of the rotation restriction of the tower is very important. The models with no intake pipe resulted in very low basal moments (or zero) since the tower base was free to rotate. The soil nonlinearity resulted in higher moments at the base.

7 CONCLUSIONS AND RECOMMENDATIONS

7.1 Conclusions

The following conclusions can be drawn from the DSSI analyses carried out for this study:

- When the embedment of the control tower in the Success Dam is considered, the seismic response in terms of displacements and accelerations of the dam, was not significantly modified.

- The use of 3D models resulted in reduced maximum shear force at the base of the control tower when compared to 2D models. For the case of no intake pipe, the reduction was 23% for the base shear force, and for the case including the intake pipe, the reduction was 44%.

- The displacements and accelerations recorded at the control points did not seem to be very sensitive to 3D effects. The effect of soil properties values was evaluated using a sensitivity analysis. The stiffness values were varied ±40% for the soils and ±10% for the foundation. The results indicated that the variation of the model stiffness did not affect significantly the base reactions values. As part of the sensitivity analysis, a variation of the Poisson's ratio was used leaving the other soil properties unchanged. The Poisson's ratio values used were 0.3 and 0.45.

- The seismic response of the Success dam as analyzed indicates that important displacements can be expected at the top of the dam. The analyses were carried out using a linear stress-strain relationship. The MCE is used in the analysis so the seismic input represents a high magnitude earthquake. On the other hand, a nonlinear analysis may decrease the maximum computed displacement.

- The influence of the control tower in the seismic response of the Success dam was evaluated by comparison of results from models with and without the structures. The time history of displacements and accelerations at the control points of analysis in the dam section was not significantly influenced by the presence of the control tower. Even when the intake pipe was included in the analysis the time histories did not vary significantly, and therefore it is concluded that the presence of the intake pipe does not considerably modify the seismic response of the dam.

- The DSSI effect on the control tower is evaluated by comparison of results presented in this thesis, and with the results presented by Cocco (2004). In that study, the embedment was accounted for by using soil springs with a P-Y formulation. As mentioned by the author, the inertial forces were not accounted for because of the nature of the P-Y proposed analysis.

- The comparison of the results of this study with previous studies indicates that the approach followed by CSI (1981) highly overestimates the demands on the control tower. This is believed to be due to differences in the input ground motion used. CSI (1981) apparently used a seismic input with higher energy, an according to the report has absolute acceleration spectral ordinates of about 1 g at periods ranging from 0.5 to 0.7 s, which is greater than the 0.45 g for the same range of periods on the MCE. The soil properties used were also different since this study did not have the same level of details in terms of available geophysical data.

7.2 Recommendations for Future Work

It is recommended to continue this line of research. The seismic response of partially embedded structures is a complex problem to evaluate, and as presented in the literature review in chapter 2, and the conclusions section of this thesis, it is important to establish the importance of several characteristics of the model in the final response of the structure, i.e. ratio of depth of embedment to total length of the structure, relationship of this ratio and the cross section area, conditions of movement at the base of the tower, etc.

It is possible that the direct comparison of results among the different studies may not be accurate, because of some differences either on the soil profile used to represent the dam, or in the seismic input finally used in the analyses. Therefore it is recommended to evaluate the methodologies using the same input to define the relevance, consistency, reliability, and applicability of the different methodologies used so far to evaluate the seismic response of the control tower at Success dam.

Other earthquake motions, soil nonlinearities and geometries should be evaluated to be able to draw general conclusions and to establish general guidelines for simplified analysis of partially embedded towers.

REFERENCES

Chopra, A. K., and Liaw, C. Y. (1975). "Earthquake Resistant Design of Intake-Outlet Towers." *Journal of the Structural Division*, 101(ST7), 1349-1366.

Chopra, A. K., and Chakrabarti, P. (1981). Earthquake Analysis of Concrete gravity dams including dam-water-foundation interaction. Earthquake engineering and structural dynamics.

Chopra, A. K., and Fok, K. L. "Evaluation of simplified earthquake analysis procedures for intake-outlet towers." *8th world conference on earthquake engineering*, San Francisco, 467-474.

Chopra, A. K. (1995). Dynamics of structures : theory and applications to earthquake engineering, Prentice Hall, Englewood Cliffs, N.J.

Chopra, A. K. (2001). Dynamics of Structures: theory and applications to earthquake engineering, Prentice Hall, NJ.

Chopra, A. K., and Earthquake Engineering Research Institute. (1979). *Soil and structure response to earthquakes*, Earthquake Engineering Research Institute, S.l.

Clough, R. a. P., J. . (2004). *Dynamics of structures*, Mc. Graw-Hill.

Cocco, L. (2004). "Evaluation of the Nonlinear Seismic Response of Intake and Control Towers with the Capacity Spectrum Method," MSc Thesis, University of Puerto Rico, Mayagüez, PR.

Cocco, L., Suarez, L., and Matheu, E.E. (2005). "Seismic Response Evaluation of Intake Towers with the Capacity Spectrum Method." University of Puerto Rico at Mayaguez. Submitted for publication to the Engineering Structures Journal.

Comartin, C. D., Niewiarowski, R. W., Rojahn, C., Applied Technology Council., and California. Seismic Safety Commission. (1996). *Seismic evaluation and retrofit of concrete buildings : products 1.2 and 1.3 of the Proposition 122 seismic retrofit practices improvement program*, Seismic Safety Commission, State of California, [Sacramento?].

Computers and Structures, I. (2002). "SAP2000 – Integrated Software for Structural Analysis and Design." CSI, ed., Berkeley, CA.

CSI. (1981). "Dynamic analysis of structures at Success Dam." Civil Systems Inc., Tulaware County, CA.

Dove, R. C. (1996). "Structural Parameter Analysis of U.S. Army Corps of Engineers Existing Intake Towers Inventory." *Technical Report SL-96-1*, US Army Corps of Engineers, Waterways Experiment Station, Vicksburg, MS.

Dove, R. C. (1998). "Performance of Lightly Reinforced Concrete Intake Towers Under Selected Loadings." *Technical Report SL-98-1*, US Army Corps of Engineers, Waterways Experiment Station, Vicksburg, MS.

Dove, R. C. (2000). "Ultimate Deflection Response of Lightly Reinforced Concrete Intake Towers." *Technical Report ERDC/SL TR-00-6*, US Army Corps of Engineers, Waterways Experiment Station, Vicksburg, MS.

Freeman, S. A. "Development and Use of Capacity Spectrum Method." *Proceedings of the 6th U.S. National Conference on Earthquake Engineering*, Seattle, Washington.

GeoSlope International Ltd (2004) “QUAKE/W” G. I. International Ltd. 2004. Canada.

Goel, R. K., and Chopra, A. K. (2004). "Evaluation of Modal and FEMA Pushover Analyses: SAC Buildings." *Earthquake Spectra*, 20(1), 225-254.

Goyal, A., and Chopra, A. K. (1989). "Earthquake Analysis and response of intake-outlet towers." *Report No. UCB/EERC-89/04*, University of California, Berkeley.

Goyal, A., and Chopra, A. K. (1989). "Earthquake Response Spectrum Analysis of Intake-Outlet Towers." *Journal of Engineering Mechanics*, 115(7), 1413-1431.

Goyal, A., and Chopra, A. K. (1989). "Hydrodynamic and Foundation Interaction Effects in Dynamics of Intake Towers: Frequency Response Functions." *Journal of Structural Engineering*, 115(6), 1371-1385.

Goyal, A., and Chopra, A. K. (1989). "Simplified Evaluation of Added Hydrodynamic Mass for Intake Towers." *Journal of Engineering Mechanics*, 115(7), 1393-1435.

Gupta, B., and Kunnath, S. K. (2000). "Adaptive Spectra-Based Pushover Procedure for Seismic Evaluation of Structures." *Earthquake Spectra*, 16(2), 367-397.

Gupta, S., and Foundation, N. S. (1980). *Hybrid modeling of soil-structure interaction*, University of California Earthquake Engineering Research Center, Berkeley, Calif. Springfield, Va.

Gupta, S., and Penzien, J. (1981). Hybrid modelling of seismic soil-structure interaction.

Gupta, S., and Penzien, J. (1981). *Hybrid modelling of soil-structure interaction for embedded structures*, Dept. of Civil Engineering University of California, Berkeley.

Itasca, C. G. (2000). *FLAC User's Manual*, Itasca Consulting Group, Inc., Minneapolis, Minnesota.

Itasca, C. G. (2002). *FLAC 3D User's Manual*, Itasca Consulting Group, Inc., Minneapolis, Minnesota.

Kramer, S. L. (1996). *Geotechnical earthquake engineering*, Prentice Hall, Upper Saddle River, N.J.

Llopis, J. L., Lee, L. T., and A., G. R. (1997). "In situ geophysical investigation to evaluate dynamic soil properties at Success dam, California." *TR GL 97-8*, U.S. Army Corps Engineers Waterways Experiment Station, Sacramento, CA.

Lysmer, J. (1975). *FLUSH : a computer program for approximate 3-D analysis of soil-structure interaction problems*, Earthquake Engineering Research Center University of California, Berkeley CA, Springfield, Va.

Schnabel, P. B., Lysmer, J., Seed, H. B., and University of California Berkeley. Earthquake Engineering Research Center. (1972). *SHAKE : a computer program for earthquake response analysis on horizontally layered sites*, Report EERC 72-12, Earthquake Engineering Research Center, College of Engineering, University of California, Berkeley, Calif.

Seed, H.B. and Idriss, I.M. (1970). "Soil moduli and damping factors for dynamic response analyses," Report No. EERC 70-10, Earthquake Engineering Research Center, University of California, Berkeley.

Suarez, L. E., Matheu, E. E., and Cocco, L. "Evaluation of Intake Towers Using the Capacity Spectrum Method." *Proceedings of the 2004 US Society of Dams Conference*, St. Louis, Missouri.

Suarez, L. E., and Montejo, L. A. (2005). "Applications of the Wavelet Transform in the Generation and Analysis of Artificial Accelerograms." Journal of Earthquake Engineering and Structural Dynamics. Submitted for publication.

Suarez, L. E., and Montejo, L. A. (2005). "Generation of Artificial Earthquakes via the Wavelet Transform." *International Journal of Solids and Structures. Submitted for publication*, in press.

USACOE. (2003). "Two-Mode Approximate and Computer Solution Methods of Analysis for a Free-Standing Intake Tower." *Engineer Manual No. 1110-2-2400*, U.S. Army Corps of Engineers, Washington, DC.

USACOE. (2004). "Information Packet for the Initial Screening Workshop of Alternative Seismic Remediation Strategies for Success Dam, Tule River, California." U.S. Army Corps of Engineers.

USACOE. (2006). "Success Seismic remediation Project" U.S. Army Corps of Engineers. *PowerPoint Presentation*.

Vucetic, M. and Dobry, R. (1991). "Effect of soil plasticity on cyclic response," Journal of Geotechnical Engineering, ASCE, Vol. 117, No. 1, pp. 89-107.